uOttawa

L'Université canadienne
Canada's university

FACULTÉ DES ÉTUDES SUPÉRIEURES ET POSTOCTORALES

uOttawa

L'Université canadienne
Canada's university

FACULTY OF GRADUATE AND POSDOCTORAL STUDIES

Sheila Ruth May Costford
AUTEUR DE LA THÈSE / AUTHOR OF THESIS

Ph.D. (Biochemistry)
GRADE / DEGREE

Department of Biochemistry
FACULTÉ, ÉCOLE, DÉPARTEMENT / FACULTY, SCHOOL, DEPARTMENT

The Roles of AMP-Activated Protein Kinase and Uncoupling Protein-3 in Skeletal Muscle Fuel Metabolism

TITRE DE LA THÈSE / TITLE OF THESIS

Mary-Ellen Harper
DIRECTEUR (DIRECTRICE) DE LA THÈSE / THESIS SUPERVISOR

CO-DIRECTEUR (CO-DIRECTRICE) DE LA THÈSE / THESIS CO-SUPERVISOR

EXAMINATEURS (EXAMINATRICES) DE LA THÈSE / THESIS EXAMINERS

Les Kozak

Ross Milne

Ilona Skerjanc

Pascal Imbeault

Gary W. Slater
Le Doyen de la Faculté des études supérieures et postdoctorales / Dean of the Faculty of Graduate and Postdoctoral Studies

The Roles of AMP-Activated Protein Kinase and Uncoupling Protein-3 in Skeletal Muscle Fuel Metabolism

Doctoral Thesis of
Sheila Costford

Supervisor
Mary-Ellen Harper, Ph.D.

Submitted to
The Faculty of Graduate and Postdoctoral Studies

In partial fulfillment of the requirements for
The Doctorate in Philosophy, Biochemistry

Your file Votre référence
ISBN: 978-0-494-41630-3
Our file Notre référence
ISBN: 978-0-494-41630-3

Abstract

The prevalence of obesity has increased at an alarming rate over the past few decades. Obesity is caused by a positive energy balance and is associated with several major health risks, such as cardiovascular disease, type 2 diabetes mellitus (T2DM) and some cancers. This research focuses on two proteins involved in energy regulation: AMP-activated protein kinase (AMPK) and uncoupling protein-3 (UCP3).

AMPK functions to maintain cellular and whole body energy homeostasis. Studies in experimental animals have demonstrated that activation of AMPK in skeletal muscle protects against insulin resistance, T2DM and obesity. **The first objective of this research was to determine whether R225W, a rare mutation in the muscle-specific γ_3 subunit of AMPK, affects activity and function in human muscle.** R225W was associated with increased basal and AMP-stimulated AMPK activities, increased muscle glycogen and decreased intramuscular triglyceride (IMTG). These findings are consistent with an important role for AMPKγ_3 in human muscle energy metabolism and highlight the attractiveness of this γ isoform as a pharmaceutical target for the treatment of metabolic disorders associated with obesity, such as T2DM.

UCP3 is a poorly understood mitochondrial inner membrane protein expressed predominantly in skeletal muscle. Although the function of UCP3 is unknown, the literature supports roles for UCP3 in facilitating fatty acid oxidation and mitigating oxidative stress. Moreover, lower levels of UCP3 have been observed in muscle of T2DM patients. **The second objective of this research was to determine if UCP3 protects from the development of insulin resistance.** UCP3 -/-, wildtype, and UCP3tg overexpressor mice were fed a 10% or 45% fat diet for 4 or 8 months. Although UCP3 overexpression protected against the accumulation of IMTG, paradoxically, both UCP3tg and UCP3 -/- mice were protected from the development of glucose intolerance and insulin resistance. UCP3tg mice were, however, protected from the development of obesity, whereas UCP3 -/- mice were not. These results therefore support a role for UCP3 in preventing the accumulation of triglyceride in both muscle and adipose tissue.

It is anticipated that these findings will lead to a better understanding of the mechanisms involved in the development of disorders of energy regulation.

Dedication

This doctoral thesis is dedicated to **David Costford**, my Dad.

Thank you for your excitement, for your encouragement and for your understanding. Thank you for lending me the car, for buying me lunch, and for slipping me a 50 when life was hard. Thank you for believing in me and for not giving up, but mostly, thank you for being there through it all.

Acknowledgements

MENTORS

Supervisor
Mary-Ellen Harper, PhD

Of all the individuals who have made an impact on my life and career, Dr. Mary-Ellen Harper has had the greatest influence during my graduate studies. She has been, and continues to be, an exceptional role model in all areas of academia, and has demonstrated and taught me the meaning of research excellence. Throughout my degree she provided me with extensive opportunities to travel the world to present my research, as well as to publish my work in peer-reviewed journals. Her excitement and passion for her research have encouraged me to pursue a career in the field of bioenergetics research, and I will be forever grateful to her for her outstanding mentorship.

Thesis Advisory Committee
Thomas Moon, PhD
Jean Marc Renaud, PhD

Dr. Thomas Moon and Dr. Jean Marc Renaud made my Thesis Advisory Committee meetings something to anticipate. I greatly appreciate their guidance and advice, the intellectual discussions in which we engaged, and most of all their humour and support.

Biochemistry Program Directors
Vasek Mezl, PhD
Ilona Skerjanc, PhD

I would like to acknowledge the guidance and support of the Biochemistry Program Directors, Dr. Vas Mezl and Dr. Ilona Skerjanc.

Department of Biochemistry, Microbiology and Immunology Faculty
John Baenziger, PhD
Steffany Bennett, PhD
Lionel Filion, PhD
Zemin Yao, PhD

I would also like to acknowledge those professors who supported and advised me in the areas of undergraduate teaching, student government and career development.

COLLEAGUES

Current Laboratory Members
Sean Crawford
Carmen Estey
Adrienne Gowing
Benny Hill
Linda Jui
Cynthia Moffat
Samantha Prevost
Mahmoud Salkhordeh
Neha Sarna
Erin Seifert, PhD
Jian Xuan

Previous Laboratory Members
Mitra Abaeian
Julie Beaulieu
Lisa Bevilacqua, PhD
Veronic Bézaire, PhD
Septimiu Bucurescu, MD
Kris Chan, MD
Shehla Chaudhry
Meredith Evans
Martin Gerrits, PhD
Basil Hubbard
Darcy MacLellan, DDS
Marianne McGee
Matthew Niedzwiecki
Dimitre Ranev
Andréanne Péloquin
Nicole Sabet
Tammy Shaw, MD
Nausheen Siddiqui, MD
Anastasia Tour
Jamie Wong

I would like to acknowledge the support of all of the current and previous members of the Mitochondrial Bioenergetics Laboratory. Specifically, I would like to emphasize the contributions of **Shehla Chaudhry** and **Sean Crawford**, both Honours Undergraduate students. Shehla worked closely with me on both the AMPK (Chapter 1) and the UCP3 (Chapters 2 and 3) projects, while Sean continues to work on phase II of the AMPK project (Appendix A).

COLLABORATORS

Ottawa Hospital Weight Management Clinic
Robert Dent, MD
Brenda Bradley

University of Ottawa Heart Institute Lipid Research Laboratory
Ruth McPherson, MD, PhD
Nihan Kavaslar, PhD
Heather Doelle
Sybil Hebert

University of California, Berkeley
Len Pennacchio, PhD
Nadav Ahituv, PhD
Wendy Schackwitz

University of Ottawa Heart Institute Molecular Function & Imaging Group
Robert Beanlands, MD
Jean da Silva, PhD
Robert deKemp, PhD
Michael Gollob, MD
May Aung
Ed Gannon
Kimberly Gardner
Michaela Garkisch
Linda Garrard

University of Ottawa School of Human Kinetics
Dany Lafontaine, PhD
Mario Lamontagne, PhD
Stéfanie Pagé

Collaborators from the Ottawa Hospital Weight Management Clinic, the University of Ottawa Heart Institute Lipid Research Laboratory and the University of California at Berkeley contributed significantly to the AMPK project (Chapter 1). Collaborators from the University of Ottawa Heart Institute Molecular Function and Imaging Group and the University of Ottawa School of Human Kinetics contributed greatly to phase II of the AMPK project (Appendix A). Specific contributions are listed immediately preceding each chapter. I would expressly like to acknowledge **Dr. Ruth McPherson** and **Dr. Bob Dent** for their dedication to the AMPK project and for their support during my graduate degree.

SUPPORT

University of Ottawa Animal Care & Veterinary Services
Eileen Franklin
Kim Yates

I would like to thank Eileen Franklin and Kim Yates, surgical technicians at the University of Ottawa Animal Care and Veterinary Services, for all their help, especially in the early years, and for their continuing friendship.

Administration
Carol Ann Kelly
Nicole Trudel

No one would graduate without the dedication of Carol Ann Kelly and Nicole Trudel, Administrative Assistants for the Biochemistry and Microbiology & Immunology graduate programs. I would like to thank both Carol Ann and Nicole for all their hard work, help and support over the past five years.

Family and Friends

I would like to acknowledge all my family and friends for their support and encouragement during my graduate degree. I would specifically like to thank **Deborah Weiss** for understanding as only a PhD candidate can understand and **Alicia Ennis** for helping me keep my life in balance and in perspective.

Table of Contents

List of Abbreviations and Symbols

Abbreviations and Acronyms

A

ACC1: acetyl-coenzyme A carboxylase-1
ACC2: acetyl-coenzyme A carboxylase-2
ACE: angiotensin-converting enzyme
ADP: adenosine diphosphate
AICAR: 5-aminoimidazole-4-carboxamid-ribosid
Akt/PKB: protein kinase B
AMP: adenosine monophosphate
AMPK: adenosine monophosphate-activated protein kinase
AMPK γ_3: adenosine monophosphate-activated protein kinase gamma-3 subunit
ANOVA: analysis of variance
ANT: adenine nucleotide translocator
ARC: arcuate nucleus
AS160: Akt/PKB (protein kinase B) substrate of 160 kilodaltons
ATP: adenosine triphosphate

B

β3 AR: beta-3 adrenergic receptor
BAT: brown adipose tissue
BMI: body mass index

C

C: cytochrome c
CART: cocaine and amphetamine regulating transcript
CBS: cystathionine beta-synthase (domain)
CCK: cholecystokinin
CDA: Canadian Diabetes Association
CDC: Center for Disease Control
cDNA: copy deoxyribonucleic acid
CoA/CoASH: coenzyme A
CT: computed tomography
C-terminus: carboxy-terminus
CTNF: ciliary neurotrophic factor
CVD: cardiovascular disease

D

DAG: diacylglycerol
DM: diabetes mellitus
DNA: deoxyribonucleic acid

E

EF2K: elongation factor-2 kinase
EGCG: (–)epigallocatechin-3-gallate
EMG: electromyography
ETC: electron transport chain
EWAT: epididymal white adipose tissue

F

FA: fatty acid
$FADH_2$: flavin adenine dinucleotide (reduced)
FDG: [^{18}F]-fluorodeoxyglucose
FFA: free fatty acids

G

GALP: galanin/galanin like peptides
GAPDH: glyceraldehyde 3-phosphate dehydrogenase
GDP: guanosine diphosphate
GLP-1: glucagon-like peptide 1
GLUT4: glucose transporter 4
GRP: gastrin releasing peptides
GS: glycogen synthase
GTP: guanosine triphosphate

H

H&E: hematoxylin and eosin
HbA1c: hemoglobin A1c
HF: high fat
HMGR: 3-hydroxy-3-methylglutaryl coenzyme A reductase

I

IBAT: interscapular brown adipose tissue
IDV: integrated densitometry value
IgG: immunoglobulin G

IL-6: interleukin-6
IMCL: intramyocellular lipid
IMTG: intramuscular triglyceride
IP: intraperitoneal
IRS-1: insulin receptor substrate-1
IV: intravenous

K

KPF: kaempferol

L

LCFA-CoA: long chain fatty acyl-coenzyme A

M

MACS: magnetic activated cell sorting
MAF: minor allele frequency
mATPase: myofibrillar adenosine triphosphatase
mDNA: mitochondrial DNA
MFI: molecular functioning and imaging
MHC: myosin heavy chain
MMLV: Moloney murine leukemia virus
MNT: medical nutrition therapy
mRNA: messenger ribonucleic acid
mTOR: mammalian target of rapamycin

N

n: sample size
NADH: nicotinamide adenine dinucleotide (reduced)
NCBI: National Center for Biotechnology Information
NHLBI: National Heart, Lung, and Blood Institute
NPY: neuropeptide Y
NS: nonsynonymous (genetics)
NS: not significant (statistics)

O

OCT: optimal cutting temperature (compound)
OsO_4: osmium tetroxide

P

PAR-Q: physical activity readiness questionnaire
PAS: Periodic Acid Schiff (stain)
PDH: pyruvate dehydrogenase (complex)
PDK1: phosphoinositide dependent kinase-1
PET: positron emission tomography
PFK2: 6-phosphofructo-2-kinase
PGC1α: peroxisome proliferator-activated receptor-γ co-activator-1α
PH: pleckstrin homology (domain)
PI(3,4,5)P_3: phosphatidylinositol (3,4,5)-triphosphate
PI(3,4)P_2: phosphatidylinositol (3,4)-bisphophate
PI3K: phosphatidylinositol-3-kinase
PKB: protein kinase B
PKCθ: protein kinase C-theta
PKCζ: protein kinase C-zeta
PMSF: phenylmethylsulphonyl fluoride
PP2A: protein phosphatase 2A
PPARγ: peroxisome proliferator-activated receptor-γ
***PRKAG3*:** gene for adenosine monophosphate-activated protein kinase gamma-3 subunit
PVN: paraventricular nucleus
PYY: peptide YY

Q

Q: ubiquinone

R

R225W: referring to mutation of residue 225 from arginine to tryptophan in the gamma-3 subunit of adenosine monophosphate-activated protein kinase
RER: respiratory exchange ratio
RN: Rendement Napole
RNA: ribonucleic acid
ROS: reactive oxygen species
RT-PCR: reverse transcription polymerase chain reaction (or real time polymerase chain reaction)

S

S: synonymous

SAMS: serine-alanine-methionine-serine (peptide)
SAS: Statistical Analysis Software
SBTI: soybean trypsin inhibitor
SD: standard deviation
SEM: standard error of the mean
SNP: single nucleotide polymorphism

T

T1DM: type 1 diabetes mellitus
T2DM: type 2 diabetes mellitus
TAG: triacylglycerol (triglyceride)
TCA Cycle: tricarboxylic acid cycle (also called the Krebs cycle or the citric acid cycle)
TZD: thiazolidinediones

U

UCP: uncoupling protein
UCP1: uncoupling protein-1
UCP3: uncoupling protein-3
UCP3 -/-: uncoupling protein-3 knockout mice
UCP3tg: uncoupling protein-3 overexpressor mice
UTR: untranslated region

W

WAT: white adipose tissue
WHO: World Health Organization
WPW: Wolff-Parkinson-White (syndrome)
WT: wildtype mice

Symbols and Chemical/Mathematical Abbreviations

cal: calories
d: day
e^-: electron
g: grams
H^+: proton
HEPES: 4-(2-hydroxyethyl)-1-piperazineethanesulfonic acid
kcal: kilocalories
kDa: kilodaltons
kg: kilograms
kJ: kilojoules
L: liters
m: meters
M: moles per liter
mg: milligrams
min: minutes
ml: milliliters
mm: millimetres
mM: millimoles per liter
mmol: millimoles
ng: nanograms
nM: nanomoles per liter
Pi: inorganic phosphate
pmol: picomoles
s: seconds
SUV: standard uptake values
µCi: microcuries
µg: micrograms
µl: microliters
µm: micrometers
µM: micromoles per liter
VCO_2: volume of carbon dioxide (production)
VO_2: volume of oxygen (consumption)
°C: degrees Celsius
γ_1: referring to adenosine monophosphate-activated protein kinase gamma-1 subunit
γ_2: referring to adenosine monophosphate-activated protein kinase gamma-2 subunit
γ_3: referring to adenosine monophosphate-activated protein kinase gamma-3 subunit
γ_{2L}: referring to long form of adenosine monophosphate-activated protein kinase gamma-2 subunit

γ_2R302Q: referring to mutation of residue 302 from arginine to glutamine in the long form of gamma-2 subunit of adenosine monophosphate-activated protein kinase

γ_2R61Q: referring to mutation of residue 61 from arginine to glutamine in the short form of gamma-2 subunit of adenosine monophosphate-activated protein kinase

γ_{2S}: referring to short form of adenosine monophosphate-activated protein kinase gamma-2 subunit

γ_3R225Q: referring to mutation of residue 225 from arginine to glutamine in the gamma-3 subunit of adenosine monophosphate-activated protein kinase

γ_3R225W: referring to mutation of residue 225 from arginine to tryptophan in the gamma-3 subunit of adenosine monophosphate-activated protein kinase

%: percent

List of Figures and Illustrations

General Introduction

Chapter 1

Chapter 2

Appendix A

List of Tables

General Introduction

"There is a state function E, called 'energy', whose differential equals the work exchanged with the surroundings during an adiabatic process."

Rudolf Julius Emanuel Clausius, 1850
((25), translated into English (24))

Energy

The first law of thermodynamics was originally proposed in 1850 by German physicist and mathematician Rudolf Clausius in his most famous paper, *Über die bewegende Kraft der Wärme* (25) ("On the Moving Force of Heat and the Laws of Heat which may be Deduced Therefrom" (24)). The first law of thermodynamics refers to the conservation of energy, the principle that energy can neither be created or destroyed, but can only be converted from one form to another. The solar energy emitted from the sun as a consequence of hydrogen fusion can be captured by photosynthetic autotrophs (higher plants, phytoplankton, algae and chloroplast-containing bacteria) and used to combine carbon dioxide and water to produce oxygen and organic materials such as glucose:

$$6\ CO_2 + 6\ H_2O + h\nu \rightarrow 6\ O_2 + C_6H_{12}O_6$$

All life on earth depends on this photosynthetic process. Heterotrophs (animals, fungi, protozoa and most bacteria) consume photosynthetic autotrophs (and other heterotrophs) in order to extract the energy

originating from the sun and convert it to a usable form, adenosine triphosphate (ATP) (Figure 1).

The utilization, storage and management of energy in living organisms are the major concepts addressed in the following thesis. This General Introduction therefore covers topics in energy catabolism, energy anabolism, energy balance, energy regulation and disorders of energy regulation.

Biological Fuel

The extractable energy consumed by heterotrophs such as humans can be in one of four forms: carbohydrate, lipid, protein or alcohol. Through catabolic processes, energy is extracted from the bonds of these molecules and repackaged as high energy phosphate bonds in ATP. ATP can then be used to fulfil cellular functions. Energy is often measured in calories (cal) or kilocalories (kcal) in biological settings. One calorie is equal to the amount of energy required to raise the temperature of 1 gram (g) of water by 1 degree Celsius (equivalent to 4.184 joules), whereas 1 kilocalorie is equal to the amount of energy required to raise the temperature of 1 kilogram (kg) of water by 1°C (equivalent to 4.184 kilojoules). It has been approximated that one gram of carbohydrate contains 4 kcal of energy, whereas protein contains 4 kcal/g, alcohol contains 7 kcal/g and fat contains 9 kcal/g (92).

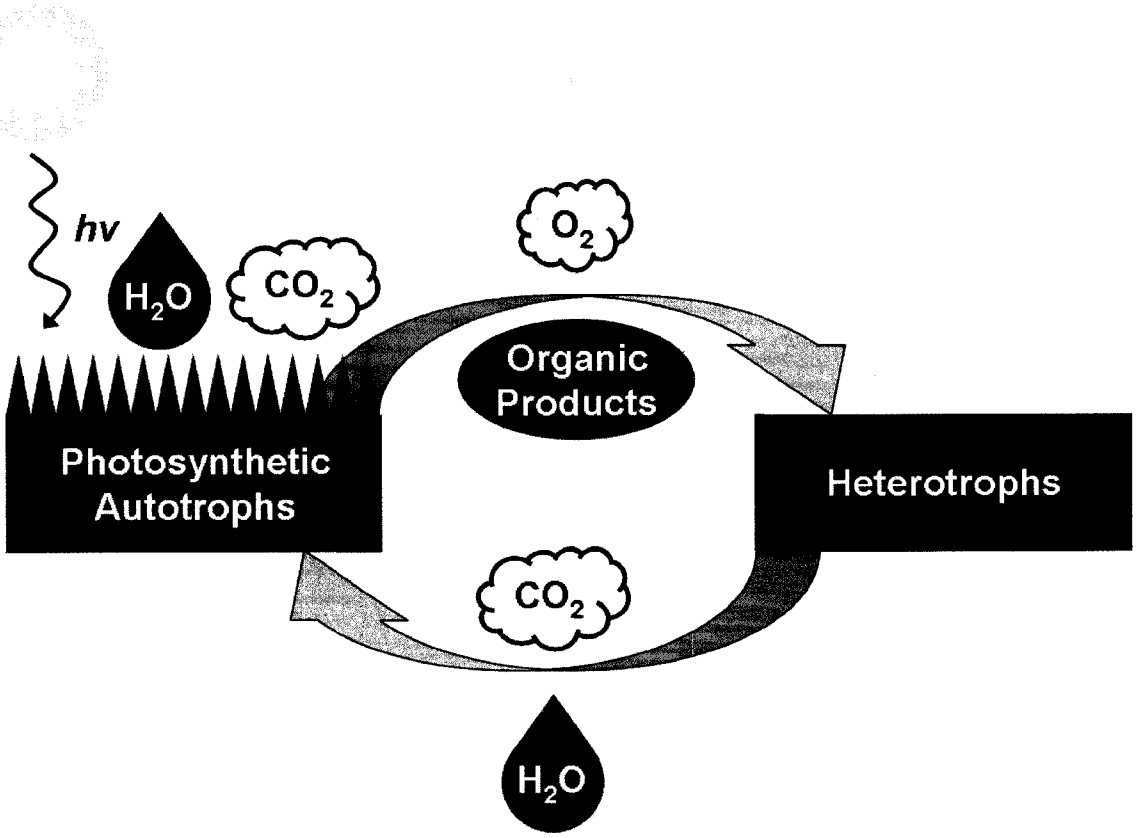

Figure 1: Biosphere energy conversion cycle for life on earth (adapted from (103)).

These approximations are termed 'Atwater Factors' and are generally adequate for the determination of caloric intake in the diet of North Americans, but they are not accurate for caloric determination of diets containing substantial amounts of fibrous plant material (145).

Energy Extraction from Fuel

Carbohydrate Catabolism

Carbohydrate digestion begins to a small extent in the mouth where salivary amylase begins to break the alpha-1,4-glycosidic linkages between monosaccharide monomers in complex carbohydrates (*e.g.*, starch). Digestion continues in the duodenum with the injection of pancreatic amylase, which performs the same function. Carbohydrate monomers, largely glucose, are taken up by the intestinal epithelial cells, and enter the portal vein. Circulating concentrations of glucose are 'sensed' by the pancreas. Under normal circumstances, as a result of elevated blood glucose levels, glucose is taken up by pancreatic beta cells through GLUT2 transporters, and insulin is released into the blood. Most peripheral glucose disposal occurs postprandially in skeletal muscle and adipose tissue. Insulin binds to the insulin receptor, initiating a cascade of intracellular signalling events, which result in the translocation of GLUT4 transporters to the plasma membrane (insulin signalling details are described in the 'Skeletal Muscle' section of this General Introduction and illustrated in Figure 8). Glucose is

then taken up into these insulin-sensitive tissues and phosphorylated to produce glucose-6-phosphate. The process of glycolysis ensues in the cytoplasm, resulting in the production of 2 pyruvate molecules for every molecule of glucose-6-phosphate (Figure 2).

In skeletal muscle, glucose can be taken up via the insulin-dependent pathway, described above, or through an insulin-independent pathway activated by muscle contraction or hypoxia (82, 89, 119, 120, 156, 164, 171). The details of this/these pathway(s) have not been completely elucidated, although there is evidence that AMP-activated protein kinase (AMPK) is responsible for some insulin-independent glucose uptake (101).

Carbohydrate monomers other than glucose, normally much less common in the human diet, enter glycolysis at various steps in the pathway. Pyruvate is converted by the pyruvate dehydrogenase (PDH) complex to the metabolite that is common to many pathways of carbohydrate, lipid and amino acid catabolism and anabolism, acetyl-CoA. Acetyl-CoA then enters the tricarboxylic acid (TCA) cycle to produce the energy-rich reducing equivalents nicotinamide adenine dinucleotide (NADH) and flavin adenine dinucleotide ($FADH_2$), as well as a small amount of usable energy in the form of guanosine triphosphate (GTP) (Figure 3).

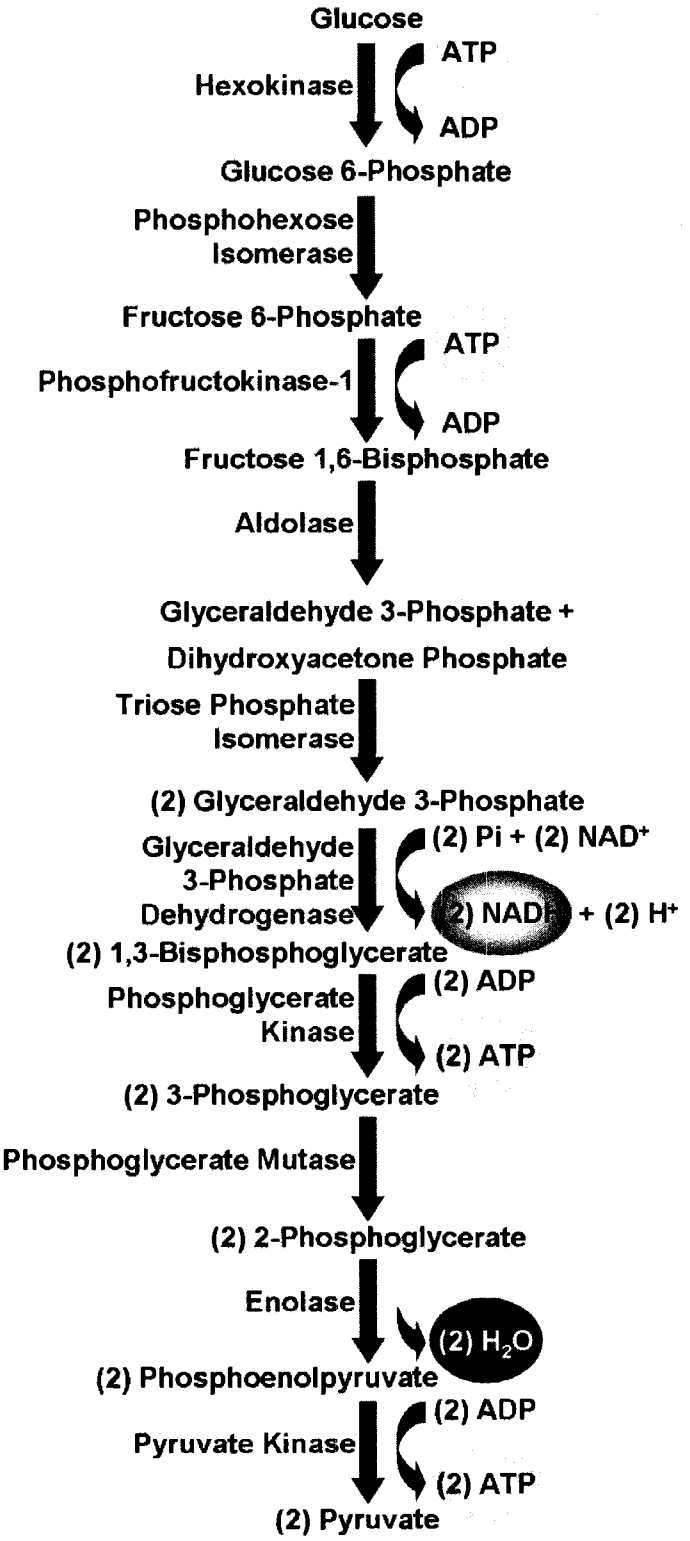

Figure 2: Glycolysis. Pi: inorganic phosphate; NADH: nicotinamide adenine dinucleotide (reduced); $FADH_2$: flavin adenine dinucleotide (reduced).

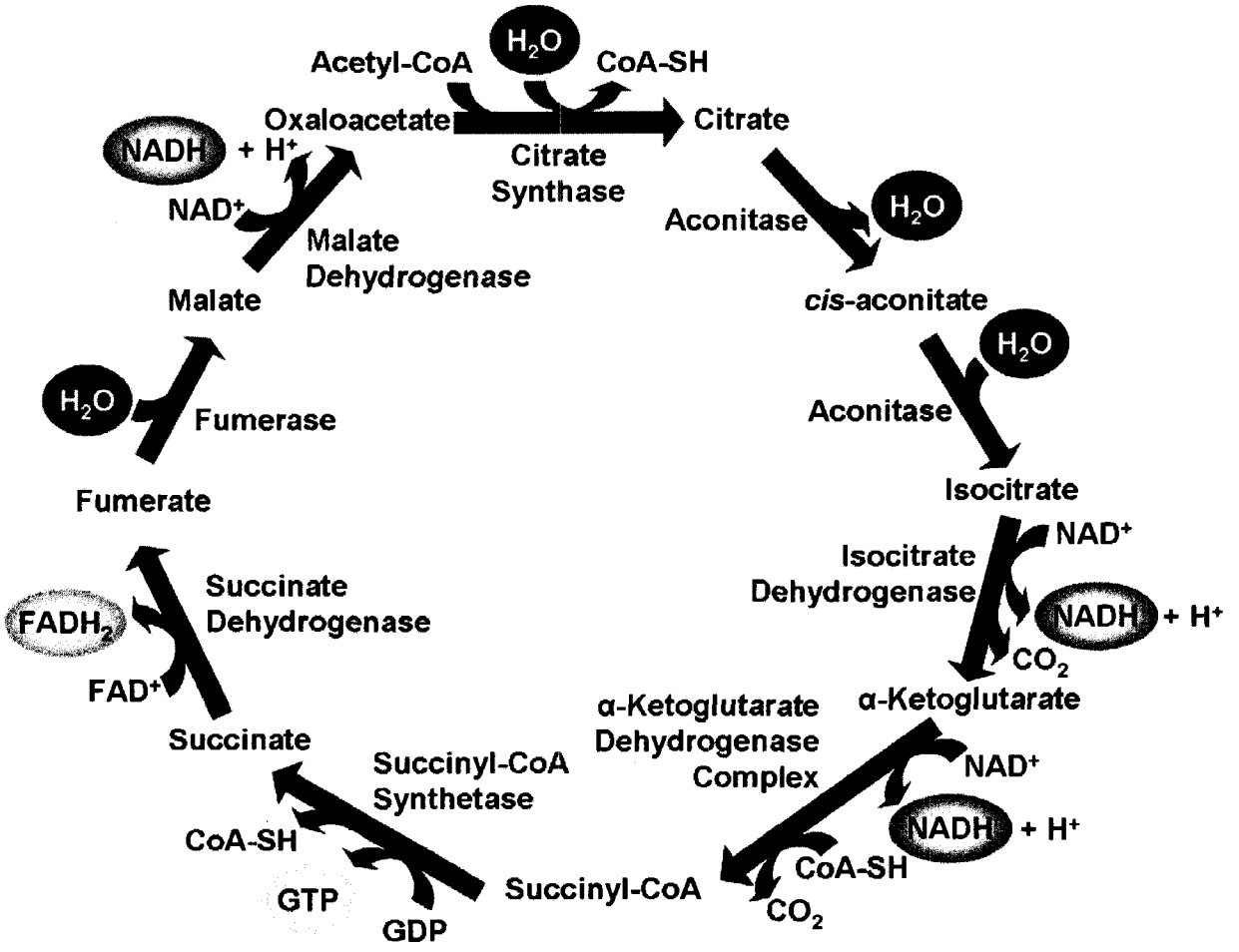

Figure 3: The tricarboxylic acid (TCA) cycle. CoA-SH: coenzyme A; NADH: nicotinamide adenine dinucleotide (reduced); GDP: guanosine diphosphate; GTP: guanosine triphosphate; $FADH_2$: flavin adenine dinucleotide (reduced).

These processes occur in the mitochondria, the 'powerhouses' of the cell (mitochondria are described in more detail in the 'The Role of Mitochondria in Energy Conversion' section of this General Introduction).

Reducing equivalents are then shuttled to the electron transport chain (ETC) located on the mitochondrial inner membrane, where equivalents donate their electrons to the first of four complexes. As electrons are passed from complex to complex, protons are pumped out of the mitochondrial matrix by three of these complexes (I, III and IV) into the intermembrane space, creating a chemical electrical potential of approximately 150 to 200 mV. Protons return to the matrix via ATP synthase (also referred to as complex V) and the energy associated with this return is used to phophorylate adenosine diphosphate (ADP) to ATP, the usable form of energy for the cell (Figure 4). Alternatively, protons can return to the mitochondrial matrix through 'proton leaks' caused by the uncoupling proteins and other poorly understood mechanisms, and these are reviewed below. Altogether the activities of the ETC and ATP synthase are referred to as oxidative phosphorylation.

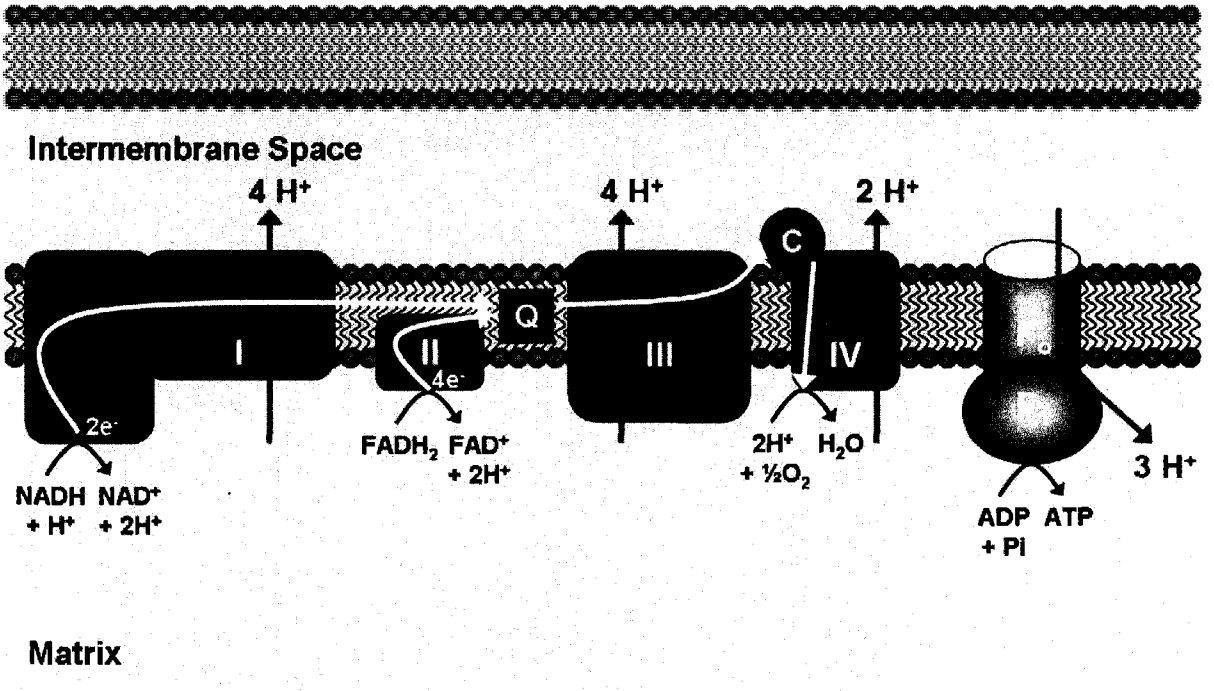

Figure 4: The electron transport chain (ETC). H^+: proton; e^-: electron; I: complex I; II: complex II; Q: ubiquinone; III: complex III; C: cytochrome c; IV: complex IV; F_o/F_1: complex V (ATP synthase); Pi: inorganic phosphate.

Intriguingly, however, this energy conversion process of oxidative phosphorylation (95) is not perfect: the energy associated with protons 'leaking back' into the matrix by any other mechanism other than through ATP synthase is lost as heat (23). This process is termed "uncoupling" (86) and may occur through particular proteins expressed on the mitochondrial inner membrane (reviewed in (113)) or through other means. The uncoupling of oxidative phosphorylation has been most extensively studied in brown adipose tissue, where it is essential in thermoregulation in small mammals and newborn humans (reviewed in (15, 63)). Uncoupling in skeletal muscle may account for up to 50% of resting energy expenditure in this tissue (121, 123) and is discussed more extensively in the 'Treatment of Energy Regulation Disorders' section of this General Introduction.

Fat Catabolism

The main form of dietary fat is triglyceride. Following ingestion, bile salts, produced by the liver and released into the duodenum, emulsify triglycerides and other dietary fats to form mixed micelles. Pancreatic lipase then releases the free fatty acids from the glycerol backbone of triglycerides. Glycerol and free fatty acids are then taken up into the mucosal epithelial cells of the intestinal wall to be reconverted back into triglyceride. Triglyceride is packaged with cholesteryl esters, phospholipids, cholesterol and apolipoproteins to form chylomicrons. These chylomicrons are released into

the lymph system and then into the blood via the thoracic duct. Lipoprotein lipase releases free fatty acids from the core of the chylomicron, which can then be taken up into the tissues. Fatty acids undergo beta-oxidation in the mitochondria (*e.g.*, Figure 5) to produce the common intermediate, acetyl-CoA (which enters the TCA cycle) and reducing equivalents (which donate their electrons to the ETC).

Protein and Alcohol Catabolism

Dietary protein is rarely used as a fuel source in the human body, and only is used to a significant extent during the consumption of hypocaloric diets, containing moderately high levels of protein. Endogenous protein (*e.g.*, of skeletal muscle) is used to a small extent during extended periods of negative energy balance. The carbon skeletons of amino acids from dietary proteins supplied in excess of amino acid requirements (*e.g.*, to support protein turnover reactions) are converted by the liver to energy-rich intermediates. They are converted to either glucose (via gluconeogenesis) or one of three ketone bodies (acetoacetate, beta-hydroxybutyrate or acetone; via ketogenesis), depending on the specific amino acid. Glucose can be released into the blood to fuel obligate glucose consumers, and ketone bodies can also be released into the blood to fuel tissues such as the heart, skeletal muscle, and the brain during fasting, when blood glucose levels are low.

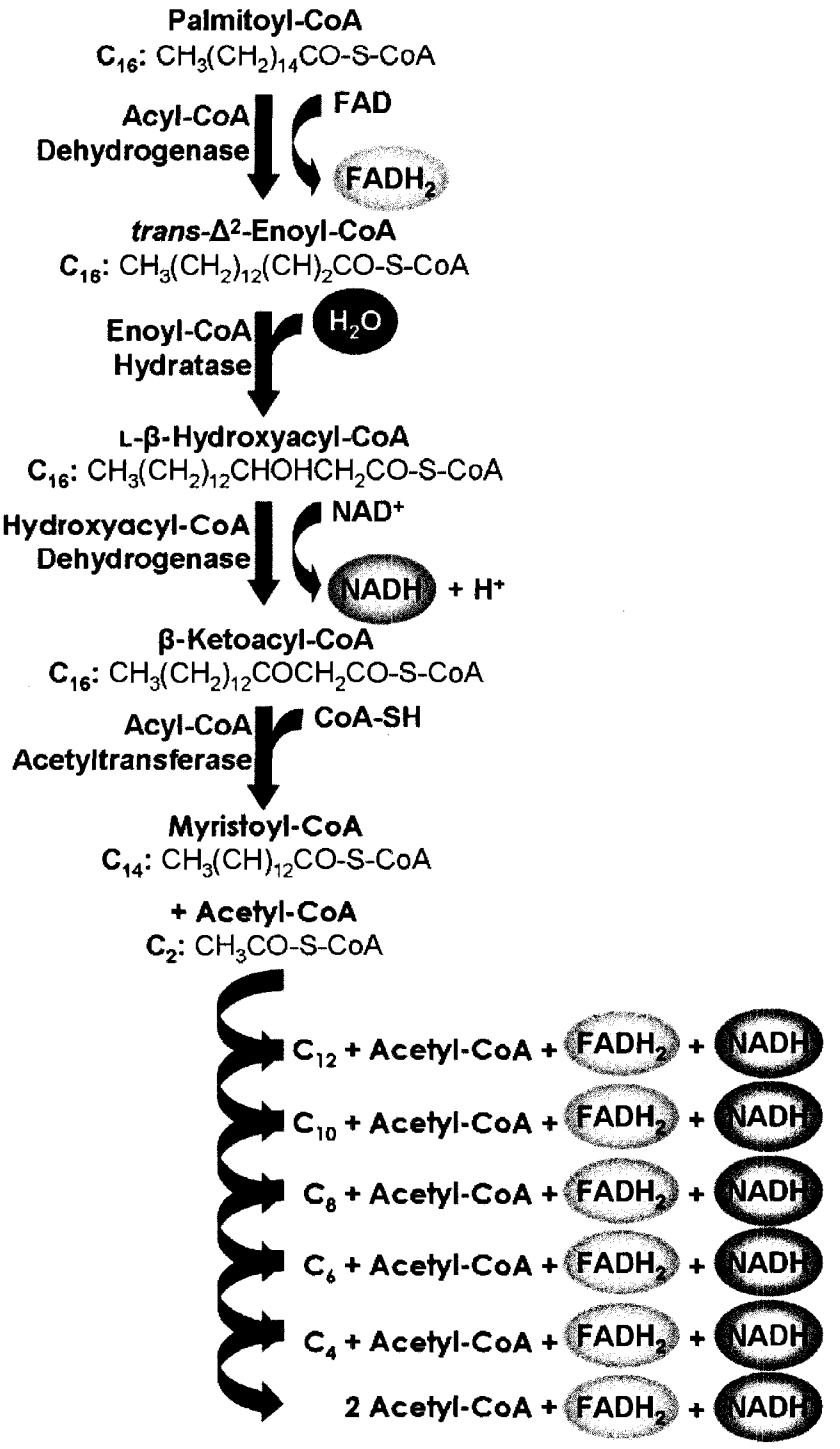

Figure 5: Beta-oxidation of palmitoyl-CoA (adapted from (103)). CoA-SH: coenzyme A; NADH: nicotinamide adenine dinucleotide (reduced); $FADH_2$: flavin adenine dinucleotide (reduced).

In most cases, energy contribution to the diet from alcohol is minimal compared to the other energy substrates, carbohydrate, lipid and protein. Alcohol (ethanol) is oxidized in the liver to acetaldehyde by alcohol dehydrogenase, and then converted to acetic acid by acetaldehyde dehydrogenase. The acetyl group from acetic acid is bound to coenzyme A to produce acetyl-CoA, which can then enter the TCA cycle for further oxidation.

The Role of Mitochondria in Energy Conversion

Mitochondria are often referred to as the 'powerhouses' of the cell as energy conversion to ATP takes place in these organelles. The mitochondrion is enclosed in two membranes: the outer more permeable membrane and the inner highly impermeable membrane. The mitochondrial inner membrane has many folds called cristae, allowing for a large membrane surface area in a small volume of space. Important metabolic processes such as beta-oxidation of fatty acids (Figure 5) and the TCA cycle (Figure 3) occur in the matrix at the interior of this organelle, whereas the ETC (Figure 4) is located on the inner membrane. A membrane potential is maintained across the inner membrane due to the efflux of protons by the ETC into the intermembrane space. This chemical potential energy is used to drive ATP synthesis as protons re-enter the matrix through ATP synthase (Figure 4). In

addition to these energy metabolic functions, mitochondria play a significant role in apoptosis and transient calcium storage.

Mitochondrial dysfunction is implicated in many disease states, including obesity, T2DM, Alzheimer's Disease, Parkinson's Disease and aging (reviewed in (112, 130)). The production of reactive oxygen species (ROS) at complexes I and III of the ETC can cause oxidative stress in high amounts, resulting in damage to mitochondrial DNA (mtDNA) and eventual cell death (reviewed in (112)). Type 2 diabetics as well as healthy offspring of individuals with T2DM have been consistently shown to have decreased mitochondrial content and oxidative capacity (87, 97, 98, 107).

Fuel Storage

Humans do not have to consume energy substrates continuously: storage mechanisms allow energy to be stockpiled for later use. Carbohydrate can be stored as glycogen in the liver (up to 10% of its weight) and in skeletal muscle (1-2% of its weight). During situations such as fasting, when blood glucose concentrations are low, glycogenolysis occurs in the liver releasing glucose back into the blood in order to fuel obligate glucose users such as the brain, the renal medulla and erythrocytes. Glycogenolysis can also occur in skeletal muscle, although the resulting glucose 6-phosphate molecules are not converted to glucose or released into the blood. They can enter

glycolysis and their energy can be extracted for use solely by the muscle. Carbohydrate is utilized as the preferential fuel in the postprandial state as well as during short-term vigorous exercise in skeletal muscle.

In humans, the amount of energy stored in the body as glycogen is relatively small compared to the amount stored as triglyceride (triacylglycerol). Fat content accounts for ~72% of the human body's energy content, whereas carbohydrate accounts for ~1% (protein accounts for ~27%) (43). Excess dietary carbohydrate is converted to acetyl-CoA, then to fatty acids, and then packaged as triglyceride for storage. Excess fatty acids are also stored as triglyceride primarily in adipose tissue, although ectopic storage of triglyceride can occur in the liver (166), the heart (17), the pancreas (153), the kidneys (36) and in skeletal muscle (109). The negative consequences associated with this phenomenon, known as 'lipotoxicity' (129, 152), is typically observed in obese subjects, although lipotoxicity in liver and skeletal muscle is more closely linked with insulin resistance (109, 166). Lipotoxicity is discussed in more detail in the 'Diabetes Mellitus' section of this General Introduction. Fatty acids (from triglyceride stores) are an important fuel substrates during fasting as well as during long-term aerobic exercise (44, 52).

Protein is not stored by the body for fuel: the carbon backbones of excess dietary amino acids are converted to ketone bodies via ketogenesis, or to

glucose via gluconeogenesis. The energy of dietary glucose can be stored as glycogen or converted to fatty acids and stored as triglyceride. Alcohol cannot be stored by the body either, and is therefore oxidized in the liver through a series of steps described above. Acetyl-CoA can be converted to fatty acid and then stored as triglyceride if it does not enter the TCA cycle for oxidation.

Energy Balance

The ability to store energy is essential for human life. Energy stores are drawn upon between meals in everyday life, and to a more extreme degree in situations of famine. Currently in developed countries, where food is easily and abundantly available, it is more likely for humans to be in a state of over-nutrition as opposed to under-nutrition. It is ideal for an individual to be in a state of energy homeostasis, or 'energy balance'. According to the energy balance equation (depicted as a scale in Figure 6), body weight will remain constant if energy consumption is equal to energy expenditure.

If energy expenditure exceeds energy intake and the scale is tipped downwards on the right, an individual will lose weight ('negative energy balance'). Conversely, and more commonly the case, if energy intake outweighs energy expenditure, the scale is tipped downwards on the left

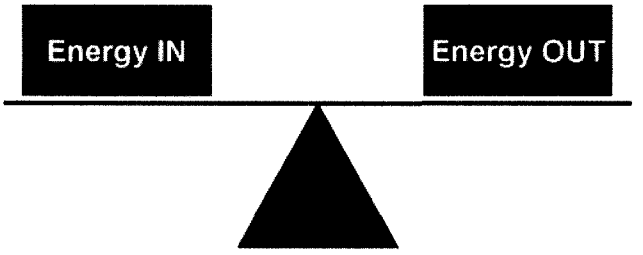

Figure 6: Energy balance. When energy consumption is equal to energy expenditure, body weight will remain constant.

and the individual will gain weight ('positive energy balance'). If an individual accumulates more body weight than is considered healthy for their height, they are classified as overweight or obese. The World Health Organization (WHO) defines overweight and obesity using the Body Mass Index (BMI). BMI is defined as the subject's weight (in kg) divided by their height (in meters, m) squared (kg/m^2). Table 1 provides BMI ranges for underweight, normal weight, overweight and obesity:

Obesity rates have been increasing worldwide at an alarming rate. According to Statistics Canada, in 2004 58.8% of Canadian adults were overweight or obese (35.4% overweight, 23.4% obese) and 26.3% of Canadian children aged 2 to 17 were overweight or obese (18.1% overweight, 8.2% obese) (142). Obesity is associated with cardiovascular disease, type 2 diabetes mellitus (T2DM) and certain cancers (reviewed in (76)). This state of energy disregulation can be caused by increased energy consumption (food intake), decreased energy expenditure, or a combination of the two. Both sides of the energy balance equation are influenced by genetic (117) and environmental factors (reviewed in (138)).

Classification	Body Mass Index (kg/m^2)
Underweight	<18.50
Normal Range	18.50 – 24.99
Overweight/Pre-Obese	25.00 – 29.99
Obese Class I	30.00 – 34.99
Obese Class II	35.00 – 39.99
Obese Class III	≥40.00

Table 1: World Health Organization Body Mass Index classifications (161, 162).

Energy Regulation

Energy Regulation at the Cellular Level

Energy homeostasis at the cellular level appears to be controlled by a 'master switch': adenosine monophosphate-activated protein kinase (AMPK). AMPK is ubiquitously expressed (16) and acts to maintain the energy status of the cell (54, 57). Appropriately also referred to as a 'fuel gauge' (56), AMPK is activated in response to metabolic stress such as muscle contraction, glucose deprivation, hypoxia or ischemia (58). When cellular ATP levels fall in response to these stresses, AMP levels rise as a result of the adenylate kinase reaction (165):

$$2\ ADP \rightarrow ATP + AMP$$

The kinase activity of AMPK is stimulated by direct binding of AMP to the regulatory gamma subunit, as well as by phosphorylation of threonine residue 172 within the kinase domain itself (60) by tumor suppressor LKB1 (59, 160) or calcium calmodulin-dependent kinase kinase-alpha/beta (CaMKKα, CaMKKβ) (61, 66, 159). AMPK is inactivated by high levels of ATP (27, 31), although the exact mechanism of this inhibition is not clear. A detailed introduction into AMPK's molecular structure and biochemical properties can be found in the Introduction of Chapter 1.

Upon activation, AMPK stimulates ATP-producing (catabolic) pathways (such as glycolysis and fatty acid oxidation) and inhibits ATP-consuming

(anabolic)pathways (such as glycogen synthesis and fatty acid synthesis) in order to restore the energy charge of the cell (reviewed in (53)). Downstream effects of AMPK activation are depicted in Figure 7.

Energy Regulation at the Whole Body Level

Interestingly, AMPK acts not only as a cellular energy sensor, but also to maintain whole body energy balance by influencing food intake in the hypothalamus (Figure 7B) (reviewed in (71)). Fasting (*i.e.*, low blood glucose levels) increases AMPK activity in the hypothalamus, increasing food intake, whereas re-feeding (*i.e.*, high glucose and insulin levels) decreases AMPK activity, eliciting the opposite effect (94). Ghrelin (originating from the gut) and neuropeptide agouti-related peptide are orexogenic peptides that stimulate AMPK activity in the hypothalamus, thereby stimulating appetite (5, 94). Conversely, the adipokine leptin acts in an anorexogenic fashion by increasing AMPK activity in the arcuate nucleus (ARC) and the paraventricular nucleus (PVN), partly through melanocortin 4 (MC4) receptor stimulation (94). AMPK therefore plays a role in whole body energy balance by increasing food intake and body weight upon its activation in the hypothalamus (5, 94) and by decreasing food intake and body weight upon its inhibition (73, 94).

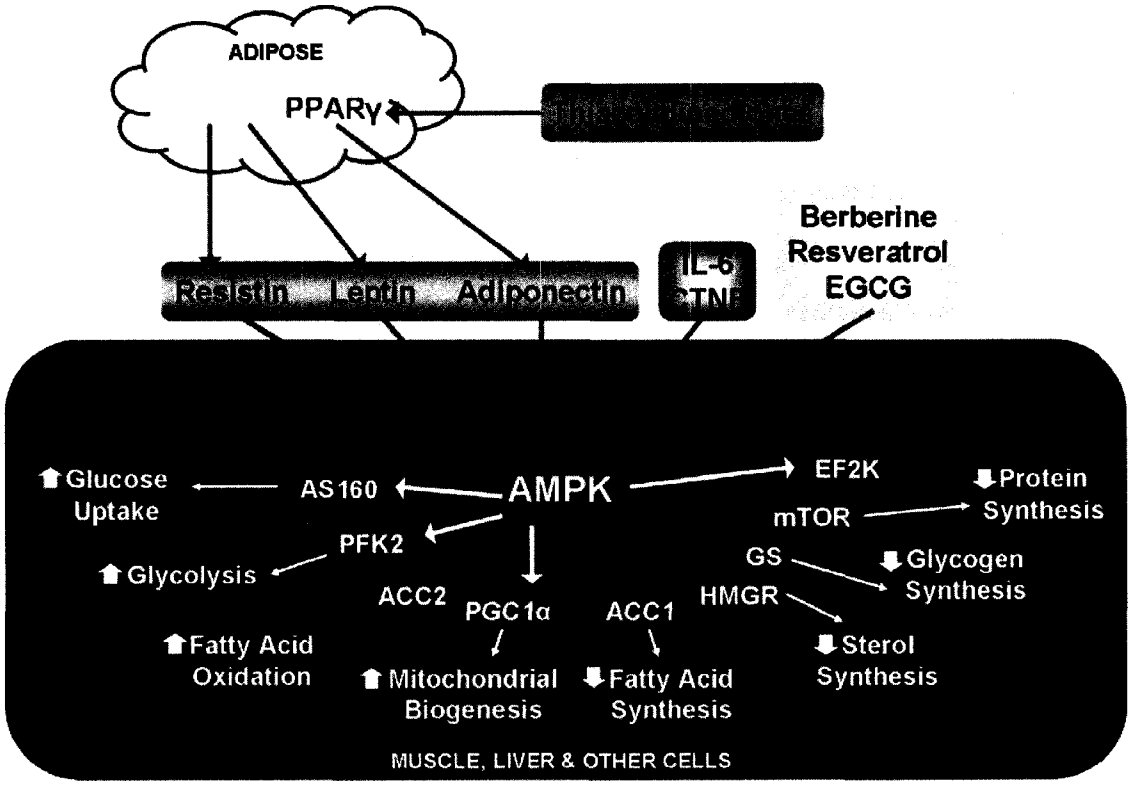

A

Figure 7A: Molecular activation and inhibition of AMPK; downstream effects of AMPK activation (adapted from (53)). PPARγ: peroxisome proliferator-activated receptor-γ; IL-6: interleukin-6; CTNF: ciliary neurotrophic factor; EGCG: (–)epigallocatechin-3-gallate; AS160: Akt/PKB substrate of 160 kDa; PFK2: 6-phosphofructo-2-kinase; ACC2: acetyl-coenzyme A carboxylase-2; PGC1α: PPARγco-activator-1α; ACC1: acetyl-coenzyme A carboxylase-1; HMGR: 3-hydroxy-3-methylglutaryl coenzyme A reductase; GS: glycogen synthase; mTOR: mammalian target of rapamycin; EF2K: elongation factor-2 kinase.

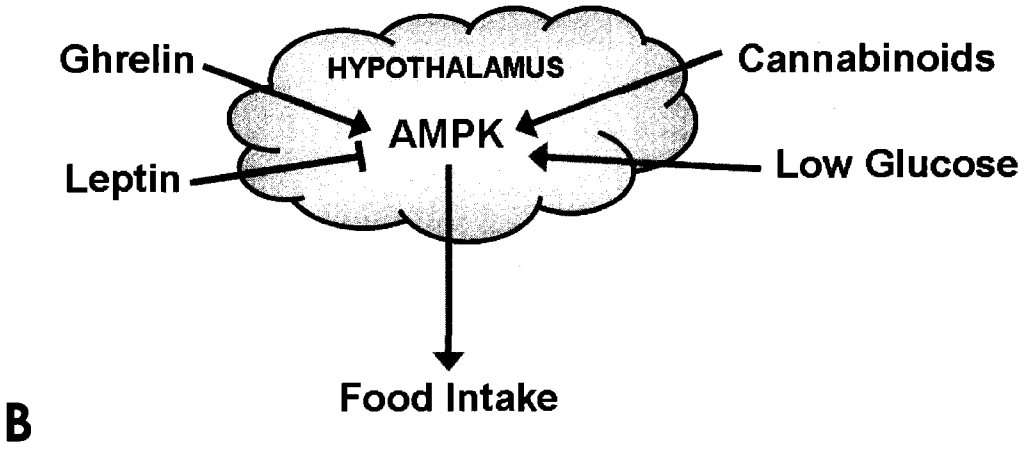

Figure 7B: Activation and downstream effects of AMPK in the hypothalamus (adapted from (53)).

Energy balance is normally very well regulated. In the current context in most societies of widely available palatable foods, however, regulatory mechanisms are being overridden. Recent research, beginning with the identification of leptin (168), has revealed that regulatory mechanisms are complex and that there are many players in the regulation of energy balance. The control of food intake occurs in the hypothalamus and involves several hypothalamic peptide systems (*e.g.*, neuropeptide Y (NPY), orexins, melanocortins, cocaine and amphetamine regulating transcript (CART), galanin/galanin like peptides (GALP) and endocannabinoids) (reviewed in (51)). Peripheral hormones released prior, during or following a meal, such as cholecystokinin (CCK), gastrin releasing peptides (GRP), glucagon-like peptide 1 (GLP-1), enterostatin, amylin, peptide YY (PYY), obestatin and ghrelin, control feelings of hunger and satiety as well as food intake (reviewed in (51)).

Diabetes Mellitus

There are two types of diabetes mellitus (DM): type 1 diabetes mellitus (T1DM), which accounts for approximately 10% of all DM worldwide, and type 2 diabetes mellitus (T2DM), which accounts for the other 90% (WHO). WHO estimates that over 180 million people currently have diabetes, and that this number will likely double by the year 2030. In Canada, more than 2

million individuals have DM and this number is expected to rise to over 3 million by the year 2010 (Canadian Diabetes Association, CDA).

Type 1 Diabetes Mellitus

T1DM is an autoimmune disease in which the immune system targets and destroys the insulin-producing beta cells in the Islets of Langerhans of the pancreas. The processes triggering T1DM are complex and still poorly understood (reviewed in (106)). As a result, individuals with T1DM are unable to produce insulin in response to high blood glucose levels and indefinitely must be regularly infused or injected with exogenous insulin. The onset of this disease is primarily in childhood and early adulthood, and has previously been termed 'early-onset' DM or 'insulin-dependent' DM.

Type 2 Diabetes Mellitus

T2DM is characterized by insulin resistance: the inability of insulin to stimulate peripheral glucose disposal and to inhibit hepatic glucose production (glycogenolysis and gluconeogenesis) (91). In the first stage of T2DM progression, often referred to as 'prediabetes', subjects paradoxically experience hyperglycemia as well as hyperinsulinemia: the pancreas is still able to sense high blood glucose levels and secrete insulin in response (91). The dysfunction lies at the level of the peripheral tissues: insulin is unable to stimulate glucose uptake (which occurs mainly in skeletal muscle) or to

suppress glucose production in the liver. In the later stages of T2DM, the beta cell fails and is unable to provide sufficient insulin in response to elevated glucose levels (91). The molecular pathogenesis of T2DM has not been fully elucidated; however, inroads have been made in our understanding of the development of insulin resistance, especially in skeletal muscle (reviewed in (99) and discussed below).

Skeletal Muscle: Energy Expenditure and Energy Substrate Storage

Skeletal muscle is a type of striated muscle having the primary function of contraction and body movement. In humans, skeletal muscle makes up approximately 42% of body weight and is responsible for 20% of energy expenditure at rest (122) (the latter percentage is greatly increased during exercise). Skeletal muscle is also responsible for 80% of postprandial peripheral glucose disposal (42). It is an insulin-sensitive tissue and therefore considered the major peripheral site of insulin resistance in T2DM (33).

Skeletal muscle is known to be a major site of glycogen storage in the body; however, it also stores lipid in the form of triglyceride. The amount of lipid stored in skeletal muscle (known as intramuscular triglyceride, IMTG, or intramyocellular lipid, IMCL) correlates very well with the degree of insulin resistance of the individual (80, 109, 111, 148, 158). Interestingly, increased IMTG stores are also observed in trained athletes without the accompanying

increase in insulin resistance. This paradox has not yet been fully explained, however, the lack of insulin resistance may be related to the higher fat oxidation to IMTG ratio in athletes compared to in sedentary individuals (reviewed in (154)).

In healthy muscle, insulin binds to the insulin receptor on the plasma membrane, initiating a cascade of intracellular signaling events to elicit the translocation of GLUT4-containing vesicles to the membrane, increasing the number of GLUT4 transporters on the membrane surface, allowing for increased glucose uptake into the cell (reviewed in (34)). The insulin signaling cascade begins with insulin binding to the alpha-subunit of the insulin receptor, activating the beta-subunit to tyrosine phosphorylate insulin receptor substrate-1 (IRS-1). These phosphorylated tyrosine residues recruit phosphatidylinositol-3-kinase (PI3K) into an active signaling complex which in turn catalyzes the phosphorylation of phosphatidylinositol (3,4)-bisphophate ($PI(3,4)P_2$) to phosphatidylinositol (3,4,5)-triphosphate ($PI(3,4,5)P_3$) at the plasma membrane. $PI(3,4,5)P_3$ recruits and binds protein kinase B (Akt/PKB), displacing its pleckstrin homology (PH) domain, allowing it to be phosphorylated by a protein complex containing mammalian target of rapamycin (mTOR) and Rictor, and by phosphoinositide dependent kinase-1 (PDK1). The details of the subsequent translocation of GLUT4-containing vesicles to the plasma membrane have not been fully elucidated, although

it is clear that the phosphorylation of Akt/PKB substrate of 160 kDa (AS160) by Akt/PKB is required (reviewed in (79, 99, 146) and illustrated in Figure 8).

Since trained athletes have high levels of IMTG but maintain insulin sensitivity, it cannot simply be the presence of excess IMTG that impedes the process of insulin-dependent glucose uptake. In the last few years it has become apparent that the accumulation of particular lipid species, specifically ceramides and diacylglycerol (DAG), interfere with insulin signaling in insulin-resistant individuals (reviewed in (99, 146)).

Skeletal muscle ceramide content as well as plasma ceramide by-product levels have been shown to be higher in insulin-resistant individuals compared to insulin-sensitive individuals (3, 48, 144). Ceramides interfere with a number of metabolic processes in the cell (reviewed in (146)). With respect to insulin signaling, ceramide activates protein phosphatase 2A (PP2A), which dephosphorylates and inactivates Akt/PKB (20, 125, 150, 173), thereby preventing GLUT4 translocation to the plasma membrane. Ceramide also activates protein kinase C-zeta (PKCζ), which phosphorylates tyrosine residue 34 in the PH-domain of Akt/PKB, preventing its translocation to the membrane and halting the insulin signaling pathway (114, 115) (illustrated in Figure 8).

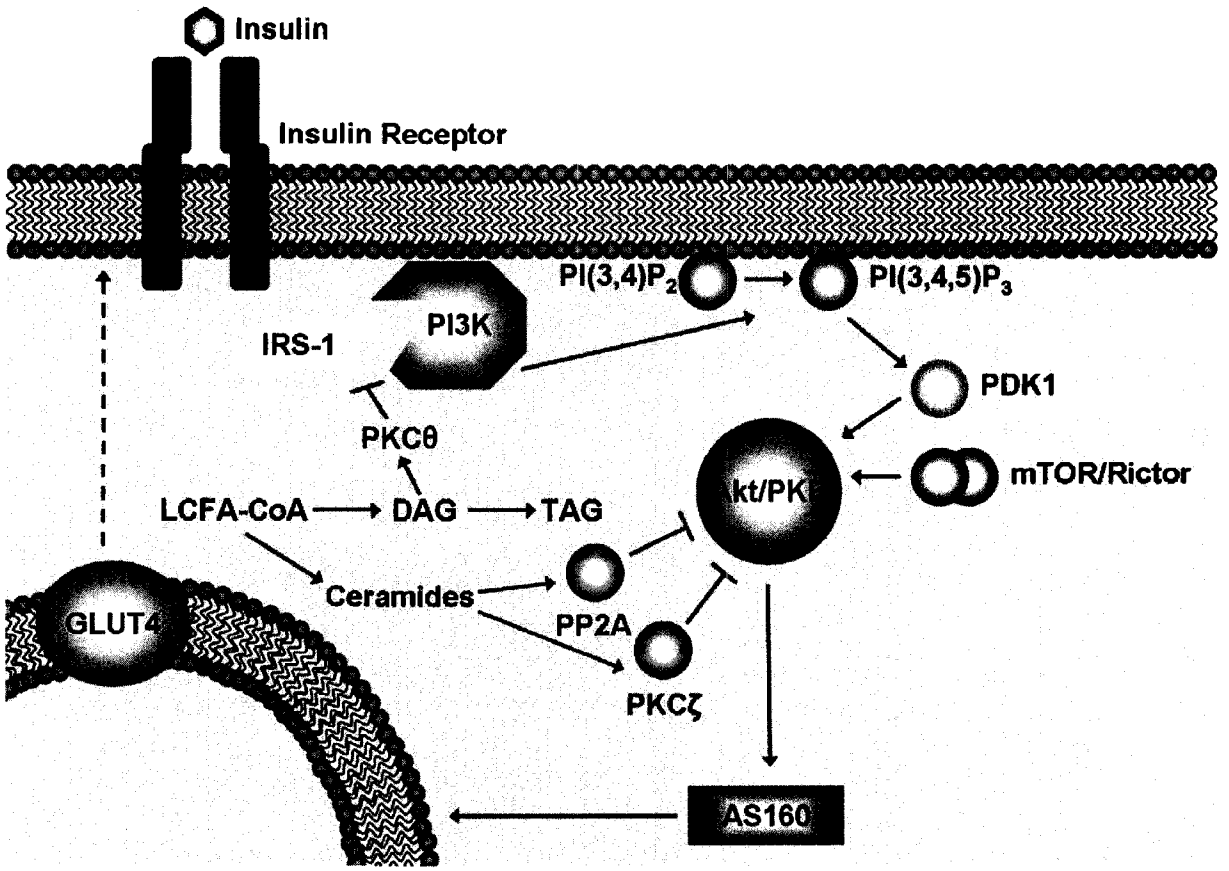

Figure 8: Interaction of ceramides and diacylglycerol in the insulin signalling pathway in skeletal muscle (adapted from (37, 99, 146)). IRS-1: insulin receptor substrate-1; PI3K: phosphatidylinositol-3-kinase; $PI(3,4)P_2$: phosphatidylinositol (3,4)-bisphophate; $PI(3,4,5)P_3$: phosphatidylinositol (3,4,5)-triphosphate; Akt/PKB: protein kinase B; AS160: Akt/PKB substrate of 160 kDa; GLUT4: glucose transporter 4; PDK1: phosphoinositide dependent kinase-1; mTOR: mammalian target of rapamycin; PKCζ: protein kinase C-zeta; PKCθ: protein kinase C-theta PP2A: protein phosphatase 2A; TAG: triacylglycerol (triglyceride); DAG: diacylglycerol; LCFA-CoA: long chain fatty acyl-coenzyme A.

Lipid-induced insulin resistance in humans results in increased DAG content in skeletal muscle and activated protein kinase C-theta (PKCθ) (67). There is evidence for DAG-activation of PKCθ in insulin-resistant subjects and subsequent serine phosphorylation of IRS-1, preventing its interaction with PI3K and further cellular insulin signaling, although the details of this pathway are not yet clear (4, 74, 84, 96, 98, 100, 167).

Skeletal muscle is made up of several different types of fibers, which have unique cellular and biochemical characteristics. There are two major classes of muscle fiber type, type 1 and type 2 (110, 118), as well as several sub-classes. Type 1 fibers, also called 'slow twitch', 'oxidative', 'slow-oxidative' or 'red' fibers, are characterized by their slow contraction time, small motor neuron, low force production, low glycolytic capacity, high resistance to fatigue, high mitochondrial content, high capillary density and high oxidative capacity (reviewed in (7, 134, 137)). These fibers rely on oxidative phosphorylation for ATP production and are typically recruited during longer term lower intensity aerobic activities (reviewed in (7, 134, 137)).

Type 2 fibers, also called 'fast twitch' fibers, have two well-characterized and quite distinct sub-classes: a and b (14, 50). Type 2a fibers, sometimes called 'fast-oxidative' or 'fast-oxidative-glycolytic' fibers, have a fast contraction time, large motor neuron, intermediate resistance to fatigue, intermediate

capillary density, high force production, high mitochondrial density, high oxidative capacity and high glycolytic capacity (reviewed in (7, 134, 137)). They tend to be recruited for longer term anaerobic activities (reviewed in (7, 134, 137)). Type 2b 'fast-glycolytic' fibers are characterized by a very fast contraction time, very large motor neuron, low resistance to fatigue, low mitochondrial density, low oxidative capacity, high glycolytic capacity and very high force output (reviewed in (7, 134, 137)). Type 1 fibers typically rely on stored triglyceride for fuel whereas type 2 fibers rely on stored glycogen and creatine-phosphate (reviewed in (7, 134, 137)). Type 2b fibers are also often referred to as type 2x fibers in the literature, but are in fact distinct from type 2b fibers. Muscle fibers originally identified as 2b in human skeletal muscle via myofibrillar adenosine triphosphatase (mATPase) staining were in fact later identified as type 2x fibers based on myosin heavy chain (MHC) isoform content (41, 136), and therefore ambiguity in the literature remains.

Type 1, type 2a and type 2b/x are considered the major classes of fiber in human skeletal muscle, however 3 additional classes have been identified: type 1c, type 2ab (also referred to as type 2ax (41, 136)) and type 2c (140). The human *vastus lateralis* is made up of 41% type 1 fibers, 1% type 1c fibers, 31% type 2a fibers, 6% type 2ab fibers, 20% type 2b fibers and 1% type 2c fibers, as determined by mATPase staining and MHC isoform content (141). A higher percentage of type 2b fibers and a lower percentage of type 1 fibers

are observed with obesity (2, 62, 78, 116, 149) and insulin resistance/T2DM (62, 78, 85, 90), however type 1 fiber percentage can be increased with exercise (reviewed in (172)), but not with weight loss alone (72). Maintaining a high percentage of type 1 fibers therefore appears to be essential for metabolic health, likely due to the high density of mitochondria and high oxidative capacity of these fibers.

Treatment of Energy Regulation Disorders

While overweight/obesity is an energy balance disorder, T2DM is a disorder of energy substrate management. These two energy regulation disorders are closely linked (19, 26, 35, 128). Overweight/obesity is an important risk factor for T2DM: according to the US Third National Health and Nutrition Examination Study (NHANES III), performed over the period of 1999 to 2002, 85.2% of adults diagnosed with T2DM were overweight or obese (30.4% overweight, 54.8% obese) (Center for Disease Control, CDC). Overweight/obesity is a risk factor for T2DM, and when excess weight is lost, subjects with T2DM can improve insulin sensitivity and glucose tolerance (47, 83).

Treatment of Obesity

As obesity is a disorder of energy balance, therapies must target either energy intake, energy expenditure, or both. According to The Obesity

Society's publication "The Practical Guide: Identification, Evaluation and Treatment of Overweight and Obesity in Adults" based on the "Guidelines on the Identification, Evaluation, and Treatment of Overweight and Obesity in Adults: Evidence Report" developed by the National Heart, Lung, and Blood Institute (NHLBI) Expert Panel (June 1998), therapies for the treatment of obesity include dietary modification, physical activity, behaviour therapy, pharmacotherapy, and weight loss surgery. It is recommended that obese subjects reduce their caloric intake by 500 to 1000 kcal per day, while maintaining a minimum daily intake of 800 kcal and losing a maximum of 2 pounds per week. Physical activity recommendations include moderate-intensity activities for 30 minutes on most, if not all, days of the week. A variety of behaviour modification strategies are recommended, including self-monitoring, stress management and social support. Sibutramine, an appetite suppressant targeting norepinephrine and serotonergic mechanisms in the brain, and orlistat, a pancreatic lipase inhibitor preventing fat uptake in the intestine, are approved in Canada for long-term weight loss. Weight loss surgery is an option only in cases of severe obesity.

The search for novel effective weight loss pharmacotherapies is ongoing. New treatments may target energy intake through endocrine/neuronal pathways of whole body energy regulation (as described above) or may target energy expenditure, likely in skeletal muscle or adipose tissue. An

active area of research and exciting potential treatment for obesity is the activation of the uncoupling of oxidative phosphorylation. When protons return to the mitochondrial matrix from the intermembrane space by any other means than through ATP synthase, the potential energy that is associated with their return is not captured as ATP and therefore lost as heat (23). Uncoupling in BAT is attributed to the original uncoupling protein, uncoupling protein-1 (UCP1) (102, 104). UCP1's activity is stimulated through sympathetic neural stimulation of adenylate kinase in brown adipocytes and the subsequent binding of fatty acids; the latter process is still poorly understood (46). The activation of UCP1 in BAT causes a dramatic increase in the leak of protons into the matrix, and subsequently in cellular oxygen consumption and heat production. However, although BAT may play a role in the prevention of obesity in rodents (88), adult humans have very small amounts of BAT, and therefore this may not be a realistic pharmaceutical target to increase whole body energy expenditure by significant amounts. A more promising mechanism for the increase of energy expenditure through UCP1 may be in the conversion of white adipose tissue (WAT) to BAT (49, 75), potentially achieved through pathways involving the beta-3 adrenergic receptor (β3 AR) (64), peroxisome proliferator-activated receptor-γ co-activator1-α (PGC1α) (163), FOXC2 (18), RIP140 (21, 22) or TLQP-21 (69) (reviewed in (28)).

Uncoupling in skeletal muscle can account for up to 50% of resting metabolic rate in this tissue (121, 123). Potential pharmaceutical targets for uncoupling in skeletal muscle, reviewed in Costford *et al.* 2007 (28), include the adenine nucleotide translocator (ANT) (12) and the activation of thyroid hormone (T3), possibly via kaempferol (KPF) (30). Uncoupling protein-3 (UCP3), a UCP1 homologue, was identified in 1997 and shown to be expressed highly selectively in skeletal muscle and at low levels in BAT (10, 155). Although the identification of the UCP1 protein and its function were determined (102, 104) prior to the identification of its gene (11, 68, 77), the identification of UCP3's gene has preceded the elucidation of its physiological function. Although it was originally hypothesized to be responsible for proton leak reactions in muscle, its physiological function has yet to be determined. UCP3 is upregulated in response to fasting (9, 93, 157) and acute exercise (132, 151), which are situations of energy deficit and therefore inconsistent with the hypothesis that UCP3 acts to 'waste' energy as an uncoupler of oxidative phosphorylation. UCP3 has also been shown to be upregulated in response to a high fat diet (126, 127). These observations led to two hypotheses for the function of UCP3: as a fatty acid effluxor during high rates of beta-oxidation (65) or as a fatty acid translocator in situations of fatty acid surplus in the mitochondrion (133). More recently, UCP3 has been implicated in the protection from ROS and oxidative damage in the mitochondria, eliciting another hypothesis involving UCP3 mediating an inducible proton leak (38-

40). The details surrounding the search for UCP3's function are discussed in the Introductions of Chapters 2 and 3 (and have been recently reviewed by Bezaire *et al.* 2007 and Costford *et al.* 2007 (8, 29)).

Treatment of Type 2 Diabetes Mellitus

The American Diabetes Association Standards of Medical Care in Diabetes 2008 (1) recommend treatment in the areas of medical nutrition therapy (MNT) (including weight loss/management), diabetes self-management education (DSME), physical activity (150 min/week of moderate to intense activity and resistance training 3 times/week), hypertension and dyslipidemia treatment (if applicable) through pharmacotherapy (*e.g.*, angiotensin-converting enzyme (ACE) inhibitors and statins, respectively), smoking cessation and cardiovascular disease (CVD) treatment (*e.g.*, metformin and thiazolidinediones (TZD)) (1). Metformin, a biguanide drug commonly prescribed to type 2 diabetics to improve glucose uptake, has been shown to indirectly activate AMPK (135, 169). Rosiglitazone and pioglitazone, both belonging to the TZD class of drugs and widely prescribed to type 2 diabetics, have also been shown to indirectly activate AMPK (45, 124). AMPK is a logical target for treatment of T2DM as AMPK increases GLUT4 translocation to the plasma membrane and glucose disposal in an insulin-independent fashion (81). Interestingly, AMPK activation during exercise has been shown to be reduced in subjects who are obese or who have T2DM

(139). A recent report revealed that patients treated with rosiglitazone have a slightly elevated risk of death from a cardiovascular event (105). This may be due to the effects of increasing AMPK activity in the heart: certain mutations in the gamma-2 subunit of AMPK lead to increased AMPK activity, glycogen accumulation in the heart and Wolff-Parkinson-White syndrome (discussed further in the introduction of Chapter 1 and reviewed in (55)). Additionally, activation of AMPK in the hypothalamus causes increased food intake (reviewed in (71)), therefore non-specific activation of AMPK in obese/T2DM patients is not ideal. A better approach would be to pharmacologically target AMPK for activation in specific tissues, such as skeletal muscle.

AMPK-Activated Protein Kinase and Uncoupling Protein-3

Electrically induced contractions in skeletal muscle have been shown to increase both AMPK activity and UCP3 mRNA (6, 108, 170). Upregulation of UCP3 mRNA can also be achieved by either acute or chronic treatment with 5-aminoimidazole-4-carboxamid-ribosid (AICAR), an established activator of AMPK (108, 143, 147, 170). Additionally, mice overexpressing UCP3 have been shown to have increased AMPK activity (131), whereas the AMPK-alpha-2 knockout mouse has decreased UCP3 mRNA expression (13, 70). Brauner *et al.* also found a correlation between UCP3 mRNA expression and alpha-2-AMPK expression in skeletal muscle of preterm newborn humans (13).

The previous studies looked at UCP3 transcript levels only, however, de Lange *et al.* recently showed increased phosphorylation of AMPK and ACC as well as increased UCP3 protein levels in rat skeletal muscle following food deprivation (32). These observations have led to the hypothesis that AMPK may control UCP3 expression. As AMPK is activated in situations of decreased cellular energy status and UCP3 expression is increased in situations where fatty acid metabolism is relied upon, it is an attractive association. However, the association is correlative at this stage. Further investigation into the molecular regulation of UCP3 by AMPK is required.

Summary

As energy regulation disorders such as obesity and T2DM become more and more prevalent in our society, the importance of research into the basic mechanisms of energy management by the human body increases. Our understanding of the integration of these pathways precludes our ability to develop novel therapies for these disorders. The next three chapters of this thesis describe the identification of the first naturally occurring gain-of-function mutation in the gamma-3 subunit of AMPK in humans, the effects of over- and under-expression of UCP3 in rodents, and the implications of each for obesity and T2DM.

References

1. 2008. Standards of medical care in diabetes--2008. Diabetes Care **31 Suppl 1:**S12-54.

2. **Abou Mrad, J., F. Yakubu, D. Lin, J. C. Peters, J. B. Atkinson, and J. O. Hill.** 1992. Skeletal muscle composition in dietary obesity-susceptible and dietary obesity-resistant rats. Am J Physiol **262:**R684-8.

3. **Adams, J. M., 2nd, T. Pratipanawatr, R. Berria, E. Wang, R. A. DeFronzo, M. C. Sullards, and L. J. Mandarino.** 2004. Ceramide content is increased in skeletal muscle from obese insulin-resistant humans. Diabetes **53:**25-31.

4. **Aguirre, V., E. D. Werner, J. Giraud, Y. H. Lee, S. E. Shoelson, and M. F. White.** 2002. Phosphorylation of Ser307 in insulin receptor substrate-1 blocks interactions with the insulin receptor and inhibits insulin action. J Biol Chem **277:**1531-7.

5. **Andersson, U., K. Filipsson, C. R. Abbott, A. Woods, K. Smith, S. R. Bloom, D. Carling, and C. J. Small.** 2004. AMP-activated protein kinase plays a role in the control of food intake. J Biol Chem **279:**12005-8.

6. **Atherton, P. J., J. Babraj, K. Smith, J. Singh, M. J. Rennie, and H. Wackerhage.** 2005. Selective activation of AMPK-PGC-1alpha or PKB-TSC2-mTOR signaling can explain specific adaptive responses to endurance or resistance training-like electrical muscle stimulation. Faseb J **19:**786-8.

7. **Baldwin, K. M., and F. Haddad.** 2001. Effects of different activity and inactivity paradigms on myosin heavy chain gene expression in striated muscle. J Appl Physiol **90:**345-57.

8. **Bezaire, V., E. L. Seifert, and M. E. Harper.** 2007. Uncoupling protein-3: clues in an ongoing mitochondrial mystery. Faseb J **21:**312-24.

9. **Boss, O., S. Samec, F. Kuhne, P. Bijlenga, F. Assimacopoulos-Jeannet, J. Seydoux, J. P. Giacobino, and P. Muzzin.** 1998. Uncoupling protein-3 expression in rodent skeletal muscle is modulated by food intake but not by changes in environmental temperature. J Biol Chem **273:**5-8.

10. **Boss, O., S. Samec, A. Paoloni-Giacobino, C. Rossier, A. Dulloo, J. Seydoux, P. Muzzin, and J. P. Giacobino.** 1997. Uncoupling protein-3: a new member of the mitochondrial carrier family with tissue-specific expression. FEBS Lett **408:**39-42.

11. **Bouillaud, F., D. Ricquier, J. Thibault, and J. Weissenbach.** 1985. Molecular approach to thermogenesis in brown adipose tissue: cDNA cloning of the mitochondrial uncoupling protein. Proc Natl Acad Sci U S A **82:**445-8.

12. **Brand, M. D., J. L. Pakay, A. Ocloo, J. Kokoszka, D. C. Wallace, P. S. Brookes, and E. J. Cornwall.** 2005. The basal proton conductance of mitochondria depends on adenine nucleotide translocase content. Biochem J **392:**353-62.

13. **Brauner, P., P. Kopecky, P. Flachs, O. Kuda, J. Vorlicek, L. Planickova, I. Vitkova, F. Andreelli, M. Foretz, B. Viollet, and J. Kopecky.** 2006. Expression of uncoupling protein 3 and GLUT4 gene in skeletal muscle of preterm newborns: possible control by AMP-activated protein kinase. Pediatr Res **60:**569-75.

14. **Brooke, M. H., and K. K. Kaiser.** 1970. Muscle fiber types: how many and what kind? Arch Neurol **23:**369-79.

15. **Cannon, B., and J. Nedergaard.** 2004. Brown adipose tissue: function and physiological significance. Physiol Rev **84:**277-359.

16. **Carling, D.** 2004. The AMP-activated protein kinase cascade--a unifying system for energy control. Trends Biochem Sci **29:**18-24.

17. **Carroll, J. F., T. M. Dwyer, A. W. Grady, G. A. Reinhart, J. P. Montani, K. Cockrell, E. F. Meydrech, and H. L. Mizelle.** 1996. Hypertension, cardiac hypertrophy, and neurohumoral activity in a new animal model of obesity. Am J Physiol **271:**H373-8.

18. **Cederberg, A., L. M. Gronning, B. Ahren, K. Tasken, P. Carlsson, and S. Enerback.** 2001. FOXC2 is a winged helix gene that counteracts obesity, hypertriglyceridemia, and diet-induced insulin resistance. Cell **106:**563-73.

19. **Chan, J. M., E. B. Rimm, G. A. Colditz, M. J. Stampfer, and W. C. Willett.** 1994. Obesity, fat distribution, and weight gain as risk factors for clinical diabetes in men. Diabetes Care **17:**961-9.

20. **Chavez, J. A., T. A. Knotts, L. P. Wang, G. Li, R. T. Dobrowsky, G. L. Florant, and S. A. Summers.** 2003. A role for ceramide, but not diacylglycerol, in the antagonism of insulin signal transduction by saturated fatty acids. J Biol Chem **278:**10297-303.

21. **Christian, M., E. Kiskinis, D. Debevec, G. Leonardsson, R. White, and M. G. Parker.** 2005. RIP140-targeted repression of gene expression in adipocytes. Mol Cell Biol **25:**9383-91.

22. **Christian, M., R. White, and M. G. Parker.** 2006. Metabolic regulation by the nuclear receptor corepressor RIP140. Trends Endocrinol Metab **17:**243-50.

23. **Christiansen, E. N., J. I. Pedersen, and H. J. Grav.** 1969. Uncoupling and recoupling of oxidative phosphorylation in brown adipose tissue mitochondria. Nature **222:**857-60.

24. **Clausius, R. J. E.** 1851. On the Moving Force of Heat and the Laws of Heat which may be Deduced Therefrom. Philosophical Magazine **2:**1–21, 102–119.

25. **Clausius, R. J. E.** 1850. Über die bewegende Kraft der Wärme. Annalen der Physik **79:**368–397, 500–524.

26. **Colditz, G. A., W. C. Willett, A. Rotnitzky, and J. E. Manson.** 1995. Weight gain as a risk factor for clinical diabetes mellitus in women. Ann Intern Med **122:**481-6.

27. **Corton, J. M., J. G. Gillespie, S. A. Hawley, and D. G. Hardie.** 1995. 5-aminoimidazole-4-carboxamide ribonucleoside. A specific method for activating AMP-activated protein kinase in intact cells? Eur J Biochem **229:**558-65.

28. **Costford, S., A. Gowing, and M. E. Harper.** 2007. Mitochondrial uncoupling as a target in the treatment of obesity. Curr Opin Clin Nutr Metab Care **10:**671-8.

29. **Costford, S. R., E. L. Seifert, V. Bezaire, F. G. M, L. Bevilacqua, A. Gowing, and M. E. Harper.** 2007. The energetic implications of uncoupling protein-3 in skeletal muscle. Appl Physiol Nutr Metab **32:**884-894.

30. **da-Silva, W. S., J. W. Harney, B. W. Kim, J. Li, S. D. Bianco, A. Crescenzi, M. A. Christoffolete, S. A. Huang, and A. C. Bianco.** 2007. The small polyphenolic molecule kaempferol increases cellular energy expenditure and thyroid hormone activation. Diabetes **56:**767-76.

31. **Davies, S. P., N. R. Helps, P. T. Cohen, and D. G. Hardie.** 1995. 5'-AMP inhibits dephosphorylation, as well as promoting phosphorylation, of the AMP-activated protein kinase. Studies using bacterially expressed human protein phosphatase-2C alpha and native bovine protein phosphatase-2AC. FEBS Lett **377:**421-5.

32. **de Lange, P., M. Moreno, E. Silvestri, A. Lombardi, F. Goglia, and A. Lanni.** 2007. Fuel economy in food-deprived skeletal muscle: signaling pathways and regulatory mechanisms. Faseb J **21:**3431-41.

33. **DeFronzo, R. A., R. Gunnarsson, O. Bjorkman, M. Olsson, and J. Wahren.** 1985. Effects of insulin on peripheral and splanchnic glucose metabolism in noninsulin-dependent (type II) diabetes mellitus. J Clin Invest **76:**149-55.

34. **Dugani, C. B., and A. Klip.** 2005. Glucose transporter 4: cycling, compartments and controversies. EMBO Rep **6:**1137-42.

35. **Dunstan, D. W., P. Z. Zimmet, T. A. Welborn, M. P. De Courten, A. J. Cameron, R. A. Sicree, T. Dwyer, S. Colagiuri, D. Jolley, M. Knuiman, R. Atkins, and J. E. Shaw.** 2002. The rising prevalence of diabetes and impaired glucose tolerance: the Australian Diabetes, Obesity and Lifestyle Study. Diabetes Care **25:**829-34.

36. **Dwyer, T. M., H. L. Mizelle, K. Cockrell, and P. Buhner.** 1995. Renal sinus lipomatosis and body composition in hypertensive, obese rabbits. Int J Obes Relat Metab Disord **19:**869-74.

37. **Dyck, D. J., G. J. Heigenhauser, and C. R. Bruce.** 2006. The role of adipokines as regulators of skeletal muscle fatty acid metabolism and insulin sensitivity. Acta Physiol (Oxf) **186:**5-16.

38. **Echtay, K. S., T. C. Esteves, J. L. Pakay, M. B. Jekabsons, A. J. Lambert, M. Portero-Otin, R. Pamplona, A. J. Vidal-Puig, S. Wang, S. J. Roebuck, and M. D. Brand.** 2003. A signalling role for 4-hydroxy-2-nonenal in regulation of mitochondrial uncoupling. Embo J **22:**4103-10.

39. **Echtay, K. S., M. P. Murphy, R. A. Smith, D. A. Talbot, and M. D. Brand.** 2002. Superoxide activates mitochondrial uncoupling protein 2 from the matrix side. Studies using targeted antioxidants. J Biol Chem **277:**47129-35.

40. **Echtay, K. S., D. Roussel, J. St-Pierre, M. B. Jekabsons, S. Cadenas, J. A. Stuart, J. A. Harper, S. J. Roebuck, A. Morrison, S. Pickering, J. C. Clapham, and M. D. Brand.** 2002. Superoxide activates mitochondrial uncoupling proteins. Nature **415:**96-9.

41. **Ennion, S., J. Sant'ana Pereira, A. J. Sargeant, A. Young, and G. Goldspink.** 1995. Characterization of human skeletal muscle fibres according to the myosin heavy chains they express. J Muscle Res Cell Motil **16:**35-43.

42. **Ferrannini, E., J. D. Smith, C. Cobelli, G. Toffolo, A. Pilo, and R. A. DeFronzo.** 1985. Effect of insulin on the distribution and disposition of glucose in man. J Clin Invest **76:**357-64.

43. **Frayn, K. N.** 1996. Metabolic Regulation: A Human Persective. Portland Press Ltd, London.

44. **Friedlander, A. L., G. A. Casazza, M. A. Horning, T. F. Buddinger, and G. A. Brooks.** 1998. Effects of exercise intensity and training on lipid metabolism in young women. Am J Physiol **275:**E853-63.

45. **Fryer, L. G., A. Parbu-Patel, and D. Carling.** 2002. The Anti-diabetic drugs rosiglitazone and metformin stimulate AMP-activated protein kinase through distinct signaling pathways. J Biol Chem **277:**25226-32.

46. **Gonzalez-Barroso, M. M., C. Fleury, F. Bouillaud, D. G. Nicholls, and E. Rial.** 1998. The uncoupling protein UCP1 does not increase the proton conductance of the inner mitochondrial membrane by functioning as a fatty acid anion transporter. J Biol Chem **273:**15528-32.

47. **Goodpaster, B. H., D. E. Kelley, R. R. Wing, A. Meier, and F. L. Thaete.** 1999. Effects of weight loss on regional fat distribution and insulin sensitivity in obesity. Diabetes **48:**839-47.

48. **Gorska, M., A. Dobrzyn, and M. Baranowski.** 2005. Concentrations of sphingosine and sphinganine in plasma of patients with type 2 diabetes. Med Sci Monit **11:**CR35-8.

49. **Guerra, C., R. A. Koza, H. Yamashita, K. Walsh, and L. P. Kozak.** 1998. Emergence of brown adipocytes in white fat in mice is under genetic control. Effects on body weight and adiposity. J Clin Invest **102:**412-20.

50. **Guth, L., and F. J. Samaha.** 1969. Qualitative differences between actomyosin ATPase of slow and fast mammalian muscle. Exp Neurol **25:**138-52.

51. **Halford, J. C., G. D. Cooper, and T. M. Dovey.** 2004. The pharmacology of human appetite expression. Curr Drug Targets **5:**221-40.

52. **Haman, F., F. Peronnet, G. P. Kenny, E. Doucet, D. Massicotte, C. Lavoie, and J. M. Weber.** 2004. Effects of carbohydrate availability on sustained shivering I. Oxidation of plasma glucose, muscle glycogen, and proteins. J Appl Physiol **96:**32-40.

53. **Hardie, D. G.** 2007. AMP-activated/SNF1 protein kinases: conserved guardians of cellular energy. Nat Rev Mol Cell Biol **8:**774-85.

54. **Hardie, D. G.** 1994. An emerging role for protein kinases: the response to nutritional and environmental stress. Cell Signal **6:**813-21.

55. **Hardie, D. G.** 2008. Role of AMP-activated protein kinase in the metabolic syndrome and in heart disease. FEBS Lett **582:**81-9.

56. **Hardie, D. G., and D. Carling.** 1997. The AMP-activated protein kinase--fuel gauge of the mammalian cell? Eur J Biochem **246:**259-73.

57. **Hardie, D. G., D. Carling, and N. Halford.** 1994. Roles of the Snf1/Rkin1/AMP-activated protein kinase family in the response to environmental and nutritional stress. Semin Cell Biol **5:**409-16.

58. **Hardie, D. G., S. A. Hawley, and J. W. Scott.** 2006. AMP-activated protein kinase--development of the energy sensor concept. J Physiol **574:**7-15.

59. **Hawley, S. A., J. Boudeau, J. L. Reid, K. J. Mustard, L. Udd, T. P. Makela, D. R. Alessi, and D. G. Hardie.** 2003. Complexes between the LKB1 tumor suppressor, STRAD alpha/beta and MO25 alpha/beta are upstream kinases in the AMP-activated protein kinase cascade. J Biol **2:**28.

60. **Hawley, S. A., M. Davison, A. Woods, S. P. Davies, R. K. Beri, D. Carling, and D. G. Hardie.** 1996. Characterization of the AMP-activated protein kinase kinase from rat liver and identification of threonine 172 as the major site at which it phosphorylates AMP-activated protein kinase. J Biol Chem **271:**27879-87.

61. **Hawley, S. A., D. A. Pan, K. J. Mustard, L. Ross, J. Bain, A. M. Edelman, B. G. Frenguelli, and D. G. Hardie.** 2005. Calmodulin-dependent protein kinase kinase-beta is an alternative upstream kinase for AMP-activated protein kinase. Cell Metab **2:**9-19.

62. **Hickey, M. S., J. O. Carey, J. L. Azevedo, J. A. Houmard, W. J. Pories, R. G. Israel, and G. L. Dohm.** 1995. Skeletal muscle fiber composition is related to adiposity and in vitro glucose transport rate in humans. Am J Physiol **268:**E453-7.

63. **Himms-Hagen, J.** 1985. Brown adipose tissue metabolism and thermogenesis. Annu Rev Nutr **5:**69-94.

64. **Himms-Hagen, J., J. Cui, E. Danforth, Jr., D. J. Taatjes, S. S. Lang, B. L. Waters, and T. H. Claus.** 1994. Effect of CL-316,243, a thermogenic beta 3-agonist, on energy balance and brown and white adipose tissues in rats. Am J Physiol **266:**R1371-82.

65. **Himms-Hagen, J., and M. E. Harper.** 2001. Physiological role of UCP3 may be export of fatty acids from mitochondria when fatty acid oxidation predominates: an hypothesis. Exp Biol Med (Maywood) **226:**78-84.

66. **Hurley, R. L., K. A. Anderson, J. M. Franzone, B. E. Kemp, A. R. Means, and L. A. Witters.** 2005. The Ca2+/calmodulin-dependent protein kinase kinases are AMP-activated protein kinase kinases. J Biol Chem **280:**29060-6.

67. **Itani, S. I., N. B. Ruderman, F. Schmieder, and G. Boden.** 2002. Lipid-induced insulin resistance in human muscle is associated with changes in diacylglycerol, protein kinase C, and IkappaB-alpha. Diabetes **51:**2005-11.

68. **Jacobsson, A., U. Stadler, M. A. Glotzer, and L. P. Kozak.** 1985. Mitochondrial uncoupling protein from mouse brown fat. Molecular cloning, genetic mapping, and mRNA expression. J Biol Chem **260:**16250-4.

69. **Jethwa, P. H., A. Warner, K. N. Nilaweera, J. M. Brameld, J. W. Keyte, W. G. Carter, N. Bolton, M. Bruggraber, P. J. Morgan, P. Barrett, and F. J.**

Ebling. 2007. VGF-derived peptide, TLQP-21, regulates food intake and body weight in Siberian hamsters. Endocrinology **148:**4044-55.

70. **Jorgensen, S. B., J. F. Wojtaszewski, B. Viollet, F. Andreelli, J. B. Birk, Y. Hellsten, P. Schjerling, S. Vaulont, P. D. Neufer, E. A. Richter, and H. Pilegaard.** 2005. Effects of alpha-AMPK knockout on exercise-induced gene activation in mouse skeletal muscle. Faseb J **19:**1146-8.

71. **Kahn, B. B., T. Alquier, D. Carling, and D. G. Hardie.** 2005. AMP-activated protein kinase: ancient energy gauge provides clues to modern understanding of metabolism. Cell Metab **1:**15-25.

72. **Kern, P. A., R. B. Simsolo, and M. Fournier.** 1999. Effect of weight loss on muscle fiber type, fiber size, capillarity, and succinate dehydrogenase activity in humans. J Clin Endocrinol Metab **84:**4185-90.

73. **Kim, E. K., I. Miller, S. Aja, L. E. Landree, M. Pinn, J. McFadden, F. P. Kuhajda, T. H. Moran, and G. V. Ronnett.** 2004. C75, a fatty acid synthase inhibitor, reduces food intake via hypothalamic AMP-activated protein kinase. J Biol Chem **279:**19970-6.

74. **Kim, J. K., J. J. Fillmore, M. J. Sunshine, B. Albrecht, T. Higashimori, D. W. Kim, Z. X. Liu, T. J. Soos, G. W. Cline, W. R. O'Brien, D. R. Littman, and G. I. Shulman.** 2004. PKC-theta knockout mice are protected from fat-induced insulin resistance. J Clin Invest **114:**823-7.

75. **Kopecky, J., G. Clarke, S. Enerback, B. Spiegelman, and L. P. Kozak.** 1995. Expression of the mitochondrial uncoupling protein gene from the aP2 gene promoter prevents genetic obesity. J Clin Invest **96:**2914-23.

76. **Kopelman, P. G.** 2000. Obesity as a medical problem. Nature **404:**635-43.

77. **Kozak, L. P., J. H. Britton, U. C. Kozak, and J. M. Wells.** 1988. The mitochondrial uncoupling protein gene. Correlation of exon structure to transmembrane domains. J Biol Chem **263:**12274-7.

78. **Kriketos, A. D., D. A. Pan, S. Lillioja, G. J. Cooney, L. A. Baur, M. R. Milner, J. R. Sutton, A. B. Jenkins, C. Bogardus, and L. H. Storlien.** 1996. Interrelationships between muscle morphology, insulin action, and adiposity. Am J Physiol **270:**R1332-9.

79. **Krook, A., H. Wallberg-Henriksson, and J. R. Zierath.** 2004. Sending the signal: molecular mechanisms regulating glucose uptake. Med Sci Sports Exerc **36:**1212-7.

80. **Krssak, M., K. Falk Petersen, A. Dresner, L. DiPietro, S. M. Vogel, D. L. Rothman, M. Roden, and G. I. Shulman.** 1999. Intramyocellular lipid

concentrations are correlated with insulin sensitivity in humans: a 1H NMR spectroscopy study. Diabetologia **42:**113-6.

81. **Kurth-Kraczek, E. J., M. F. Hirshman, L. J. Goodyear, and W. W. Winder.** 1999. 5' AMP-activated protein kinase activation causes GLUT4 translocation in skeletal muscle. Diabetes **48:**1667-71.

82. **Lee, A. D., P. A. Hansen, and J. O. Holloszy.** 1995. Wortmannin inhibits insulin-stimulated but not contraction-stimulated glucose transport activity in skeletal muscle. FEBS Lett **361:**51-4.

83. **Lemieux, S., D. Prud'homme, A. Nadeau, A. Tremblay, C. Bouchard, and J. P. Despres.** 1996. Seven-year changes in body fat and visceral adipose tissue in women. Association with indexes of plasma glucose-insulin homeostasis. Diabetes Care **19:**983-91.

84. **Li, J., K. DeFea, and R. A. Roth.** 1999. Modulation of insulin receptor substrate-1 tyrosine phosphorylation by an Akt/phosphatidylinositol 3-kinase pathway. J Biol Chem **274:**9351-6.

85. **Lillioja, S., A. A. Young, C. L. Culter, J. L. Ivy, W. G. Abbott, J. K. Zawadzki, H. Yki-Jarvinen, L. Christin, T. W. Secomb, and C. Bogardus.** 1987. Skeletal muscle capillary density and fiber type are possible determinants of in vivo insulin resistance in man. J Clin Invest **80:**415-24.

86. **Loomis, W. F., and F. Lipmann.** 1948. Reversible inhibition of the coupling between phosphorylation and oxidation. J Biol Chem **173:**807.

87. **Lowell, B. B., and G. I. Shulman.** 2005. Mitochondrial dysfunction and type 2 diabetes. Science **307:**384-7.

88. **Lowell, B. B., S. S. V, A. Hamann, J. A. Lawitts, J. Himms-Hagen, B. B. Boyer, L. P. Kozak, and J. S. Flier.** 1993. Development of obesity in transgenic mice after genetic ablation of brown adipose tissue. Nature **366:**740-2.

89. **Lund, S., G. D. Holman, O. Schmitz, and O. Pedersen.** 1995. Contraction stimulates translocation of glucose transporter GLUT4 in skeletal muscle through a mechanism distinct from that of insulin. Proc Natl Acad Sci U S A **92:**5817-21.

90. **Marin, P., B. Andersson, M. Krotkiewski, and P. Bjorntorp.** 1994. Muscle fiber composition and capillary density in women and men with NIDDM. Diabetes Care **17:**382-6.

91. **McGarry, J. D.** 2002. Banting lecture 2001: dysregulation of fatty acid metabolism in the etiology of type 2 diabetes. Diabetes **51:**7-18.

92. **Merrill, A. L., and B. K. Watt.** 1955. Energy value of foods - basis and derivation. Agricultural Handbook No. 74.

93. **Millet, L., H. Vidal, F. Andreelli, D. Larrouy, J. P. Riou, D. Ricquier, M. Laville, and D. Langin.** 1997. Increased uncoupling protein-2 and -3 mRNA expression during fasting in obese and lean humans. J Clin Invest **100:**2665-70.

94. **Minokoshi, Y., T. Alquier, N. Furukawa, Y. B. Kim, A. Lee, B. Xue, J. Mu, F. Foufelle, P. Ferre, M. J. Birnbaum, B. J. Stuck, and B. B. Kahn.** 2004. AMP-kinase regulates food intake by responding to hormonal and nutrient signals in the hypothalamus. Nature **428:**569-74.

95. **Mitchell, P.** 1966. Chemiosmotic coupling in oxidative and photosynthetic phosphorylation. Biol Rev Camb Philos Soc **41:**445-502.

96. **Moeschel, K., A. Beck, C. Weigert, R. Lammers, H. Kalbacher, W. Voelter, E. D. Schleicher, H. U. Haring, and R. Lehmann.** 2004. Protein kinase C-zeta-induced phosphorylation of Ser318 in insulin receptor substrate-1 (IRS-1) attenuates the interaction with the insulin receptor and the tyrosine phosphorylation of IRS-1. J Biol Chem **279:**25157-63.

97. **Mootha, V. K., C. M. Lindgren, K. F. Eriksson, A. Subramanian, S. Sihag, J. Lehar, P. Puigserver, E. Carlsson, M. Ridderstrale, E. Laurila, N. Houstis, M. J. Daly, N. Patterson, J. P. Mesirov, T. R. Golub, P. Tamayo, B. Spiegelman, E. S. Lander, J. N. Hirschhorn, D. Altshuler, and L. C. Groop.** 2003. PGC-1alpha-responsive genes involved in oxidative phosphorylation are coordinately downregulated in human diabetes. Nat Genet **34:**267-73.

98. **Morino, K., K. F. Petersen, S. Dufour, D. Befroy, J. Frattini, N. Shatzkes, S. Neschen, M. F. White, S. Bilz, S. Sono, M. Pypaert, and G. I. Shulman.** 2005. Reduced mitochondrial density and increased IRS-1 serine phosphorylation in muscle of insulin-resistant offspring of type 2 diabetic parents. J Clin Invest **115:**3587-93.

99. **Morino, K., K. F. Petersen, and G. I. Shulman.** 2006. Molecular mechanisms of insulin resistance in humans and their potential links with mitochondrial dysfunction. Diabetes **55 Suppl 2:**S9-S15.

100. **Mothe, I., and E. Van Obberghen.** 1996. Phosphorylation of insulin receptor substrate-1 on multiple serine residues, 612, 632, 662, and 731, modulates insulin action. J Biol Chem **271:**11222-7.

101. **Mu, J., J. T. Brozinick, Jr., O. Valladares, M. Bucan, and M. J. Birnbaum.** 2001. A role for AMP-activated protein kinase in contraction- and hypoxia-regulated glucose transport in skeletal muscle. Mol Cell **7:**1085-94.

102. **Nedergaard, J., and O. Lindberg.** 1982. The brown fat cell. Int Rev Cytol **74:**187-286.

103. **Nelson, D. L., and M. M. Cox.** 2005. Lehninger Principles of Biochemistry Fourth Edition. W. H. Freeman and Company **New York**.

104. **Nicholls, D. G., and R. M. Locke.** 1984. Thermogenic mechanisms in brown fat. Physiol Rev **64:**1-64.

105. **Nissen, S. E., and K. Wolski.** 2007. Effect of rosiglitazone on the risk of myocardial infarction and death from cardiovascular causes. N Engl J Med **356:**2457-71.

106. **Oldstone, M. B.** 2005. Molecular and cellular mechanisms, pathogenesis, and treatment of insulin-dependent diabetes obtained through study of a transgenic model of molecular mimicry. Curr Top Microbiol Immunol **296:**65-87.

107. **Patti, M. E., A. J. Butte, S. Crunkhorn, K. Cusi, R. Berria, S. Kashyap, Y. Miyazaki, I. Kohane, M. Costello, R. Saccone, E. J. Landaker, A. B. Goldfine, E. Mun, R. DeFronzo, J. Finlayson, C. R. Kahn, and L. J. Mandarino.** 2003. Coordinated reduction of genes of oxidative metabolism in humans with insulin resistance and diabetes: Potential role of PGC1 and NRF1. Proc Natl Acad Sci U S A **100:**8466-71.

108. **Pedersen, S. B., S. Lund, E. S. Buhl, and B. Richelsen.** 2001. Insulin and contraction directly stimulate UCP2 and UCP3 mRNA expression in rat skeletal muscle in vitro. Biochem Biophys Res Commun **283:**19-25.

109. **Perseghin, G., P. Scifo, F. De Cobelli, E. Pagliato, A. Battezzati, C. Arcelloni, A. Vanzulli, G. Testolin, G. Pozza, A. Del Maschio, and L. Luzi.** 1999. Intramyocellular triglyceride content is a determinant of in vivo insulin resistance in humans: a 1H-13C nuclear magnetic resonance spectroscopy assessment in offspring of type 2 diabetic parents. Diabetes **48:**1600-6.

110. **Peter, J. B., R. J. Barnard, V. R. Edgerton, C. A. Gillespie, and K. E. Stempel.** 1972. Metabolic profiles of three fiber types of skeletal muscle in guinea pigs and rabbits. Biochemistry **11:**2627-33.

111. **Phillips, D. I., S. Caddy, V. Ilic, B. A. Fielding, K. N. Frayn, A. C. Borthwick, and R. Taylor.** 1996. Intramuscular triglyceride and muscle insulin sensitivity: evidence for a relationship in nondiabetic subjects. Metabolism **45:**947-50.

112. **Pieczenik, S. R., and J. Neustadt.** 2007. Mitochondrial dysfunction and molecular pathways of disease. Exp Mol Pathol **83:**84-92.

113. **Porter, R. K.** 2006. A new look at UCP 1. Biochim Biophys Acta **1757:**446-8.

114. **Powell, D. J., E. Hajduch, G. Kular, and H. S. Hundal.** 2003. Ceramide disables 3-phosphoinositide binding to the pleckstrin homology domain of protein kinase B (PKB)/Akt by a PKCzeta-dependent mechanism. Mol Cell Biol **23:**7794-808.

115. **Powell, D. J., S. Turban, A. Gray, E. Hajduch, and H. S. Hundal.** 2004. Intracellular ceramide synthesis and protein kinase Czeta activation play an essential role in palmitate-induced insulin resistance in rat L6 skeletal muscle cells. Biochem J **382:**619-29.

116. **Pujol, A., L. Lefaucheur, P. Ecolan, L. Picon, and L. Penicaud.** 1993. Fiber type composition and enzyme activities of muscles in two models of obese rats. Comp Biochem Physiol B **106:**269-72.

117. **Rankinen, T., A. Zuberi, Y. C. Chagnon, S. J. Weisnagel, G. Argyropoulos, B. Walts, L. Perusse, and C. Bouchard.** 2006. The human obesity gene map: the 2005 update. Obesity (Silver Spring) **14:**529-644.

118. **Ranvier, L.** 1873. Proprietés et structures différentes des muscles rouges et des muscles blanc, chez les lapins et chez les raises. C R hepd Séanc Acad Sci (Paris) **77:**1030-1043.

119. **Richter, E. A., L. P. Garetto, M. N. Goodman, and N. B. Ruderman.** 1984. Enhanced muscle glucose metabolism after exercise: modulation by local factors. Am J Physiol **246:**E476-82.

120. **Richter, E. A., L. P. Garetto, M. N. Goodman, and N. B. Ruderman.** 1982. Muscle glucose metabolism following exercise in the rat: increased sensitivity to insulin. J Clin Invest **69:**785-93.

121. **Rolfe, D. F., and M. D. Brand.** 1996. Contribution of mitochondrial proton leak to skeletal muscle respiration and to standard metabolic rate. Am J Physiol **271:**C1380-9.

122. **Rolfe, D. F., and G. C. Brown.** 1997. Cellular energy utilization and molecular origin of standard metabolic rate in mammals. Physiol Rev **77:**731-58.

123. **Rolfe, D. F., J. M. Newman, J. A. Buckingham, M. G. Clark, and M. D. Brand.** 1999. Contribution of mitochondrial proton leak to respiration rate in working skeletal muscle and liver and to SMR. Am J Physiol **276:**C692-9.

124. **Saha, A. K., P. R. Avilucea, J. M. Ye, M. M. Assifi, E. W. Kraegen, and N. B. Ruderman.** 2004. Pioglitazone treatment activates AMP-activated protein kinase in rat liver and adipose tissue in vivo. Biochem Biophys Res Commun **314:**580-5.

125. **Salinas, M., R. Lopez-Valdaliso, D. Martin, A. Alvarez, and A. Cuadrado.** 2000. Inhibition of PKB/Akt1 by C2-ceramide involves activation of ceramide-activated protein phosphatase in PC12 cells. Mol Cell Neurosci **15:**156-69.

126. **Samec, S., J. Seydoux, and A. G. Dulloo.** 1998. Interorgan signaling between adipose tissue metabolism and skeletal muscle uncoupling protein homologs: is there a role for circulating free fatty acids? Diabetes **47:**1693-8.

127. **Samec, S., J. Seydoux, and A. G. Dulloo.** 1998. Role of UCP homologues in skeletal muscles and brown adipose tissue: mediators of thermogenesis or regulators of lipids as fuel substrate? Faseb J **12:**715-24.

128. **Satman, I., T. Yilmaz, A. Sengul, S. Salman, F. Salman, S. Uygur, I. Bastar, Y. Tutuncu, M. Sargin, N. Dinccag, K. Karsidag, S. Kalaca, C. Ozcan, and H. King.** 2002. Population-based study of diabetes and risk characteristics in Turkey: results of the turkish diabetes epidemiology study (TURDEP). Diabetes Care **25:**1551-6.

129. **Schaffer, J. E.** 2003. Lipotoxicity: when tissues overeat. Curr Opin Lipidol **14:**281-7.

130. **Schapira, A. H.** 2006. Mitochondrial disease. Lancet **368:**70-82.

131. **Schrauwen, P., D. G. Hardie, B. Roorda, J. C. Clapham, A. Abuin, M. Thomason-Hughes, K. Green, P. M. Frederik, and M. K. Hesselink.** 2004. Improved glucose homeostasis in mice overexpressing human UCP3: a role for AMP-kinase? Int J Obes Relat Metab Disord **28:**824-8.

132. **Schrauwen, P., M. K. Hesselink, I. Vaartjes, E. Kornips, W. H. Saris, J. P. Giacobino, and A. Russell.** 2002. Effect of acute exercise on uncoupling protein 3 is a fat metabolism-mediated effect. Am J Physiol Endocrinol Metab **282:**E11-7.

133. **Schrauwen, P., W. H. Saris, and M. K. Hesselink.** 2001. An alternative function for human uncoupling protein 3: protection of mitochondria against accumulation of nonesterified fatty acids inside the mitochondrial matrix. Faseb J **15:**2497-502.

134. **Scott, W., J. Stevens, and S. A. Binder-Macleod.** 2001. Human skeletal muscle fiber type classifications. Phys Ther **81:**1810-6.

135. **Shaw, R. J., K. A. Lamia, D. Vasquez, S. H. Koo, N. Bardeesy, R. A. Depinho, M. Montminy, and L. C. Cantley.** 2005. The kinase LKB1 mediates glucose homeostasis in liver and therapeutic effects of metformin. Science **310:**1642-6.

136. **Smerdu, V., I. Karsch-Mizrachi, M. Campione, L. Leinwand, and S. Schiaffino.** 1994. Type IIx myosin heavy chain transcripts are expressed in type IIb fibers of human skeletal muscle. Am J Physiol **267:**C1723-8.

137. **Spangenburg, E. E., and F. W. Booth.** 2003. Molecular regulation of individual skeletal muscle fibre types. Acta Physiol Scand **178:**413-24.

138. **Speakman, J. R.** 2004. Obesity: the integrated roles of environment and genetics. J Nutr **134:**2090S-2105S.

139. **Sriwijitkamol, A., D. K. Coletta, E. Wajcberg, G. B. Balbontin, S. M. Reyna, J. Barrientes, P. A. Eagan, C. P. Jenkinson, E. Cersosimo, R. A. DeFronzo, K. Sakamoto, and N. Musi.** 2007. Effect of acute exercise on AMPK signaling in skeletal muscle of subjects with type 2 diabetes: a time-course and dose-response study. Diabetes **56:**836-48.

140. **Staron, R. S.** 1991. Correlation between myofibrillar ATPase activity and myosin heavy chain composition in single human muscle fibers. Histochemistry **96:**21-4.

141. **Staron, R. S., F. C. Hagerman, R. S. Hikida, T. F. Murray, D. P. Hostler, M. T. Crill, K. E. Ragg, and K. Toma.** 2000. Fiber type composition of the vastus lateralis muscle of young men and women. J Histochem Cytochem **48:**623-9.

142. **StatisticsCanada.** 2004. Canadian Community Health Survey.

143. **Stoppani, J., A. L. Hildebrandt, K. Sakamoto, D. Cameron-Smith, L. J. Goodyear, and P. D. Neufer.** 2002. AMP-activated protein kinase activates transcription of the UCP3 and HKII genes in rat skeletal muscle. Am J Physiol Endocrinol Metab **283:**E1239-48.

144. **Straczkowski, M., I. Kowalska, A. Nikolajuk, S. Dzienis-Straczkowska, I. Kinalska, M. Baranowski, M. Zendzian-Piotrowska, Z. Brzezinska, and J. Gorski.** 2004. Relationship between insulin sensitivity and sphingomyelin signaling pathway in human skeletal muscle. Diabetes **53:**1215-21.

145. **SubcommitteeOnTheTenthEditionOfTheRecommendedDietaryAllowances, FoodAndNutritionBoard, CommissionOnLifeSciences, and NationalResearchCouncil.** 1989. Recommended Dietary Allowances: 10th Edition. National Academy of Sciences.

146. **Summers, S. A.** 2006. Ceramides in insulin resistance and lipotoxicity. Prog Lipid Res **45:**42-72.

147. **Suwa, M., H. Nakano, and S. Kumagai.** 2003. Effects of chronic AICAR treatment on fiber composition, enzyme activity, UCP3, and PGC-1 in rat muscles. J Appl Physiol **95:**960-8.

148. **Szczepaniak, L. S., E. E. Babcock, F. Schick, R. L. Dobbins, A. Garg, D. K. Burns, J. D. McGarry, and D. T. Stein.** 1999. Measurement of intracellular triglyceride stores by H spectroscopy: validation in vivo. Am J Physiol **276:**E977-89.

149. **Tanner, C. J., H. A. Barakat, G. L. Dohm, W. J. Pories, K. G. MacDonald, P. R. Cunningham, M. S. Swanson, and J. A. Houmard.** 2002. Muscle fiber type is associated with obesity and weight loss. Am J Physiol Endocrinol Metab **282:**E1191-6.

150. **Teruel, T., R. Hernandez, and M. Lorenzo.** 2001. Ceramide mediates insulin resistance by tumor necrosis factor-alpha in brown adipocytes by maintaining Akt in an inactive dephosphorylated state. Diabetes **50:**2563-71.

151. **Tsuboyama-Kasaoka, N., N. Tsunoda, K. Maruyama, M. Takahashi, H. Kim, S. Ikemoto, and O. Ezaki.** 1998. Up-regulation of uncoupling protein 3 (UCP3) mRNA by exercise training and down-regulation of UCP3 by denervation in skeletal muscle. Biochem Biophys Res Commun **247:**498-503.

152. **Unger, R. H., and L. Orci.** 2001. Diseases of liporegulation: new perspective on obesity and related disorders. Faseb J **15:**312-21.

153. **Unger, R. H., and Y. T. Zhou.** 2001. Lipotoxicity of beta-cells in obesity and in other causes of fatty acid spillover. Diabetes **50 Suppl 1:**S118-21.

154. **van Loon, L. J., and B. H. Goodpaster.** 2006. Increased intramuscular lipid storage in the insulin-resistant and endurance-trained state. Pflugers Arch **451:**606-16.

155. **Vidal-Puig, A., G. Solanes, D. Grujic, J. S. Flier, and B. B. Lowell.** 1997. UCP3: an uncoupling protein homologue expressed preferentially and abundantly in skeletal muscle and brown adipose tissue. Biochem Biophys Res Commun **235:**79-82.

156. **Wallberg-Henriksson, H., and J. O. Holloszy.** 1985. Activation of glucose transport in diabetic muscle: responses to contraction and insulin. Am J Physiol **249:**C233-7.

157. **Weigle, D. S., L. E. Selfridge, M. W. Schwartz, R. J. Seeley, D. E. Cummings, P. J. Havel, J. L. Kuijper, and H. BeltrandelRio.** 1998. Elevated free fatty acids induce uncoupling protein 3 expression in muscle: a potential explanation for the effect of fasting. Diabetes **47:**298-302.

158. **Weiss, R., S. Dufour, S. E. Taksali, W. V. Tamborlane, K. F. Petersen, R. C. Bonadonna, L. Boselli, G. Barbetta, K. Allen, F. Rife, M. Savoye, J. Dziura, R. Sherwin, G. I. Shulman, and S. Caprio.** 2003. Prediabetes in obese youth: a syndrome of impaired glucose tolerance, severe insulin resistance, and altered myocellular and abdominal fat partitioning. Lancet **362:**951-7.

159. **Woods, A., K. Dickerson, R. Heath, S. P. Hong, M. Momcilovic, S. R. Johnstone, M. Carlson, and D. Carling.** 2005. Ca2+/calmodulin-dependent protein kinase kinase-beta acts upstream of AMP-activated protein kinase in mammalian cells. Cell Metab **2:**21-33.

160. **Woods, A., S. R. Johnstone, K. Dickerson, F. C. Leiper, L. G. Fryer, D. Neumann, U. Schlattner, T. Wallimann, M. Carlson, and D. Carling.** 2003. LKB1 is the upstream kinase in the AMP-activated protein kinase cascade. Curr Biol **13:**2004-8.

161. **WorldHealthOrganization.** 2000. Obesity: preventing and managing the global epidemic. WHO Technical Report Series **894**.

162. **WorldHealthOrganization.** 1995. Physical status: the use and interpretation of anthropometry. WHO Technical Report Series **854**.

163. **Wu, Z., P. Puigserver, U. Andersson, C. Zhang, G. Adelmant, V. Mootha, A. Troy, S. Cinti, B. Lowell, R. C. Scarpulla, and B. M. Spiegelman.** 1999. Mechanisms controlling mitochondrial biogenesis and respiration through the thermogenic coactivator PGC-1. Cell **98:**115-24.

164. **Yeh, J. I., E. A. Gulve, L. Rameh, and M. J. Birnbaum.** 1995. The effects of wortmannin on rat skeletal muscle. Dissociation of signaling pathways for insulin- and contraction-activated hexose transport. J Biol Chem **270:**2107-11.

165. **Yeh, L. A., K. H. Lee, and K. H. Kim.** 1980. Regulation of rat liver acetyl-CoA carboxylase. Regulation of phosphorylation and inactivation of acetyl-CoA carboxylase by the adenylate energy charge. J Biol Chem **255:**2308-14.

166. **Yki-Jarvinen, H.** 2005. Fat in the liver and insulin resistance. Ann Med **37:**347-56.

167. **Yu, C., Y. Chen, G. W. Cline, D. Zhang, H. Zong, Y. Wang, R. Bergeron, J. K. Kim, S. W. Cushman, G. J. Cooney, B. Atcheson, M. F. White, E. W. Kraegen, and G. I. Shulman.** 2002. Mechanism by which fatty acids inhibit insulin activation of insulin receptor substrate-1 (IRS-1)-associated phosphatidylinositol 3-kinase activity in muscle. J Biol Chem **277:**50230-6.

168. **Zhang, Y., R. Proenca, M. Maffei, M. Barone, L. Leopold, and J. M. Friedman.** 1994. Positional cloning of the mouse obese gene and its human homologue. Nature **372:**425-32.

169. **Zhou, G., R. Myers, Y. Li, Y. Chen, X. Shen, J. Fenyk-Melody, M. Wu, J. Ventre, T. Doebber, N. Fujii, N. Musi, M. F. Hirshman, L. J. Goodyear, and D. E. Moller.** 2001. Role of AMP-activated protein kinase in mechanism of metformin action. J Clin Invest **108:**1167-74.

170. **Zhou, M., B. Z. Lin, S. Coughlin, G. Vallega, and P. F. Pilch.** 2000. UCP-3 expression in skeletal muscle: effects of exercise, hypoxia, and AMP-activated protein kinase. Am J Physiol Endocrinol Metab **279:**E622-9.

171. **Zierath, J. R.** 1995. In vitro studies of human skeletal muscle: hormonal and metabolic regulation of glucose transport. Acta Physiol Scand Suppl **626:**1-96.

172. **Zierath, J. R., and J. A. Hawley.** 2004. Skeletal muscle fiber type: influence on contractile and metabolic properties. PLoS Biol **2:**e348.

173. **Zinda, M. J., C. J. Vlahos, and M. T. Lai.** 2001. Ceramide induces the dephosphorylation and inhibition of constitutively activated Akt in PTEN negative U87mg cells. Biochem Biophys Res Commun **280:**1107-15.

Chapter 1

Gain-of-Function R225W Mutation in Human AMPKγ_3 Causing Increased Glycogen and Decreased Triglyceride in Skeletal Muscle

Sheila R. Costford[1†], Nihan Kavaslar[2†], Nadav Ahituv[4], Shehla N. Chaudhry[1], Wendy S. Schackwitz[4,5], Robert Dent[3], Len A. Pennacchio[4], Ruth McPherson[2†] and Mary-Ellen Harper[1†]

PLoS ONE. 2007 Sep 19;2(9):e903.

[1]Department of Biochemistry, Microbiology and Immunology, Faculty of Medicine, University of Ottawa, Ottawa ON Canada K1H 8M5
[2]Division of Cardiology and Lipoprotein and Atherosclerosis Research Group, University of Ottawa Heart Institute, 40 Ruskin St., Ottawa, ON Canada K1Y 4W7
[3]Ottawa Hospital Weight Management Clinic, 1053 Carling Ave., Ottawa, ON Canada K1Y 4E9
[4]Genomics Division, One Cyclotron Rd., MS 84-171, Lawrence Berkeley National Laboratory, Berkeley, CA 94720, USA
[5]U.S. Department of Energy Joint Genome Institute, Walnut Creek, CA 94598 USA.
[†]These authors contributed equally to this work.

Brief Description of Contents

This manuscript, published in PLoS ONE in September of 2007, describes the identification of the first mutation in the gamma-3 subunit of AMP-activated protein kinase in humans, R225W. Findings demonstrate that this mutation results in an overall increase in both basal and AMP-stimulated AMPK activity in muscle fibers isolated, grown up and differentiated in culture from *vastus lateralis* biopsies of R225W carriers. Carriers also display increased muscle glycogen content and decreased intramuscular triglyceride, but with no change in fiber type ratio. Results are consistent with an important regulatory role for AMPKγ_3 in human skeletal muscle metabolism and have broad implications for the treatment of type 2 diabetes mellitus.

Contribution of Collaborators

Sheila R. Costford

Collected *vastus lateralis* samples at muscle biopsies, processed muscle biopsies for histology and myoblast isolation, isolated myoblasts, maintained cell cultures, performed AMPK isolations and activity determinations, took micrographs of PAS staining for glycogen, OsO_4 staining for IMTG and fiber typing, performed imaging analysis/quantification of muscle glycogen content, IMTG and fiber typing. Analyzed data for the above described experiments. Table/Figure contributions: Figure 9, Figure 11, Figure 12, Figure 14, Figure 15 and Figure 16. Assisted in the writing, editing and submission of the manuscript.

Nihan Kavaslar

Collected, isolated and sent DNA samples to the Pennacchio lab for gene resequencing. Analyzed clinical and blood chemistry results. Isolated RNA from muscle biopsies and assessed the levels of mRNA for AMPKgamma-3. Table/Figure contributions: Figure 10, Table 2 and Table 3. Assisted in the interpretation of findings. Assisted in writing the manuscript.

Nadav Ahituv and Wendy Schackwitz

Resequenced a total of 58 genes, including the gene for the gamma-3 subunit of AMPK. Conducted Polyphen and SIFT analyses. Read and provided constructive suggestions for the manuscript.

Shehla N. Chaudhry

Assisted in the collection of most *vastus lateralis* samples at muscle biopsies, assisted in the processing of muscle biopsies for histology and myoblast isolation, isolation myoblasts, maintenance of cell cultures, performance of AMPK isolations and activity determinations, the capture of micrographs of PAS staining for glycogen, OsO_4 staining for IMTG and fiber typing, the performance of imaging analysis/quantification of muscle glycogen content, IMTG and fiber typing.

Robert Dent

Clinician for one of the probands. Contacted and recruited this subject and members of her family. Conducted some muscle biopsies. Supervised hyperinsulinemic-euglycemic clamps. Assisted in interpretation of findings and in the writing of the manuscript.

Len Pennacchio

Planned and supervised the resequencing of the 58 genes and the Polyphen and SIFT analyses. Read and provided constructive suggestions for the manuscript.

Ruth McPherson

As Principal Investigator of the Thin Gene Study, Dr McPherson contacted and recruited the other proband and members of their family. Assisted in the design of the study. Conducted some muscle biopsies and supervised hyperinsulinemic-euglycemic clamps. Assisted in data analysis and interpretation of findings. Assisted in writing the manuscript.

Mary-Ellen Harper

Assisted in study design, and the overall organization amongst collaborators. Assisted in data analysis and interpretation. Assisted in writing the manuscript and submitting it for publication.

Abstract

Background

AMP-activated protein kinase (AMPK) is a heterotrimeric enzyme that is evolutionarily conserved from yeast to mammals and functions to maintain cellular and whole body energy homeostasis. Studies in experimental animals demonstrate that activation of AMPK in skeletal muscle protects against insulin resistance, type 2 diabetes and obesity. The regulatory γ_3 subunit of AMPK is expressed exclusively in skeletal muscle; however, its importance in controlling overall AMPK activity is unknown. While evidence is emerging that gamma subunit mutations interfere specifically with AMP activation, there remains some controversy regarding the impact of gamma subunit mutations (11, 23, 37). Here we report the first gain-of-function mutation in the muscle-specific regulatory γ_3 subunit in humans.

Methods and Findings

We sequenced the exons and splice junctions of the AMPK γ_3 gene (*PRKAG3*) in 761 obese and 759 lean individuals, identifying 87 sequence variants including a novel R225W mutation in subjects from two unrelated families. The γ_3R225W mutation is homologous in location to the γ_2R302Q mutation in patients with Wolff-Parkinson-White syndrome and to the γ_3R225Q mutation originally linked to an increase in muscle glycogen content in purebred Hampshire Rendement

Napole (RN^-) pigs. We demonstrate in differentiated muscle satellite cells obtained from the *vastus lateralis* of R225W carriers that the mutation is associated with an approximate doubling of both basal and AMP-activated AMPK activities. Moreover, subjects bearing the R225W mutation exhibit a ~90% increase of skeletal muscle glycogen content and a ~30% decrease in intramuscular triglyceride (IMTG).

Conclusions

We have identified for the first time a mutation in the skeletal muscle-specific regulatory γ_3 subunit of AMPK in humans. The γ_3R225W mutation has significant functional effects as demonstrated by increases in basal and AMP-activated AMPK activities, increased muscle glycogen and decreased IMTG. Overall, these findings are consistent with an important regulatory role for AMPK γ_3 in human muscle energy metabolism.

Introduction

AMP-activated protein kinase (AMPK) is a serine/threonine kinase that is evolutionarily conserved from yeast to mammals and functions as a highly responsive energy sensor in cells (6, 24, 25, 29). It acts both centrally and peripherally to coordinate multiple inputs from various hormones, peptides and nutrients to maintain overall energy homeostasis. In response to cellular stress in the periphery, AMPK inhibits anabolic pathways and stimulates catabolic pathways to restore cellular energy charge. *In vitro* and experimental animal studies have demonstrated that altered activity of AMPK has significant implications for a number of cardiovascular risk factors, including type 2 diabetes (24, 25, 29). In skeletal muscle, AMPK activation stimulates glucose uptake, fatty acid uptake and oxidation, and mitochondrial biogenesis (29). Thus AMPK activation in skeletal muscle protects against the development of insulin resistance, type 2 diabetes and obesity (7, 9, 10, 38).

AMPK has a heterotrimeric structure and is composed of an α-catalytic, a β-regulatory and a γ-regulatory subunit. The α-catalytic subunit has two isoforms (α_1, α_2), the β-regulatory subunit has two isoforms (β_1, β_2), and the γ-regulatory subunit has three isoforms (γ_1, γ_2, γ_3) (12, 14). Figure 9 depicts the three γ isoforms and their structural characteristics.

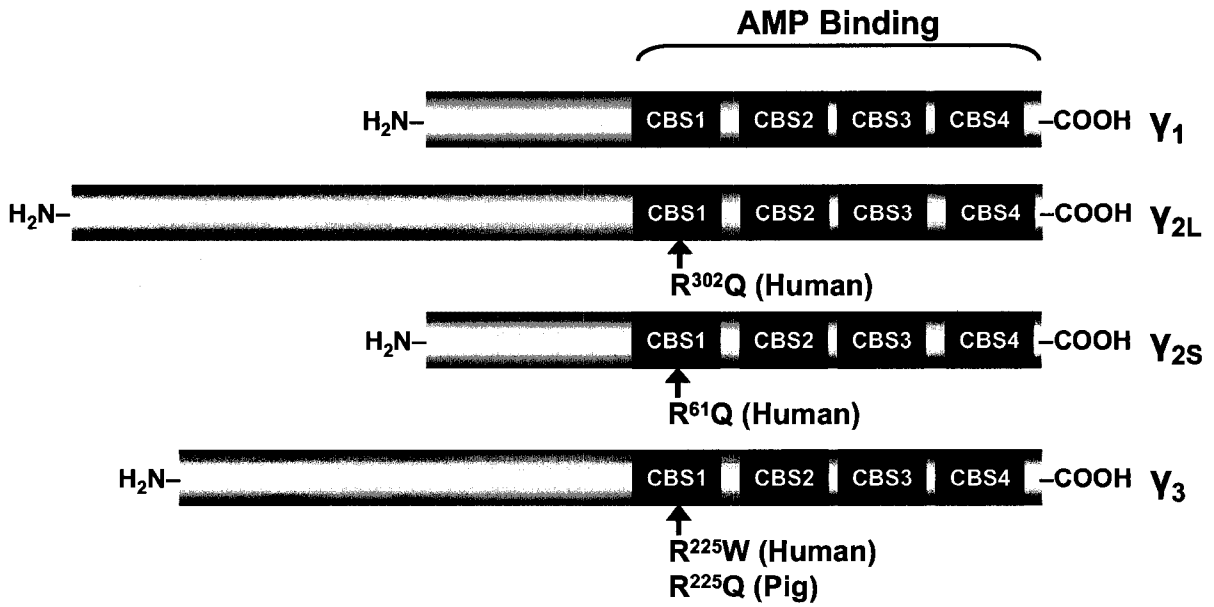

Figure 9: γ subunit isoforms showing the 4 tandem repeats of CBS domains responsible for AMP and ATP binding. Locations of the human R225W and the porcine R225Q mutations in the γ_3 subunit as well as the R302Q and R61Q mutations in the γ_2 long and short forms, respectively, are indicated. Figure adapted from (12).

The various isoforms of each subunit are encoded by distinct genes, with alternative promoters and splice variants, adding to genetic and post-translational complexities (29). Most isoforms are expressed to some extent in all tissues, although mRNA expression data indicate that the γ_3 subunit is more abundant in skeletal muscle than in any other tissue (31). The relative proportions of the γ subunits in human skeletal muscles are as yet unknown. Several exercise studies in humans have measured γ subunit protein levels in the *vastus lateralis* muscle. In these studies, protein levels were expressed as percentage of sedentary controls, pretraining values, or untrained muscles as opposed to absolute relative values (18, 35, 39). A more recent study provided evidence that only 3 out of the 12 possible AMPK complex combinations are expressed in human *vastus lateralis*: $\alpha_1/\beta_2/\gamma_1$, $\alpha_2/\beta_2/\gamma_1$ and $\alpha_2/\beta_2/\gamma_3$ (8). The only heterotrimer shown to be phosphorylated and activated during high intensity exercise was the complex containing the γ_3 isoform. The activity associated with the other two heterotrimers either remained unchanged or decreased during exercise (8). The γ_2 long and short isoforms (γ_{2L} and γ_{2S}, respectively) result from alternative splicing of a common transcript in heart and other tissues (13, 22, 30). While both long and short isoforms are expressed in heart, γ_{2S} is predominant in skeletal muscle (13).

To date the only published mutations in the AMPK genes in humans are in the γ_2-regulatory subunit, the predominant γ isoform in cardiac muscle. While AMPK

activity stimulates fatty acid oxidation, glucose uptake and glycolysis in the heart, its regulation is complex, and still not well understood (11, 17, 37). At least six different missense mutations within the CBS domains of γ_2 have been shown to cause the excess storage of glycogen in pronounced glycogen-associated vacuoles(15). This excess storage of glycogen results in a complex phenotype, including Wolff-Parkinson-White (WPW) syndrome, conduction system disease and cardiac hypertrophy (4, 21, 22). In purebred Hampshire Rendement Napole (RN) pigs, a naturally occurring R225Q mutation in the γ_3 subunit of AMPK was identified and linked to increased glycogen storage in skeletal muscle (32) and to increased resynthesis of glycogen after exercise when R225Q AMPKγ_3 is overexpressed in transgenic mice (6).

In the context of our ongoing goal of identifying genes that underlie predisposition for diabetes and obesity, we searched for genetic variation in human *PRKAG3*. Of the 24 novel coding variants identified, we focused on the R225W mutation due to the established importance of the mutation in porcine AMPK γ_3 and the homologous mutations in the γ_2 subunit of human AMPK. We determined the functional significance of this mutation in differentiated muscle cells from the *vastus lateralis* of R225W carriers compared to matched controls.

Here we describe a previously unreported R225W mutation in the human AMPK γ_3 gene, *PRKAG3,* found in two independent kindreds. We show that the R225W

mutation causes increased basal and AMP-activated AMPK activity, as well as increased muscle glycogen storage and decreased intramuscular triglyceride (IMTG).

Methods

Subjects and Sequence Analysis

The coding exons and splice junctions of the human AMPK γ_3 gene (NCBI accession no. NM_017431) were resequenced in obese Caucasian subjects from the Ottawa Hospital Weight Management Clinic and in lean healthy Caucasian individuals who participated in a study of leanness at the University of Ottawa Heart Institute. The cohorts consisted of 761 obese subjects with a mean BMI of 39.9 kg/m^2 and >90th percentile adjusted for age and sex, and 759 lean subjects with a mean BMI of 20.1 kg/m^2 and <25th percentile adjusted for age and sex. The study was approved by the institutional review boards of the University of Ottawa Heart Institute and the Ottawa Hospital. Informed written consent was obtained from all participants. A total of 58 genes were sequenced as part of this study and detailed findings have been presented elsewhere (2). Selection criteria for our patient population as well as methods for DNA isolation, sequencing and data analysis have been described previously (1).

Predictions of the possible functional implications of the variants were made using PolyPhen (http://genetics.bwh.harvard.edu/pph/) and SIFT (http://blocks.fhcrc.org/sift/SIFT.html) programs (34, 36). The R225W variant, which is found in the second CBS domain (Figure 1), was identified to be

functionally damaging by both programs. This variant was intriguing since it is analogous to the R225Q mutation causing increased muscle glycogen content in pigs, as well as having the same amino acid location as the mutations in the human γ_2 subunit that are known to alter AMPK protein function and cause Wolff-Parkinson-White syndrome. We thus contacted subjects that were identified as carrying the R225W mutation in the initial study cohorts, and screened their available family members for further study (Figure 10).

The region of the AMPKG3 gene with the R225W variation was sequenced in DNA samples from family members to determine whether they carried the same variation. Subject characteristics are described in Table 2.

Skeletal Muscle Biopsies and Cell Culture

Five subjects with the R225W mutation and five control subjects were matched for gender, age, weight, BMI, as well as amount and intensity of self-reported weekly physical activity. These subjects refrained from physical activity for three days prior to undergoing additional studies in the post-absorptive state after an overnight fast. Percutaneous skeletal muscle biopsies of the *vastus lateralis* muscle were obtained from R225W carriers and their matched controls using a 5mm Bergstrom needle (Opitek) under local anaesthesia with 1% lidocaine. *Vastus lateralis* is commonly selected for studies of human muscle metabolism

and was chosen for biopsy in the current study due to the demonstrated importance of the γ_3 subunit in this muscle (8).

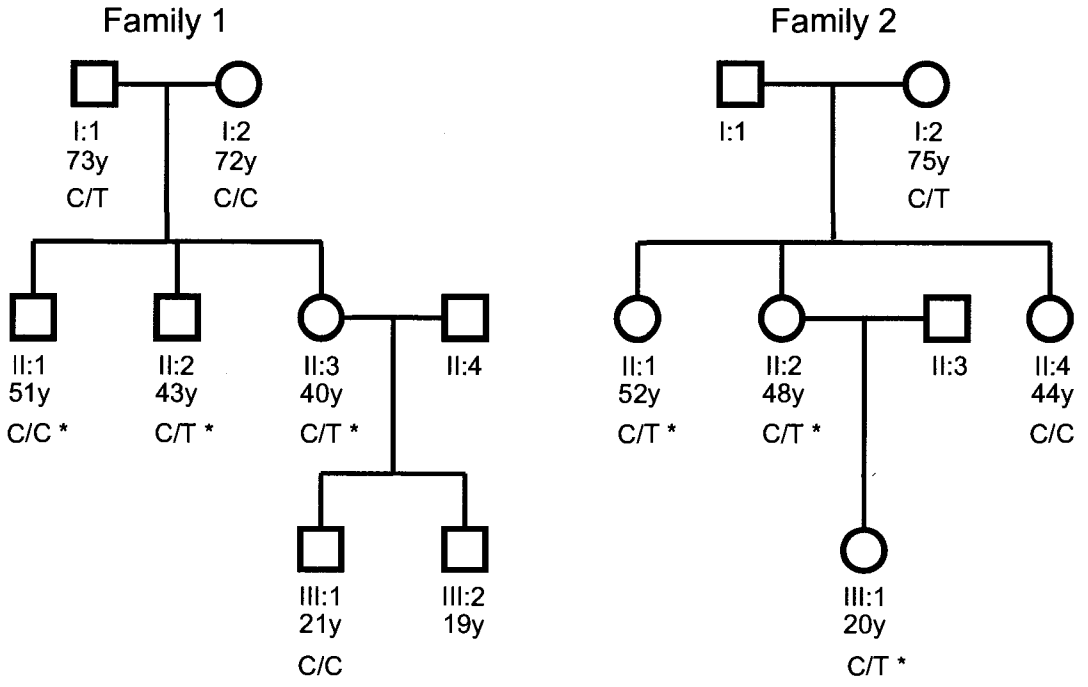

Figure 10: Families of the two probands with the PRKAG3-R225W mutation. *Subjects who underwent muscle biopsy.

	R225W (n=5)	Controls (n=5)
Age (years)	40.6 ± 12.4	42.8 ± 12.9
Weight (kg)	82.5 ± 23.2	80.9 ± 27.1
BMI (kg/m^2)	29.1 ± 9.0	29.2 ± 10.3
Total Cholesterol (mmol/L)	5.54 ± 0.70	4.52 ± 0.66
Body Fat (%)	34.6 ± 10.4	35.6 ± 8.7
Basal Metabolic Rate (kJ)	6773.8 ± 1201.1	5380.4 ± 2134.9
HDL-C (mmol/L)	1.29 ± 0.26	1.52 ± 0.70
LDL-C (mmol/L)	3.22 ± 0.47	2.55 ± 0.35
TC:HDL	4.40 ± 0.71	3.44 ± 1.24
Triglycerides (mmol/L)	2.27 ± 1.00	1.11 ± 0.61
Glucose (mmol/L)	4.94 ± 0.61	5.16 ± 0.63
Insulin (pmol/L)	54.2 ± 10.1	47.4 ± 35.8
HbA1c	0.0522 ± 0.0031	0.0544 ± 0.0013

Table 2: Characteristics of PRKAG3-R225W subjects and controls who underwent muscle biopsy. Blood chemistry measurements were conducted following an overnight fast. Means +/- SD. n=5, Student's *t*-test, no significant differences between R225W and control subjects.

A 10 mg sample of the biopsy was flash frozen in O.C.T. compound for muscle fiber typing, glycogen content determination and IMTG determination. A 25 mg sample of tissue was subjected to trypsin digestion and cells were grown to ~70% confluency in Ham's F10 media (supplemented with 1% antibiotic-antimycotic, 2.5 μg/mL gentamycin, 12.4% FBS, 0.41 mg/mL BSA, 826 nM dexamethazone, 8.3 ng/mL epidermal growth factor, 0.41 mg/mL fetuin, and 25 pmol insulin). Isolation of satellite cells was achieved via immuno-sorting using primary anti-5.1H11 (Developmental Studies Hybridoma Bank) and secondary MACS goat anti-mouse IgG microbeads. After the suspension was passed through a magnetic field, labelled cells were isolated, eluted and then grown up in culture. Upon reaching 80% confluency, cells were differentiated for ~10 days in Dulbecco's modified Eagle's medium (supplemented with 2% horse serum, 1% antibiotic-antimycotic and 2.5 μg/mL gentamycin).

AMPK Isolation

Approximately 10 days after differentiation, myotubes were incubated on ice while shaking in the presence of lysis buffer (30 mM HEPES, 2.5 mM EGTA, 3 mM EDTA, 70 mM KCl, 0.1% Nonidet P-40, 20 mM β-glycerophosphate, 20 mM NaF, 2 mM NaPPi, 1 mM Na_3VO_4, 200 μM PMSF and 1 μM pepstatin A). Partial purification of AMPK from the cell lysate was carried out as detailed in (26, 28). The cell lysate was incubated at a 1:1 ratio with 30% polyethylene glycol 6000 for 1 hour. Resulting purified protein was dissolved in assay buffer (62.5 mM Na

HEPES, 62.5 mM NaCl, 62.5 mM NaF, 6.25 mM Na pyrophosphate, 1.25 mM EDTA, 1.25 mM EGTA, 1 mM dithiothreitol, 1 mM PMSF, 5 μg/mL SBTI and 1 μM pepstatin A) and then quantified using the bicinchoninic assay.

AMPK Activity Determination

The SAMS peptide assay was carried out as detailed in (16, 26) with minor modifications: 13 μL reaction buffer (20 mM HEPES-NaOH, 0.4 mM dithiothreitol, 0.01% Brij-35 with or without 300 μM AMP), 10 μL of 562 μM SAMS substrate peptide, 10 μCi [^{32}P]ATP (3000 Ci/mmol), and 6 μg of partially purified AMPK were incubated with constant shaking at 30°C for 15 minutes. Negative controls consisted of all reagents except SAMS substrate peptide and AMP. All reactions were carried out in triplicate. AMPK activity was expressed as pmol of ^{32}P-radiolabeled phosphate incorporated into the SAMS peptide per minute per mg of protein.

Quantitative RT-PCR Analysis

RNA from muscle biopsy samples was extracted using Trizol (Invitrogen) and treated with DNaseI (Ambion). cDNA was generated from 0.5 μg of RNA using random decamer primers (Ambion) with MMLV reverse transcriptase (Invitrogen). Amplicons of AMPKG3 and GAPDH genes were cloned into pCR 2.1-TOPO (Invitrogen). Serial dilutions of these constructs were used to generate standard curves, following assessment of primer efficiency and analysis of

melting curve profiles. Quantitative real-time PCR analysis was performed in a LightCycler system (Roche) using FastStart DNA MasterPLUS SYBR Green I kit (Roche). The primers for real-time PCR were designed using LightCycler Probe Design Software v1.0 (Roche). Following 30 cycles of amplification with 1.0 µl of cDNA and 0.5 µM of F and R primers per reaction, expression of AMPKG3 was normalized to expression of GAPDH. Primer sequences: F: 5'-CAGAGGACACTATGTCTGG-3' and R: 5'-GCTTGGGATTGAGGACT-3' (AMPKG3), F: 5'-GATTTGGCCGTATTGGG-3' and R: 5'-TCCACGACATACTCAGC-3' (GAPDH).

Western Blotting and Densitometry

To determine protein levels of the γ_3 isoform, the same purified protein extracts that were used for the AMPK activity assay were subjected to immunoblotting. Electrophoresis was carried out using a 12% polyacrylamide gel. Following transfer to nitrocellulose membranes, primary antibodies were incubated at a 1:1000 dilution overnight at 4°C (AMPKγ_1, AMPKγ_3 and β-actin antibodies were from Cell Signaling Technology, Danvers, MA). The secondary antibody was a peroxidase-conjugated goat anti-rabbit IgG (Santa Cruz Inc., Santa Cruz, CA) and was incubated at a 1:500 dilution for one hour at room temperature. For detection, blots were processed using enhanced chemiluminescence kits (Amersham Pharmacia; Baie d'Urfe, QC, Canada). β-actin was used as the loading control and densitometry was carried out to determine relative protein levels (values expressed as γ isoform integrated densitometry value (IDV)

divided by β-actin IDV).

Muscle Glycogen Content Determination

Glycogen content was determined using Periodic Acid Schiff (PAS) staining. Frozen tissues were cut as 10 μm cross sections and mounted on Superfrost slides. After Schiff staining, sections were counterstained with Harris's hematoxylin. Imaging software (Northern Eclipse) was used to analyze tissues at 200X magnification with an Axiophot digital light microscope (Axiophot 2, Zeiss, Oberkochen, Germany). 2-3 fields of view in each of 3 sections per patient were analyzed for glycogen content as a proportion of surface area of each field.

Intramuscular Triglyceride (IMTG) Content

IMTG content was determined using osmium tetroxide (OsO_4) staining. Frozen tissues were cut as 10 μm cross sections and mounted on Superfrost slides and fixed in 10% neutral buffered formalin. IMTG was stained black with 1% OsO_4 and then cells were counterstained with hematoxylin and eosin (H&E). Imaging software (Northern Eclipse) was used to analyze tissues at 200X magnification with an Axiophot digital light microscope (Axiophot 2, Zeiss, Oberkochen, Germany). 2-3 fields of view in each of 3 sections per patient were analyzed for IMTG content as a proportion of surface area of each field.

Fiber Typing

Frozen tissues were cut as 10 μm cross sections and mounted on Superfrost slides. Sections were stained using the Vectastain ABC-AP kit (Vector Laboratories). Type 1 fibers were identified by using A4.840 as the primary antibody (Developmental Studies Hybridoma Bank), which is specific to the C-terminal part of the beta slow myosin heavy chain in type I skeletal muscle fibers. Biotinylated goat anti-mouse IgG (BA-9200, Vector Laboratories) was used as the secondary antibody, and then cells were stained red using SK-5100 (Vector Laboratories). Type 2a fibers were identified by using N2.261 as the primary antibody (Developmental Studies Hybridoma Bank), which is specific to the N-terminal part of the beta slow myosin heavy chain in adult skeletal myosin heavy chain type IIA. BA-9200 was used as the secondary antibody, and then cells were stained blue using SK-5300 (Vector Laboratories). Type 2b/x fibers were identified as unstained cells. Fiber type ratios were determined by counting numbers of each fiber type in 2-3 fields of view in 3 sections per patient.

Statistical Analysis

The management of clinical and genotypic data was carried out with SAS statistical software (Version 9.1, SAS Institute Inc., Cary, NC). A one-way ANOVA with Tukey post-test was used to determine differences in AMPK activity (Figure

11). Student's *t* tests were used to assess mRNA levels, protein levels, glycogen content, intramuscular triglyceride and fiber type ratio (Figures 12-15).

Results

AMPK γ_3 Sequence Variants

We sequenced the exons and intron/exon boundaries of *PRKAG3*, which codes for the subunit of AMPK that is specific to skeletal muscle. We studied 761 obese subjects with a mean BMI of 39.9 kg/m^2 and >90th percentile adjusted for age and gender, and 759 lean subjects with a mean BMI of 20.1 kg/m^2 and <25th percentile adjusted for age and gender. We identified 87 genetic variants in *PRKAG3* and its flanking regions. Of the six common (minor allele frequency >0.05) variants, three were intronic polymorphisms (IVS2+45, IVS6+31 and IVS10+85), one was a synonymous variant (G180G), and two were non-synonymous variants (P71A and R340W). The 81 rare variants included one SNP in the upstream region, one in the 5' UTR, 50 intronic SNPs, 10 synonymous and 16 nonsynonymous coding variants, one frameshift mutation that leads to a stop codon and two SNPs in the 3' UTR. The frequency and functional prediction for the coding variants are outlined in Table 3.

Of the 30 coding *PRKAG3* variants observed in this study, 24 were not listed in the current SNP database (dbSNPbuild126). Computational predictions of the severity of missense substitutions were made using PolyPhen (36) and SIFT (34).

Variant	Allele	MAF (Obese)	MAF (Lean)	S/NS	Functional Prediction	
					PolyPhen	SIFT
E70E	G>A	0	0.001	S	-	-
P71A (rs692243)	C>G	0.179	0.160	NS	possibly damaging	tolerated
E76Q	G>C	0	0.001	NS	benign	tolerated
E85E	G>A	0.001	0	S	-	-
T87T	C>T	0.003	0.003	S	-	-
D103G	A>G	0.001	0	NS	benign	tolerated
V107fs	indel	0.001	0	frameshift	stop codon	stop codon
G113V	G>T	0	0.001	NS	possibly damaging	tolerated
F139F (rs12328317)	C>T	0.001	0.001	S	-	-
L153V (rs35050588)	C>G	0.001	0	NS	benign	tolerated
L161P	T>C	0.001	0	NS	benign	tolerated
G171S	G>A	0.001	0	NS	benign	tolerated
P179P	C>T	0.001	0	S	-	-
G180G (rs35658907)	C>T	0.026	0.034	S	-	-
G180S	G>A	0	0.001	NS	benign	tolerated
Y194Y	C>T	0.001	0	S	-	-
M197T	T>C	0.001	0	NS	possibly damaging	affected
E211Q	G>C	0.001	0	NS	benign	tolerated
R225W	C>T	0.001	0.001	NS	probably damaging	affected
R225Q	G>A	0	0.001	NS	benign	tolerated
Q260R	A>G	0.001	0.006	NS	benign	tolerated
L269T	T>C	0.001	0	NS	possibly damaging	affected
R307C	C>T	0.001	0	NS	probably damaging	affected
P313P	G>A	0.001	0.001	S	-	-
R340W (rs33985460)	C>T	0.053	0.056	NS	probably damaging	affected
R340Q	G>A	0.001	0	NS	benign	tolerated
R446M	G>T	0	0.001	NS	possibly damaging	tolerated
A482V (rs34720726)	C>T	0.002	0	NS	benign	affected
D485N	G>A	0.005	0.001	NS	benign	tolerated
L487L	C>T	0.001	0	S	-	-

Table 3: Coding variants in the PRKAG3 gene observed in this study. (MAF: minor allele frequency; S/NS: synonymous/nonsynonymous)

Given the established importance of homologous mutations in Rendement Napole (RN^-) pigs (γ_3R225Q) (3, 27, 32) and in the γ_2 subunit (R302Q/R61Q) in human patients (22), we pursued the functional significance of the novel R225W mutation identified in two unrelated subjects. A total of 11 subjects from the two families were screened for the R225W mutation. Two family members in the first family and three family members in the second family were observed to carry the mutation (Figure 10). Other sequence variants that are predicted to have functional implications according to PolyPhen and SIFT are shown in Table 3. Of interest are variants M197T, I269T, R307C and R340Q, all of which occur at similarly low frequencies in our cohorts.

Characteristics of R225W and Matched Control Subjects

The five carriers of the R225W variant were matched with control subjects on the basis of gender, age, weight, and BMI. The R225W carriers and control subjects were also well-matched for amount and intensity of self-reported weekly physical activity. Two brothers of the proband in the first family, and the sister and daughter of the proband in the second family consented to muscle biopsies and were included in the study (Figure 10). No significant differences were noted in fasting values for plasma lipids, glucose, insulin, or HbA1c in this small cohort (Table 2). During a hyperinsulinemic glucose clamp study, the rate of glucose infusion required to maintain euglycemia in the last hour of the clamp was somewhat higher in the 2 carriers of the R225W variant as compared

to 2 closely matched controls but did not reach a nominal standard of significance (7.3 ± 0.8 *vs.* 5.4± 2.4 ml/kg/min, p=0.16).

Basal and AMP-Activated AMPK Activity

We determined that the R225W mutation had an overall effect on AMPK activity. Myocytes derived from *vastus lateralis* biopsies were immunopurified and differentiated into myotubes, following which total AMPK activity was assayed using the 'gold-standard' SAMS peptide assay (16, 26) in purified protein extracts. Results demonstrated that the basal (p=0.015) as well as the AMP-activated (p=0.001) AMPK activities in subjects with the R225W mutation were two-fold higher compared to that found in controls (Figure 11).

Control subjects exhibited a 0.054 pmol/min/mg mean increase in activity upon AMP-stimulation, whereas R225W carriers showed a mean increase of 0.108 pmol/min/mg, representing a 65% and a 58% increase from basal activity, respectively. Although R225W carriers demonstrate twice the AMP-stimulated AMPK activity of control subjects, the similar percent increases indicate that R225W AMPK is likely activated by AMP with a similar magnitude to control AMPK. R225W AMPK is therefore not constitutively active or AMP-independent, as it is able to be further activated by AMP.

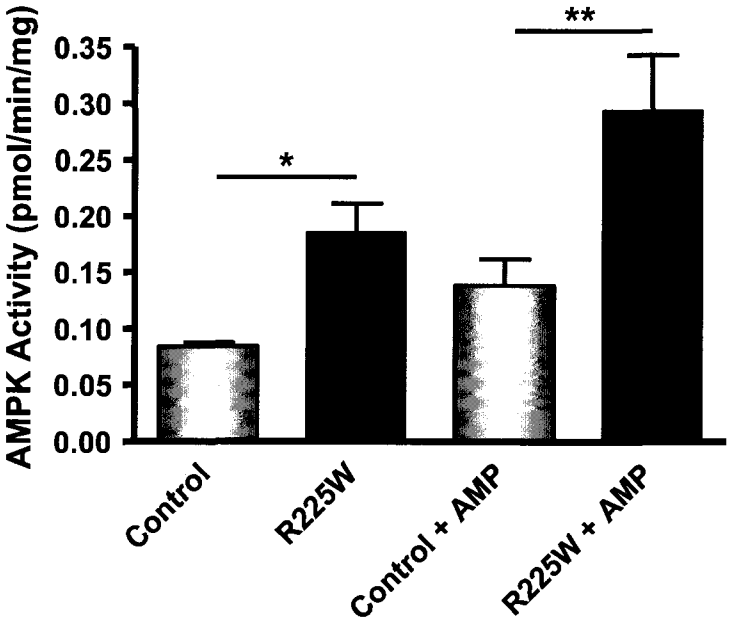

Figure 11: Basal and AMP-activated AMPK activities in differentiated skeletal muscle cells from R225W carriers and matched control subjects. Means +/- SD. n=3, One-way ANOVA, Tukey post-test, *p=0.015, **p=0.001.

Expression of AMPK γ Isoforms

AMPKγ_3 mRNA levels in skeletal muscle biopsy samples were detected by RT-PCR analysis. There was no difference in AMPKγ_3 mRNA levels between R225W carriers and control subjects (p=0.083, 2-tailed t-test). AMPKγ_1 and γ_3 protein levels were detected by Western blotting in the same purified protein extracts as used for the AMPK activity assay. β-actin was used as the loading control and densitometry was carried out to determine relative protein levels. There were no differences in either AMPKγ_1 or γ_3 protein levels between R225W carriers and control subjects (p=0.389 and p=0.229, respectively) (Figure 12a and b).

Importantly, the only three complexes that normally contribute to AMPK activity in human *vastus lateralis* are $\alpha_1\beta_2\gamma_1$, $\alpha_2\beta_2\gamma_1$ and $\alpha_2\beta_2\gamma_3$ (8). We think that the R225W variant is affecting AMPK activity without affecting the level of transcription or translation of the *PRKAG3* gene.

Skeletal Muscle Glycogen Content

To determine the effect of the R225W mutation on skeletal muscle glycogen content, we used Periodic Acid Schiff (PAS) staining of cryo-sectioned *vastus lateralis* muscle. As shown in Figure 13, muscle of R225W carriers had approximately 90% more muscle glycogen content than controls (p=0.002). This result was expected as the Hampshire RN$^-$ pigs carrying the R225Q γ_3AMPK mutation have increased muscle glycogen content (32).

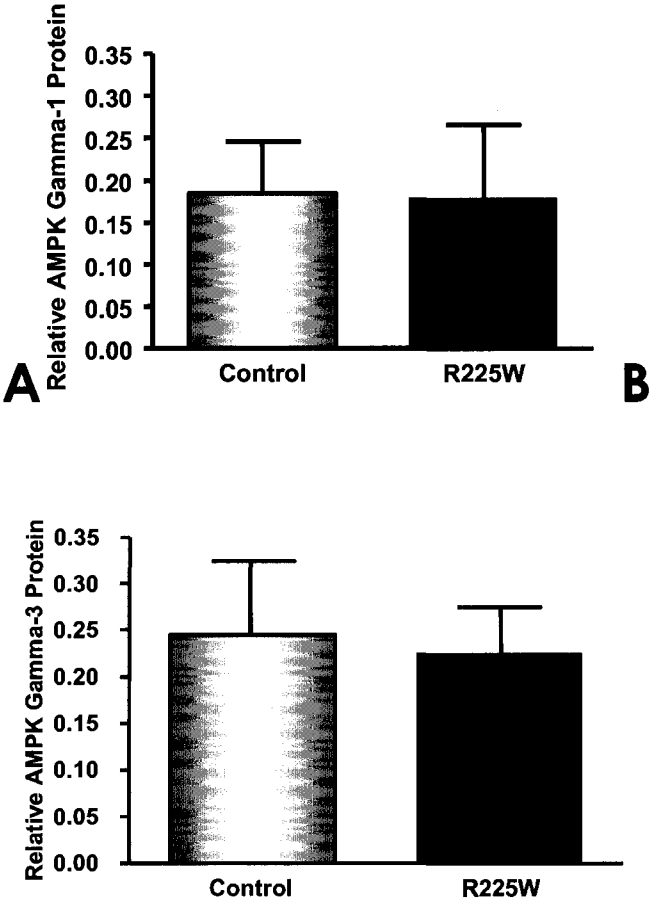

Figure 12: Relative protein levels of the γ_1 (A) and γ_3 (B) isoforms in differentiated skeletal muscle cells from R225W carriers and matched control subjects. The integrated densitometry value (IDV) for each γ subunit was divided by the IDV of the loading control, β-actin. Means +/- SD. n=2-4, Student's *t*-test, p=0.389 (A), p=0.229 (B).

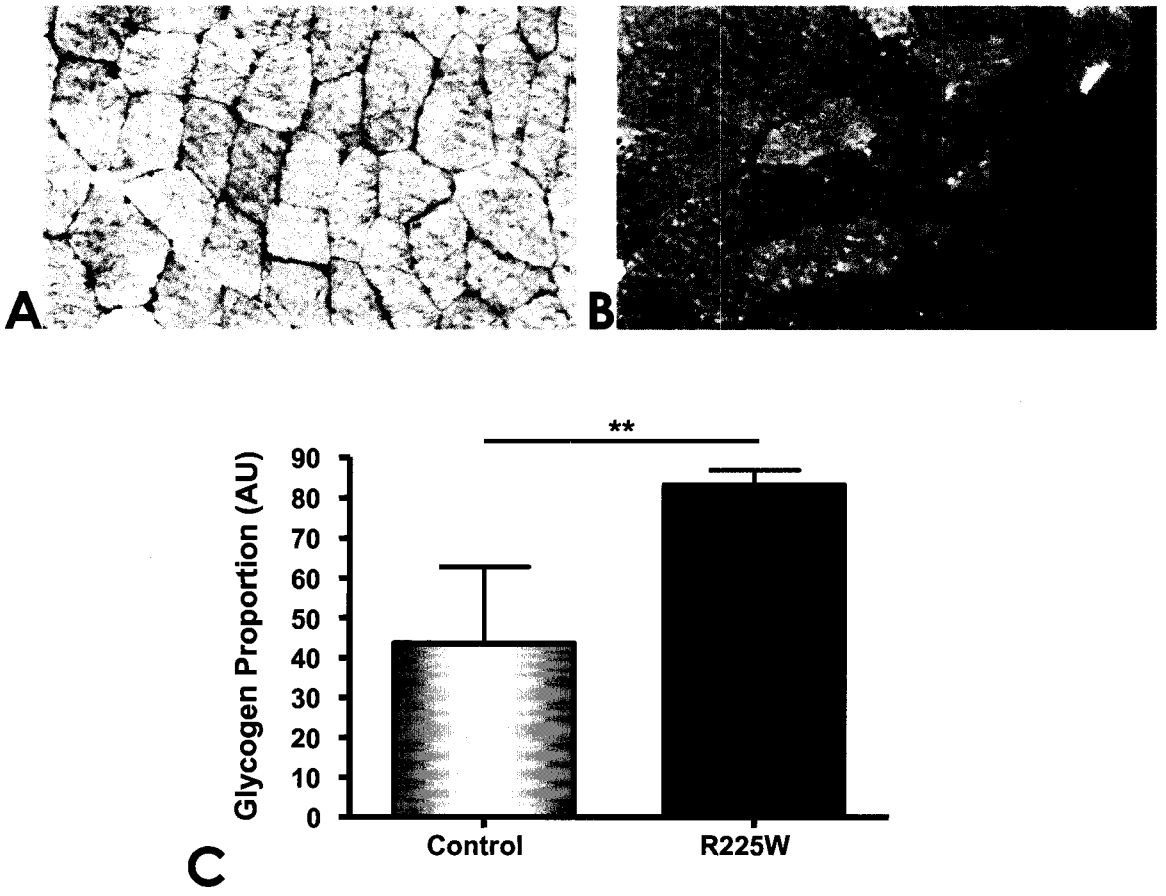

Figure 13: Glycogen content of *vastus lateralis* for R225W and control subjects. Muscle sections were prepared and stained with PAS, as described in the methods section (A: control, B: R225W). C: quantification of glycogen content via imaging software. Means +/- SD. n=5, Student's *t*-test, **p=0.002.

Intramuscular Triglyceride (IMTG) Content

We hypothesized that IMTG would be reduced in skeletal muscle of subjects with the R225W variant, given observations in transgenic mice expressing the homologous mutation in the AMPK γ_3 gene and fed a high fat diet (6). Osmium tetroxide (OsO_4) staining of sections of the *vastus lateralis* muscle indicated lower IMTG levels in the R225W carriers as compared to matched controls ($p=0.032$) (Figure 14).

Vastus Lateralis Muscle Fiber Type Composition

Finally, we determined whether or not there were differences in muscle fiber type composition in the biopsied muscle. Immunohistochemistry of the sections revealed a similar proportional distribution of fiber types in subjects with the R225W mutation compared to controls (Figure 15).

Fiber type ratio is an important measure due to its influence on muscle glycogen content and IMTG content. Since there are no differences in fiber type ratio between R225W subjects and controls, differences in glycogen and IMTG cannot be attributed to fiber type composition.

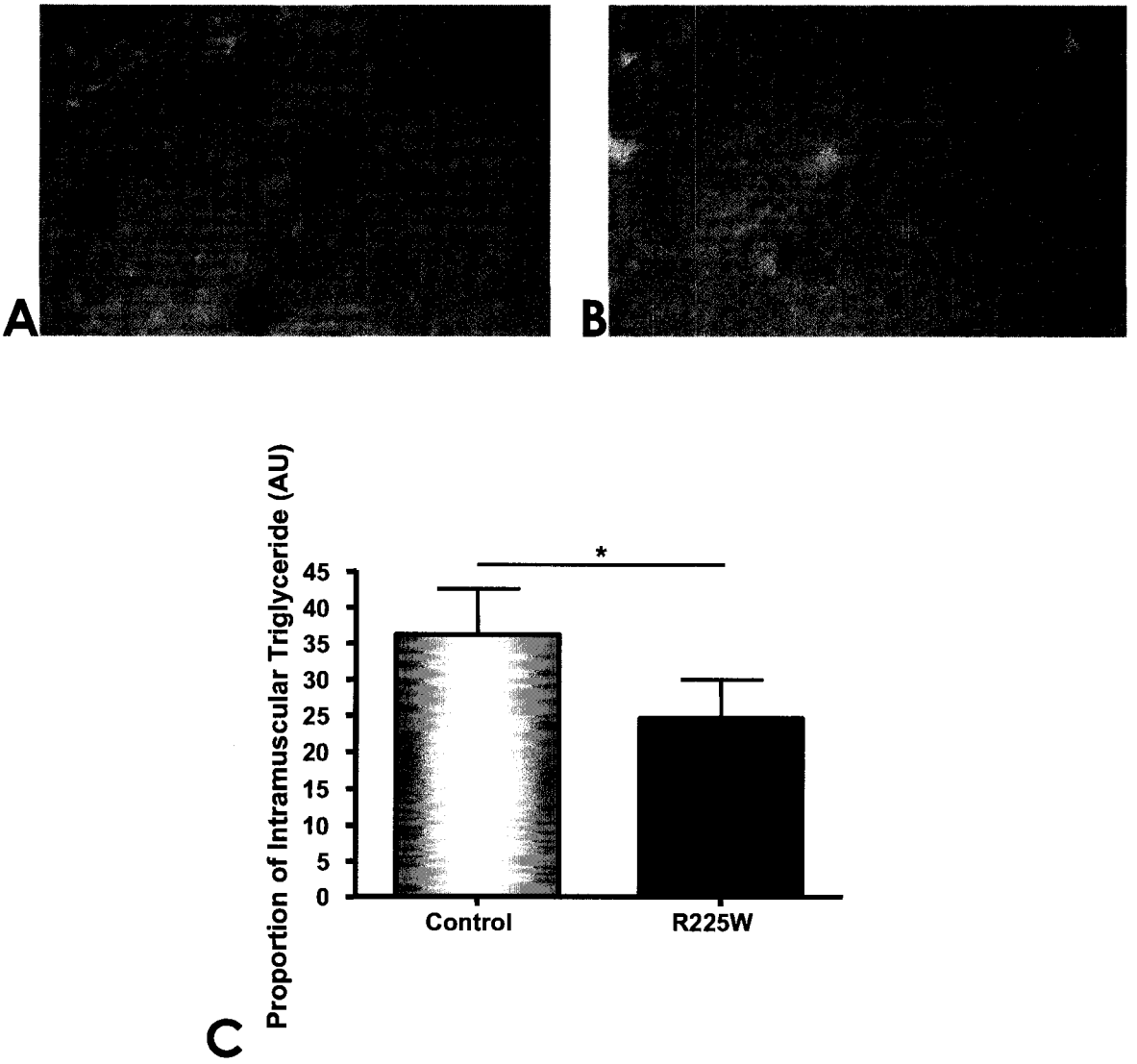

Figure 14: Intramuscular triglyceride content of *vastus lateralis* for R225W and control subjects. Muscle sections were prepared and stained with OsO_4, as described in the methods section (A: control, B: R225W). C: quantification of IMTG via imaging software. Means +/- SD. n=4, Student's *t*-test, *p=0.032.

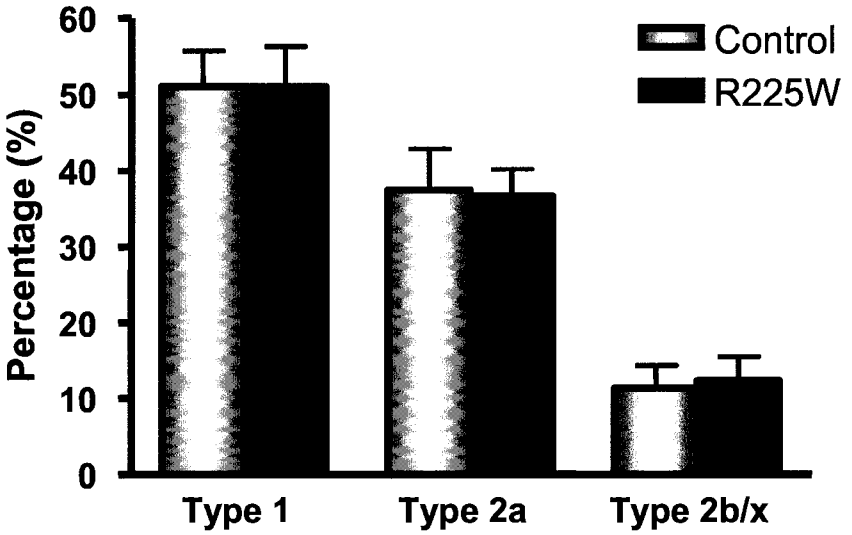

Figure 15: Fiber type ratios of *vastus lateralis* for R225W versus control subjects, expressed as percentage of each fiber type. Means +/- SD. n=5, Student's *t*-test for each fiber type, no significant differences between R225W and control subjects (Type 1: p=0.992, Type 2a: p=0.896, Type 2b/x: p=0.834).

Discussion

AMPK is widely recognized as a key metabolic regulator of energy expenditure in peripheral tissues and of energy intake in the hypothalamus. In this study we focused on the functional importance of a rare mutation in *PRKAG3* encoding the AMPK regulatory γ_3 subunit that is expressed exclusively in skeletal muscle. While the functions of the three AMPK subunits have not been fully characterized, it is becoming increasingly clear that the γ subunit is a major regulator of holoenzyme activity (17, 24, 25, 29). The γ subunit is thought to be involved in AMP binding, and in the regulation of glycogen content as variants in its CBS domains affect glycogen metabolism in skeletal and cardiac muscle (4, 13, 15, 32, 40). This is the first report of functional effects of nonsynonymous sequence variants in the γ_3 subunit in humans. We have demonstrated that the R225W mutation increases basal and AMP-activated AMPK activities in differentiated muscle cells obtained from the *vastus lateralis* of carriers (Figure 11), and that γ_1 and γ_3 protein levels are unchanged in R225W carriers (Figure 12). Normally in human *vastus lateralis*, the complexes that contribute to AMPK activity are $\alpha_1\beta_2\gamma_1$, $\alpha_2\beta_2\gamma_1$ and $\alpha_2\beta_2\gamma_3$ (8). Future studies will need to assess the subunit combinations that contribute to AMPK activity in R225W carriers. We have also demonstrated that R225W results in increased skeletal muscle glycogen content (Figure 13) and decreased IMTG content (Figure 14), while there was no change in muscle fiber type composition (Figure 15).

Further studies are required to characterize the effects of R225W on metabolic responses to challenges such as acute and chronic exercise. However, given the literature on Hampshire RN- pigs with an analogous γ_3 mutation (3, 27, 32), and the Tg-R225Qγ_3 mice (5, 20), it is anticipated that the human R225W variant would result in improved capacity during chronic exercise challenges due to their increased muscle glycogen. The natural occurrence of mutations in AMPKγ_3 was first discovered in Hampshire RN- pigs (3, 32). The single missense mutation, arginine 225 to glutamine (R225Q) results in a dominant mutation that is homologous to the γ_3 R225W variant described here. R225Q causes an approximate 70% increase in skeletal muscle glycogen, but no change in heart and liver glycogen content, resulting in poor meat quality. Other phenotypic effects include lower muscle fat content and increased oxidative capacity. Furthermore, Hampshire RN- pigs carrying the mutation showed normal resting levels of glucose and insulin as well as normal glucose tolerance tests. When challenged with exercise, it was found that R225Q pigs depleted their glycogen stores at normal rates, but re-synthesized glycogen at faster rates than control pigs due to increased muscle glucose uptake rates (3, 27). This limited evidence indicated no functional impairments associated with the increased glycogen in skeletal muscle. Our findings that human R225W carriers have an approximate 90% increase in skeletal muscle glycogen, an approximate 30% decrease in intramuscular triglyceride, and normal levels of plasma lipids, glucose, insulin

and HbA1c are consistent with the animal studies described above. Future studies will investigate the physiological response of these subjects to exercise challenges.

Recently mice bearing the homologous human AMPK γ_3 transgene, Tg-R225Q, were developed to study the effects of the naturally occurring pig mutation. The R225Q mutation produced a fully dominant protein (6) with increased AMPK activity. ACC phosphorylation was increased in the basal state as well as after stimulation with AICAR (an artificial activator of AMPK), indicating that the mutated AMPK could be activated (6). Glycogen content of various muscles in mice bearing the R225Q mutation have 1.5-2 times the glycogen content of controls (40), consistent with our findings in humans. Moreover, exercise increased ACC phosphorylation and decreased intramuscular triglyceride (IMTG) in the *gastrocnemius* muscle of transgenic, compared to wild-type, mice. Tg-R225Q mice thus oxidized more fat in the AMP-stimulated state (during exercise) compared to wild-type controls (5). As demonstrated in the current study, the R225Wγ_3 mutation in humans is a gain-of-function mutation that exhibits increased basal and AMP-activated activity of AMPK. It should be noted that total cellular AMPK activity was assayed in this study, not immuno-purified γ_3 activity. Therefore, the R225W mutation in γ_3 has an important effect overall on total AMPK activity in skeletal muscle. It will be of interest in future studies to determine whether the $\alpha_1\beta_2\gamma_1$, $\alpha_2\beta_2\gamma_1$ and $\alpha_2\beta_2\gamma_3$ subunit combinations

normally found in human *vastus lateralis* are also formed in skeletal muscle of R225W carriers.

Interestingly, this novel mutation is analogous to the γ_2 subunit mutation that causes inherited cardiac arrhythmias and cardiac hypertrophy (4, 21, 22). While it is known that AMPK activity stimulates fatty acid oxidation, glucose uptake and glycolysis in the heart, its regulation is complex, and still not well understood (17). Missense mutations within the CBS domains of γ_2 have been shown to cause the excess storage of glycogen in pronounced glycogen-associated vacuoles (15). This excess storage of glycogen is thought to result in myocyte hypertrophy, and gives rise to WPW syndrome and cardiac conduction disease (15). The enhanced skeletal muscle glycogen deposition demonstrated in carriers of the analogous γ_3 mutation is consistent with the above results in the heart. Subsequent introduction of some of the γ_2 mutations into the AMPK homologue in yeast (SNF1/SNF4) produced a constitutively active enzyme, indicating that these heterozygous missense mutations were dominant in their effect (4). Our findings indicate that the γ_3 R225W mutation increases basal AMPK activity, but results in a protein that can be further activated by AMP, unlike the latter γ_2 mutations.

In summary, we report the identification of human subjects bearing a R225W mutation in *PRKAG3* which causes increased basal and AMP-stimulated AMPK

activity, increased glycogen content and decreased IMTG in skeletal muscle. These findings are relevant to an improved understanding of the regulatory role that AMPK plays in skeletal muscle energy metabolism. The γ_3 subunit represents an attractive pharmacological target due to its exclusive expression in skeletal muscle. It has already been demonstrated that Metformin, commonly prescribed for treatment of type 2 diabetes, acts via stimulation of AMPK (19, 33, 41); and although it is not possible to draw conclusions regarding therapeutics from this study, it is tempting to hypothesize that the stimulation of AMPK activity in skeletal muscle alone, without affecting AMPK activity in the brain or heart, could be effective in the treatment of obesity and type 2 diabetes mellitus.

Acknowledgements

We would like to thank Linda Jui for histochemistry work, Heather Doelle, Brenda Bradley and Sybil Hébert for patient recruitment and assistance with clinical studies, Thet Naing for technical assistance, and Dr. Michael Gollob for critically reading the manuscript. The authors would also like to express their sincere thanks to the subjects who participated in this research.

References

1. **Ahituv, N., N. Kavaslar, W. Schackwitz, A. Ustaszewska, J. M. Collier, S. Hebert, H. Doelle, R. Dent, L. A. Pennacchio, and R. McPherson.** 2006. A PYY Q62P variant linked to human obesity. Hum Mol Genet **15**:387-91.

2. **Ahituv, N., N. Kavaslar, W. Schackwitz, A. Ustaszewska, J. Martin, S. Hebert, H. Doelle, B. Ersoy, G. Kryukov, S. Schmidt, N. Yosef, E. Ruppin, R. Sharan, C. Vaisse, S. Sunyaev, R. Dent, J. Cohen, R. McPherson, and L. A. Pennacchio.** 2007. Medical sequencing at the extremes of human body mass. Am J Hum Genet **80**:779-91.

3. **Andersson, L.** 2003. Identification and characterization of AMPK gamma 3 mutations in the pig. Biochem Soc Trans **31**:232-5.

4. **Arad, M., D. W. Benson, A. R. Perez-Atayde, W. J. McKenna, E. A. Sparks, R. J. Kanter, K. McGarry, J. G. Seidman, and C. E. Seidman.** 2002. Constitutively active AMP kinase mutations cause glycogen storage disease mimicking hypertrophic cardiomyopathy. J Clin Invest **109**:357-62.

5. **Barnes, B. R., Y. C. Long, T. L. Steiler, Y. Leng, D. Galuska, J. F. Wojtaszewski, L. Andersson, and J. R. Zierath.** 2005. Changes in Exercise-Induced Gene Expression in 5'-AMP-Activated Protein Kinase {gamma}3-Null and {gamma}3 R225Q Transgenic Mice. Diabetes **54**:3484-9.

6. **Barnes, B. R., S. Marklund, T. L. Steiler, M. Walter, G. Hjalm, V. Amarger, M. Mahlapuu, Y. Leng, C. Johansson, D. Galuska, K. Lindgren, M. Abrink, D. Stapleton, J. R. Zierath, and L. Andersson.** 2004. The 5'-AMP-activated protein kinase gamma3 isoform has a key role in carbohydrate and lipid metabolism in glycolytic skeletal muscle. J Biol Chem **279**:38441-7.

7. **Bergeron, R., S. F. Previs, G. W. Cline, P. Perret, R. R. Russell, 3rd, L. H. Young, and G. I. Shulman.** 2001. Effect of 5-aminoimidazole-4-carboxamide-1-beta-D-ribofuranoside infusion on in vivo glucose and lipid metabolism in lean and obese Zucker rats. Diabetes **50**:1076-82.

8. **Birk, J. B., and J. F. Wojtaszewski.** 2006. Predominant alpha2/beta2/gamma3 AMPK activation during exercise in human skeletal muscle. J Physiol **577**:1021-32.

9. **Buhl, E. S., N. Jessen, R. Pold, T. Ledet, A. Flyvbjerg, S. B. Pedersen, O. Pedersen, O. Schmitz, and S. Lund.** 2002. Long-term AICAR administration reduces metabolic disturbances and lowers blood pressure in rats displaying features of the insulin resistance syndrome. Diabetes **51:**2199-206.

10. **Buhl, E. S., N. Jessen, O. Schmitz, S. B. Pedersen, O. Pedersen, G. D. Holman, and S. Lund.** 2001. Chronic treatment with 5-aminoimidazole-4-carboxamide-1-beta-D-ribofuranoside increases insulin-stimulated glucose uptake and GLUT4 translocation in rat skeletal muscles in a fiber type-specific manner. Diabetes **50:**12-7.

11. **Burwinkel, B., J. W. Scott, C. Buhrer, F. K. van Landeghem, G. F. Cox, C. J. Wilson, D. Grahame Hardie, and M. W. Kilimann.** 2005. Fatal congenital heart glycogenosis caused by a recurrent activating R531Q mutation in the gamma 2-subunit of AMP-activated protein kinase (PRKAG2), not by phosphorylase kinase deficiency. Am J Hum Genet **76:**1034-49.

12. **Carling, D.** 2004. The AMP-activated protein kinase cascade--a unifying system for energy control. Trends Biochem Sci **29:**18-24.

13. **Cheung, P. C., I. P. Salt, S. P. Davies, D. G. Hardie, and D. Carling.** 2000. Characterization of AMP-activated protein kinase gamma-subunit isoforms and their role in AMP binding. Biochem J **346 Pt 3:**659-69.

14. **Crute, B. E., K. Seefeld, J. Gamble, B. E. Kemp, and L. A. Witters.** 1998. Functional domains of the alpha1 catalytic subunit of the AMP-activated protein kinase. J Biol Chem **273:**35347-54.

15. **Daniel, T., and D. Carling.** 2002. Functional analysis of mutations in the gamma 2 subunit of AMP-activated protein kinase associated with cardiac hypertrophy and Wolff-Parkinson-White syndrome. J Biol Chem **277:**51017-24.

16. **Davies, S. P., D. Carling, and D. G. Hardie.** 1989. Tissue distribution of the AMP-activated protein kinase, and lack of activation by cyclic-AMP-dependent protein kinase, studied using a specific and sensitive peptide assay. Eur J Biochem **186:**123-8.

17. **Dyck, J. R. B., and G. D. Lopaschuk.** 2006. AMPK alterations in cardiac physiology and pathology: enemy or Ally? J Physiol (Lond):jphysiol.2006.109389.

18. **Frosig, C., S. B. Jorgensen, D. G. Hardie, E. A. Richter, and J. F. Wojtaszewski.** 2004. 5'-AMP-activated protein kinase activity and protein expression are regulated by endurance training in human skeletal muscle. Am J Physiol Endocrinol Metab **286:**E411-7.

19. **Fryer, L. G., A. Parbu-Patel, and D. Carling.** 2002. The Anti-diabetic drugs rosiglitazone and metformin stimulate AMP-activated protein kinase through distinct signaling pathways. J Biol Chem **277:**25226-32.

20. **Fujii, N., N. Jessen, and L. J. Goodyear.** 2006. AMP-activated protein kinase and the regulation of glucose transport. Am J Physiol Endocrinol Metab **291:**E867-77.

21. **Gollob, M. H., M. S. Green, A. S. Tang, T. Gollob, A. Karibe, A. S. Ali Hassan, F. Ahmad, R. Lozado, G. Shah, L. Fananapazir, L. L. Bachinski, and R. Roberts.** 2001. Identification of a gene responsible for familial Wolff-Parkinson-White syndrome. N Engl J Med **344:**1823-31.

22. **Gollob, M. H., J. J. Seger, T. N. Gollob, T. Tapscott, O. Gonzales, L. Bachinski, and R. Roberts.** 2001. Novel PRKAG2 mutation responsible for the genetic syndrome of ventricular preexcitation and conduction system disease with childhood onset and absence of cardiac hypertrophy. Circulation **104:**3030-3.

23. **Hamilton, S. R., D. Stapleton, J. B. O'Donnell, Jr., J. T. Kung, S. R. Dalal, B. E. Kemp, and L. A. Witters.** 2001. An activating mutation in the gamma1 subunit of the AMP-activated protein kinase. FEBS Lett **500:**163-8.

24. **Hardie, D. G., and D. Carling.** 1997. The AMP-activated protein kinase--fuel gauge of the mammalian cell? Eur J Biochem **246:**259-73.

25. **Hardie, D. G., and K. Sakamoto.** 2006. AMPK: a key sensor of fuel and energy status in skeletal muscle. Physiology (Bethesda) **21:**48-60.

26. **Hardie, D. G., Salt, I. P., Davies, S. P.** 2000. Analysis of the role of the AMP-activated protein kinase in the response to cellular stress. Methods Mol. Biol. **99:**63-74.

27. **Hedegaard, J., P. Horn, R. Lametsch, H. Sondergaard Moller, P. Roepstorff, C. Bendixen, and E. Bendixen.** 2004. UDP-glucose pyrophosphorylase is upregulated in carriers of the porcine RN- mutation in the AMP-activated protein kinase. Proteomics **4:**2448-54.

28. **Ingham, K. C.** 1990. Precipitation of proteins with polyethylene glycol. Methods Enzymol **182:**301-6.

29. **Kahn, B. B., T. Alquier, D. Carling, and D. G. Hardie.** 2005. AMP-activated protein kinase: ancient energy gauge provides clues to modern understanding of metabolism. Cell Metab **1:**15-25.

30. **Lang, T., L. Yu, Q. Tu, J. Jiang, Z. Chen, Y. Xin, G. Liu, and S. Zhao.** 2000. Molecular cloning, genomic organization, and mapping of PRKAG2, a heart abundant gamma2 subunit of 5'-AMP-activated protein kinase, to human chromosome 7q36. Genomics **70:**258-63.

31. **Mahlapuu, M., C. Johansson, K. Lindgren, G. Hjalm, B. R. Barnes, A. Krook, J. R. Zierath, L. Andersson, and S. Marklund.** 2004. Expression profiling of the gamma-subunit isoforms of AMP-activated protein kinase suggests a major role for gamma3 in white skeletal muscle. Am J Physiol Endocrinol Metab **286:**E194-200.

32. **Milan, D., J. T. Jeon, C. Looft, V. Amarger, A. Robic, M. Thelander, C. Rogel-Gaillard, S. Paul, N. Iannuccelli, L. Rask, H. Ronne, K. Lundstrom, N. Reinsch, J. Gellin, E. Kalm, P. L. Roy, P. Chardon, and L. Andersson.** 2000. A mutation in PRKAG3 associated with excess glycogen content in pig skeletal muscle. Science **288:**1248-51.

33. **Musi, N., M. F. Hirshman, J. Nygren, M. Svanfeldt, P. Bavenholm, O. Rooyackers, G. Zhou, J. M. Williamson, O. Ljunqvist, S. Efendic, D. E. Moller, A. Thorell, and L. J. Goodyear.** 2002. Metformin increases AMP-activated protein kinase activity in skeletal muscle of subjects with type 2 diabetes. Diabetes **51:**2074-81.

34. **Ng, P. C., and S. Henikoff.** 2002. Accounting for human polymorphisms predicted to affect protein function. Genome Res **12:**436-46.

35. **Nielsen, J. N., K. J. Mustard, D. A. Graham, H. Yu, C. S. MacDonald, H. Pilegaard, L. J. Goodyear, D. G. Hardie, E. A. Richter, and J. F. Wojtaszewski.** 2003. 5'-AMP-activated protein kinase activity and subunit expression in exercise-trained human skeletal muscle. J Appl Physiol **94:**631-41.

36. **Ramensky, V., P. Bork, and S. Sunyaev.** 2002. Human non-synonymous SNPs: server and survey. Nucleic Acids Res **30:**3894-900.

37. **Scott, J. W., S. A. Hawley, K. A. Green, M. Anis, G. Stewart, G. A. Scullion, D. G. Norman, and D. G. Hardie.** 2004. CBS domains form energy-sensing modules whose binding of adenosine ligands is disrupted by disease mutations. J Clin Invest **113**:274-84.

38. **Winder, W. W., and D. G. Hardie.** 1999. AMP-activated protein kinase, a metabolic master switch: possible roles in type 2 diabetes. Am J Physiol **277**:E1-10.

39. **Wojtaszewski, J. F., J. B. Birk, C. Frosig, M. Holten, H. Pilegaard, and F. Dela.** 2005. 5'AMP activated protein kinase expression in human skeletal muscle: effects of strength training and type 2 diabetes. J Physiol **564**:563-73.

40. **Yu, H., M. F. Hirshman, N. Fujii, J. M. Pomerleau, L. E. Peter, and L. J. Goodyear.** 2006. Muscle-specific overexpression of wild type and R225Q mutant AMP-activated protein kinase gamma3-subunit differentially regulates glycogen accumulation. Am J Physiol Endocrinol Metab **291**:E557-65.

41. **Zhou, G., R. Myers, Y. Li, Y. Chen, X. Shen, J. Fenyk-Melody, M. Wu, J. Ventre, T. Doebber, N. Fujii, N. Musi, M. F. Hirshman, L. J. Goodyear, and D. E. Moller.** 2001. Role of AMP-activated protein kinase in mechanism of metformin action. J Clin Invest **108**:1167-74.

Chapter 2

Effects of the Presence, Absence and Overexpression of Uncoupling Protein-3 on Adiposity and Fuel Metabolism in Congenic Mice

Sheila R. Costford, Shehla N. Chaudhry, Mahmoud Salkhordeh, and Mary-Ellen Harper

Am J Physiol Endocrinol Metab. 2006 Jun;290(6):E1304-12. Epub 2006 Jan 24.

Department of Biochemistry, Microbiology and Immunology
Faculty of Medicine, University of Ottawa
451 Smyth Rd., Ottawa, Ontario
Canada, K1H 8M5

Running Head: Effects of UCP3 on Adiposity and Fuel Metabolism

Brief Description of Contents

This manuscript was published electronically in January 2006 and then published in print in the American Journal of Physiology: Endocrinology and Metabolism in June of 2006. It describes the whole body energetics and development of insulin resistance in mice overexpressing or lacking uncoupling protein-3 (UCP3) compared to wildtype control animals. Paradoxically, both overexpressor and knockout mice showed protection from the development of insulin resistance as assessed by glucose and insulin tolerance tests. Overexpressor mice were leaner, had lower fat pad weights, and when challenged with a high fat diet, stored less intramuscular triglyceride (IMTG). Knockout mice took up more 2-deoxy-D-[1-^{3}H]-glucose into brown adipose tissue, incorporated more 2-deoxy-D-[1-^{3}H]-glucose into liver glycogen and when challenged with a high fat diet, stored more IMTG. Results are consistent with a role for UCP3 in preventing accumulation of triglyceride in both adipose tissue and muscle.

Contribution of Collaborators

Sheila R. Costford

Mouse colony maintenance: changed cages, fed mice, weighed mice and rodent diet. Performed all experiments (with the exception of histological staining), analyzed all data, contributed all tables and figures, wrote the first draft of the manuscript, participated in the editing and submission of the manuscript.

Shehla N. Chaudhry

Assisted with mouse colony maintenance and the performance of all experiments (with the exception of histological staining).

Mahmoud Salkhordeh

Assisted with mouse colony maintenance and the performance of glucose and insulin tolerance tests, as well as 2-deoxy-[1-^{3}H]-glucose-6-phosphate uptake into tissues and incorporation into liver glycogen experiments.

Mary-Ellen Harper

Conceived and designed the study, contributed to data analysis, edited and submitted manuscript.

Abstract

Uncoupling protein-3 (UCP3) is a poorly understood mitochondrial inner membrane protein expressed predominantly in skeletal muscle. The aim of this study was to examine the effects of the absence or constitutive physiological overexpression of *UCP3* on whole body energy metabolism, glucose tolerance and muscle triglyceride content. Congenic male *Ucp3 -/-*, wildtype, and *UCP3tg* overexpressor mice were fed a 10% fat diet for 4 or 8 months following weaning. *UCP3tg* mice had lower body weights and were less metabolically efficient than wildtype or *Ucp3 -/-* mice, but were not hyperphagic. *UCP3tg* mice had smaller epididymal white adipose tissue and brown adipose tissue (BAT) depots, however there were no differences in muscle weights. Glucose and insulin tolerance tests revealed that both *UCP3tg* and *Ucp3 -/-* mice were protected from development of impaired glucose tolerance and were more sensitive to insulin. 2-deoxy-D-[1-^{3}H]-glucose tracer studies showed increased uptake of glucose into BAT and increased storage of liver glycogen in *Ucp3 -/-* mice. Assessments of intramuscular triglyceride (IMTG) revealed decreases in quadriceps of *UCP3tg* mice compared to wildtype and *Ucp3 -/-* mice. When challenged with a 45% fat diet, *Ucp3 -/-* mice showed increased accumulation of IMTG compared to wildtype mice, which in turn had greater IMTG than *UCP3tg*

mice. Results are consistent with a role for UCP3 in preventing accumulation of triglyceride in both adipose tissue and muscle.

Key Words: Intramuscular triglyceride, obesity, glucose tolerance, insulin resistance, skeletal muscle

Introduction

Lipotoxicity is the detrimental accumulation of lipids and lipid metabolites in tissues other than adipose tissue (e.g., liver, heart or skeletal muscle). The accumulation of triglyceride in muscle (intramuscular triglyceride, IMTG) correlates well with impaired insulin-stimulated glucose uptake (27, 28). While IMTG is not related to BMI, age, fasting plasma triglycerides, non-esterified fatty acids, glucose or insulin, it is a determinant of insulin resistance (21). Insulin resistance is the best predictor of type 2 diabetes mellitus, and therefore there is a keen interest in understanding processes that are related to the accumulation of lipid in muscle.

There is evidence of a potential link between uncoupling protein-3 (UCP3) in muscle and protection against the development of type 2 diabetes. F1 generation mice overexpressing human *UCP3* 20-fold normal in skeletal muscle showed reduced fasting glucose and insulin levels, as well as increased glucose tolerance in response to an oral glucose tolerance test (9, 10). Interestingly, these mice were also reported to be hyperphagic despite being protected from the development of obesity. Patients with type 2 diabetes have been shown to have decreased UCP3 expression in *vastus lateralis* (30), and although initial studies revealed a negative correlation

between *UCP3* mRNA levels and BMI (31), later studies showed no association between UCP3 protein levels and body mass index (30).

UCP3 is a mitochondrial inner membrane protein of unknown function expressed predominantly in skeletal muscle (6). Since its identification in 1997, it has also been found to be expressed in brown adipose tissue (BAT), at low levels in the heart, and in certain parts of the brain (34, 35). *UCP3* was named due to its 57% sequence homology to uncoupling protein-1 (UCP1) (6, 34), which is expressed exclusively in BAT and serves to uncouple oxidative phosphorylation, resulting in the dissipation of energy as heat in response to cold or overfeeding (26). It was originally hypothesized that UCP3 would act to uncouple oxidative phosphorylation in muscle as UCP1 does in BAT (13), and, in fact, overexpression studies of *UCP3* in yeast yielded increased uncoupling (20, 38). However, it has since been demonstrated that this observed uncoupling may have been artifactual, due to very high levels of protein expression in the mitochondrial inner membrane (16, 32).

Physiologically, UCP3 expression is increased in response to fasting (3, 5, 8, 24), acute exercise (11, 33), and elevation of plasma lipids via high fat diet (14) or infusion of Intralipid (37), conditions in which reliance on fat oxidation is increased, regardless of any increases or decreases in energy expenditure. Moreover, unlike UCP1, UCP3 does not increase in response to cold

adaptation (5). These findings suggest that UCP3 is not likely involved in dissipating energy through uncoupling of oxidative phosphorylation, which would be detrimental to the organism during dietary energy deficits, but may indicate that UCP3 is involved in facilitating fat oxidation. A mechanism through which UCP3 could facilitate fatty acid oxidation was proposed (19) to involve a mitochondrial thioesterase functioning in tandem with UCP3. The former liberates the CoASH, which is in high demand during fatty acid oxidation, and the latter exports excess fatty acid anions. While several reports support such a role (4, 23, 25, 36), the molecular mechanism remains to be proved. Moreover, there is strong support for a role for UCP3 in the protection from reactive oxygen species (7, 23). Altogether, findings are consistent with the possibility that low levels of UCP3 could impair fat oxidation and therefore result in the accumulation of lipid in muscle, the onset of insulin resistance and the development of type 2 diabetes.

Our purpose here was to assess the metabolic impacts of the absence, presence and physiological levels of overexpression of *UCP3* in mice. We hypothesized that transgenic *UCP3* overexpressor mice (*UCP3tg*) would be protected from the development of insulin resistance whereas *Ucp3* knockout mice (*Ucp3* -/-) would be predisposed to the development of insulin resistance. Strengths of this study include the use of congenic lines of

mice, a defined diet, and levels of UCP3 overexpression that are physiological.

Materials and Methods

Treatment of Animals

Congenic male *Ucp3* -/-, wildtype (WT) and *UCP3tg* C57BL/6 mice (n=60) were housed individually and fed a defined rodent diet with 10 kcal% fat (Research Diets, D12450C, New Brunswick, NJ) *ad libitum* from weaning. An additional group of congenic male *Ucp3* -/-, wildtype and *UCP3tg* mice (n=15) were fed a 45 kcal% fat diet (Research Diets, D12451, New Brunswick, NJ) *ad libitum* from weaning for further intramuscular triglyceride studies. The D12450C diet consisted of 20% protein, 70% carbohydrate and 10% fat whereas the D12451 diet consisted of 20% protein, 35% carbohydrate and 45% fat by kcal. Protein from both diets was from casein and L-cysteine, carbohydrate was from corn starch, maltodextrin and sucrose, and fat was from soybean oil and lard. Food was given to mice inside the clear polycarbonate cages in which they were housed. *UCP3tg* mice, which overexpress human *UCP3* in skeletal muscle (~66-fold increase in mRNA) and at low levels in BAT (50% increase in mRNA), were provided originally by Dr. John Clapham at Glaxo-Smith-Kline (UK), the F1 generation of which has been previously described (10). *Ucp3* -/- mice on a mixed genetic background have also been previously described (15). Mice used in the current study had been backcrossed 10 generations into the C57BL/6 background to minimize effects of genetic background. Overexpressor mice

express UCP3 protein levels in skeletal muscle that are 2-2.5 fold of wildtype levels (4). Mice were maintained at 23°C with light from 0600-1800 and were studied from weaning to 4 or 8 months on the defined diets. Animals were cared for in accordance with the principles and guidelines of the Canadian Council on Animal Care and the Institute of Laboratory Animal Resources (National Research Council). The study was approved by the Animal Care Committee of the University of Ottawa.

Whole Body Analyses

Food intake was measured and mice were weighed semi-weekly from weaning to sacrifice. Food intake was calculated by dividing the total amount of energy ingested over the lifespan of the mouse by the number of days the mouse consumed the defined diet (4 or 8 months). The results are expressed as mean kcal ingested per day. Metabolic efficiency was calculated as total body weight gained divided by total amount of food consumed over 4 or 8 months and is expressed as mg body weight gained per kcal ingested. Naso-anal length and rectal body temperature were measured prior to sacrifice at the same time every day (Physitemp Thermalert, Model TH-8, Clifton, New Jersey).

Glucose and Insulin Tolerance Tests

Glucose and insulin tolerance tests were carried out (one week apart to allow mice to recover) after 1, 3, 4 and 8 months on the diet. Mice were fasted for 16 hours with water *ad libitum* prior to the test. Fasting blood glucose was determined by bleeding mice from the saphenous vein onto a glucometer (One Touch Basic, LifeScan, Burnaby, British Columbia). Mice were given an interperitoneal injection of 1 mg glucose (10% dextrose in sterile saline) or 1 x 10^{-4} units human insulin (Humalog Rapid Acting, Eli Lilly, in sterile saline) per g body weight. Blood glucose was assessed again at 10, 20, 30 and 120 min post-injection.

Indirect Calorimetry

Oxygen consumption (VO_2) and carbon dioxide production (VCO_2) of mice were measured using a customized four-chamber Oxymax system with automatic temperature and light controls (Columbus Instruments, Columbus, OH). Temperature was maintained at 24°C and lights were on from 0600-1800. System settings included a flow rate of 0.5 L/min, a sample line-purge time of 2 min, and a measurement period of 60 s every twelve min. Mice were placed in separate 2.5 L calorimetry chambers with *ad libitum* access to the defined diet and water. 24-hour energy expenditure was expressed as percent relative cumulative frequencies of all points collected throughout a

24-hour period, as described previously (2, 29). Respiratory exchange ratios (RER) were calculated as the ratio of VCO_2 divided by VO_2.

Analysis of 2-Deoxy-[1-^{3}H]-glucose-6-phosphate in Tissue

This procedure was carried out as detailed in Wang *et al.*, 2003 (36), with minor modifications. At 4 months, half of the mice were fasted for 16 hours. Mice were given an intraperitoneal injection of 0.5 µCi 2-deoxy-[1-^{3}H]-glucose mixed with 10% dextrose to provide a fixed specific activity at 1 g glucose per kg body weight. Mice were decapitated 70 min post-injection, and quadriceps, gastrocnemius, diaphragm, interscapular brown adipose tissue (BAT), epididymal white adipose tissue (EWAT), liver, pancreas and heart were dissected and flash frozen in liquid nitrogen. Thawed tissues were homogenized in 2% $HClO_4$ (10 µl per mg tissue) and left at 4°C overnight. Homogenates were centrifuged for 10 min at 2000 g and supernatants were neutralized to pH 7.4 with 2 M KOH. Total [^{3}H]-radioactivity was measured in half the volume of the supernatant, and the other half of the supernatant was added to a column filled with anion exchange resin (Ag1-X8) (BioRad, Mississauga, Ontario, Canada). Free 2-deoxyglucose was eluted with 12 ml of water and 2-deoxyglucose-6-phosphate was eluted with 10 ml 0.4 M ammonium acetate/0.5 M formic acid. [^{3}H]-radioactivity was measured in 2-deoxyglucose and 2-deoxyglucose-6-phosphate eluantes. Tissue glucose

uptake (pmol/g/min wet tissue) was calculated by dividing tissue [^{3}H]-2-deoxyglucose-6-phosphate activity by the glucose specific activity.

Analysis of 2-Deoxy-[1-^{3}H]-glucose-6-phosphate in Liver Glycogen

This procedure was carried out as detailed in Wang *et al.*, 2003 (36), with minor modifications. Liver samples were homogenized, extracted and neutralized as tissues undergoing [^{3}H]-2-deoxyglucose-6-phosphate analysis. 500 µl KOH containing 2.5% oyster glycogen and 100 µl 0.2% Na_2SO_4 were added to 500 ul of neutralized supernatant. Glycogen was precipitated with 1 ml ethanol, centrifuged for 15 min at 850 g at 4°C, and the pellet was washed with 66% ethanol before resuspension in 1 ml distilled water and counted for [^{3}H]-radioactivity.

Intramuscular Triglyceride Determination

After 8 months, quadriceps muscles from mice fed the 10% fat diet and from mice fed the 45% fat diet were fixed in 10% buffered neutral formalin. Tissues were trimmed no thicker than 4mm, rinsed in dH_2O, and left in 0.17M potassium dichromate 0.08M osmium tetroxide solution for 8 hours (1). Tissues were left under running H_2O for 2 hours and then processed in an automatic tissue processor, embedded in paraffin and cut in 5um sections. Tissues were mounted on glass slides and then incubated at 42°C overnight. Imaging software (Northern Eclipse) was used to analyze tissues at 10X magnification

with an Axiophot light microscope (Axiophot, Zeiss, Oberkochen, Germany). Images from fields in 9-12 sections per mouse were selected and converted into 8-bit grayscale. The number of sections per mouse depended on the amount of quadriceps muscle available for histological staining, and therefore varied somewhat. Images (fields of view) consisted of the entire section (this was consistent between mice). Threshold was set at 0 to 99. IMTG was measured as a proportion of surface area of each field.

Brown Adipose Tissue Histology

Brown adipose tissue (BAT) was fixed in 10% buffered neutral formalin and subjected to standard histological methods for staining with hematoxylin and eosin.

Results

Whole Body

UCP3tg mice had lower body weights than both wildtype and *Ucp3 -/-* mice at both 4 and 8 months, however there were no differences in linear growth, as assessed by naso-anal length (Table 4).

At 8 months, *UCP3tg* mice were less metabolically efficient than both wildtype and *Ucp3 -/-* mice. This trend was also present at 4 months, but did not reach statistical significance. There were no differences in food intake or body temperature between genotypes at either 4 or 8 months (Table 4). *UCP3tg* mice had lower quadriceps weights compared to wildtype mice at 4 months, but this difference disappeared by 8 months (Table 5).

UCP3tg mice had lower diaphragm weights compared to wildtype and *Ucp3 -/-* mice at 4 months, but these differences also disappeared by 8 months (Table 5). *UCP3tg* mice had lower EWAT and BAT weights than both wildtype and *Ucp3 -/-* mice at both 4 and 8 months (Table 5). *UCP3tg* mice also had lower liver weights compared to wildtype mice at both 4 and 8 months (Table 5).

4 months	***UCP3tg***	**WT**	*Ucp3* **-/-**	**p-value**
Body Weight (g)	29.3 ± 1.1	35.2 ± 0.9	35.1 ± 1.2	<0.01 *UCP3tg* vs WT *UCP3tg* vs *Ucp3* -/-
Metabolic Efficiency (mg/kcal)	17.7 ± 0.7	19.5 ± 0.9	19.0 ± 0.7	>0.05
Food Intake (kcal/d)	9.4 ± 0.4	9.6 ± 0.2	9.8 ± 0.2	>0.05
8 months	***UCP3tg***	**WT**	*Ucp3* **-/-**	**p-value**
Body Weight (g)	34.3 ± 1.6	41.2 ± 0.7	40.0 ± 2.4	<0.01 *UCP3tg* vs WT <0.05 *UCP3tg* vs *Ucp3* -/-
Body Temp (°C)	34.0 ± 0.9	35.0 ± 0.9	35.4 ± 0.6	>0.05
Naso-Anal Length (cm)	8.4 ± 0.3	8.3 ± 0.2	8.4 ± 0.2	>0.05
Metabolic Efficiency (mg/kcal)	8.3 ± 0.7	10.9 ± 0.3	10.7 ± 1.0	<0.01 *UCP3tg* vs WT <0.05 *UCP3tg* vs *Ucp3* -/-
Food Intake (kcal/d)	11.6 ± 0.2	12.0 ± 0.2	12.0 ± 0.5	>0.05

Table 4: Whole body measurements. Means ± SEM, n=10. One-way ANOVA, Tukey post-test. *UCP3tg* mice have lower body weights at 4 and 8 months, as well as lower metabolic efficiencies at 8 months.

4 months Tissue (g)	***UCP3tg***	**WT**	*Ucp3* **-/-**	**p-value**
Soleus	0.03 ± 0.00	0.03 ± 0.00	0.03 ± 0.00	>0.05
Gastrocnemius	0.31 ± 0.01	0.34 ± 0.01	0.33 ± 0.02	>0.05
Quadriceps	0.27 ± 0.02	0.34 ± 0.01	0.31 ± 0.02	<0.01 *UCP3tg* vs WT
Diaphragm	0.06 ± 0.01	0.09 ± 0.01	0.10 ± 0.00	<0.01 *UCP3tg* vs WT *UCP3tg* vs *Ucp3 -/-*
EWAT	0.94 ± 0.14	1.72 ± 0.17	1.60 ± 0.17	<0.01 *UCP3tg* vs WT <0.05 *UCP3tg* vs *Ucp3 -/-*
BAT	0.09 ± 0.01	0.14 ± 0.01	0.13 ± 0.01	<0.05 *UCP3tg* vs WT *UCP3tg* vs *Ucp3 -/-*
Pancreas	0.20 ± 0.01	0.21 ± 0.01	0.21 ± 0.02	>0.05
Liver	0.99 ± 0.04	1.19 ± 0.04	1.12 ± 0.07	<0.05 *UCP3tg* vs WT
Heart	0.16 ± 0.01	0.16 ± 0.01	0.16 ± 0.01	>0.05
Spleen	0.08 ± 0.01	0.06 ± 0.01	0.07 ± 0.00	>0.05

8 months Tissue (g)	***UCP3tg***	**WT**	*Ucp3 -/-*	**p-value**
Soleus	0.02 ± 0.00	0.03 ± 0.00	0.03 ± 0.01	>0.05
Gastrocnemius	0.34 ± 0.01	0.32 ± 0.01	0.33 ± 0.01	>0.05
Quadriceps	0.31 ± 0.02	0.32 ± 0.01	0.30 ± 0.02	>0.05
Diaphragm	0.10 ± 0.01	0.10 ± 0.01	0.11 ± 0.01	>0.05
EWAT	1.39 ± 0.20	2.18 ± 0.09	2.14 ± 0.31	<0.01 *UCP3tg* vs WT <0.05 *UCP3tg* vs *Ucp3 -/-*
BAT	0.20 ± 0.03	0.37 ± 0.02	0.35 ± 0.06	<0.01 *UCP3tg* vs WT <0.05 *UCP3tg* vs *Ucp3 -/-*
Pancreas	0.22 ± 0.01	0.22 ± 0.01	0.22 ± 0.02	>0.05
Liver	1.41 ± 0.11	2.07 ± 0.14	1.97 ± 0.30	<0.05 *UCP3tg* vs WT
Heart	0.32 ± 0.16	0.16 ± 0.01	0.17 ± 0.01	>0.05
Spleen	0.08 ± 0.01	0.09 ± 0.00	0.09 ± 0.00	>0.05

Table 5: Tissue wet weights. Means ± SEM, n=10. One-way ANOVA, Tukey post-test. *UCP3tg* mice have lower epididymal white adipose tissue (EWAT), brown adipose tissue (BAT) and liver weights. Differences in muscle weights disappear by 8 months.

Indirect Calorimetry

There were no differences in respiratory exchange ratios (RER) between genotypes at either 4 or 8 months (Figure 16A,B), indicating that there was no shift in fuel preference at the level of the whole body in either *UCP3tg* or *Ucp3* -/- mice. There were no differences in oxygen consumption between genotypes after either 4 months or 8 months on the diet (Figure 17A,B), indicating that energy expenditure was similar between genotypes.

Glucose Tolerance

Surprisingly, both *UCP3tg* and *Ucp3* -/- mice showed protection from the development of glucose intolerance, as measured by glucose tolerance test (Figure 18). Initially, after 1 month on the diet, only *Ucp3* -/- showed better glucose tolerance compared to wildtype mice (Figure 18A). At 3 months, however, both *UCP3tg* and *Ucp3* -/- mice showed better glucose tolerance than the wildtype mice (Figure 18B). At 4 months the differences in glucose tolerance between the genotypes narrowed, but statistical significance was maintained and both *UCP3tg* and *Ucp3* -/- mice had better glucose tolerance than wildtype mice (Figure 18C). After 8 months on the diet, both *UCP3tg* and *Ucp3* -/- mice still showed protection from the development of glucose intolerance, however, *Ucp3* -/- were more glucose tolerant than both wildtype and *UCP3tg* mice (Figure 18D). These results were unexpected and point to possible compensatory mechanisms in the *Ucp3* -/- mice.

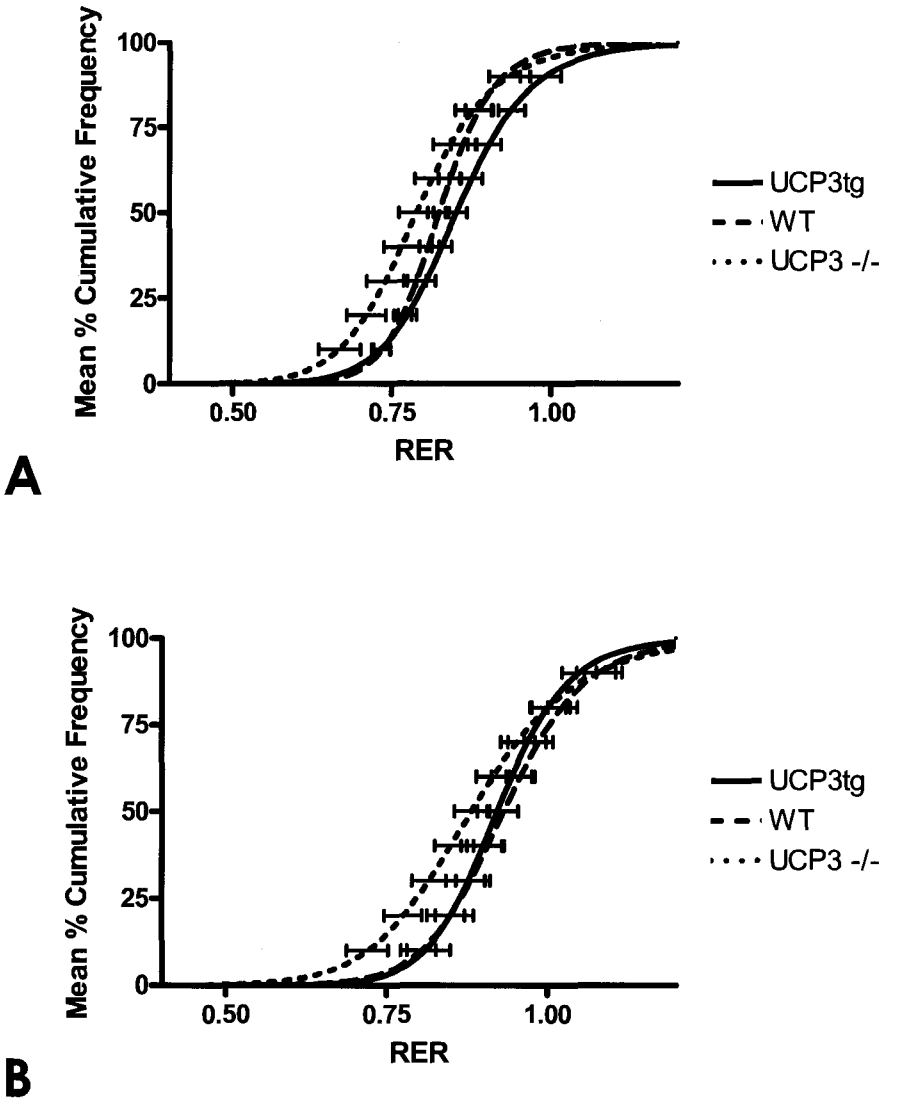

Figure 16: Percent relative cumulative frequency of respiratory exchange ratios (RER) at 4 months (A) and 8 months (B). Means ± SEM, n=6-10 (a), n=5-10 (b). One-way ANOVA with Tukey post-test was used to test for differences in means at 10, 20, 30, 40, 50, 60, 70, 80 and 90th percentile values. No significant differences between groups.

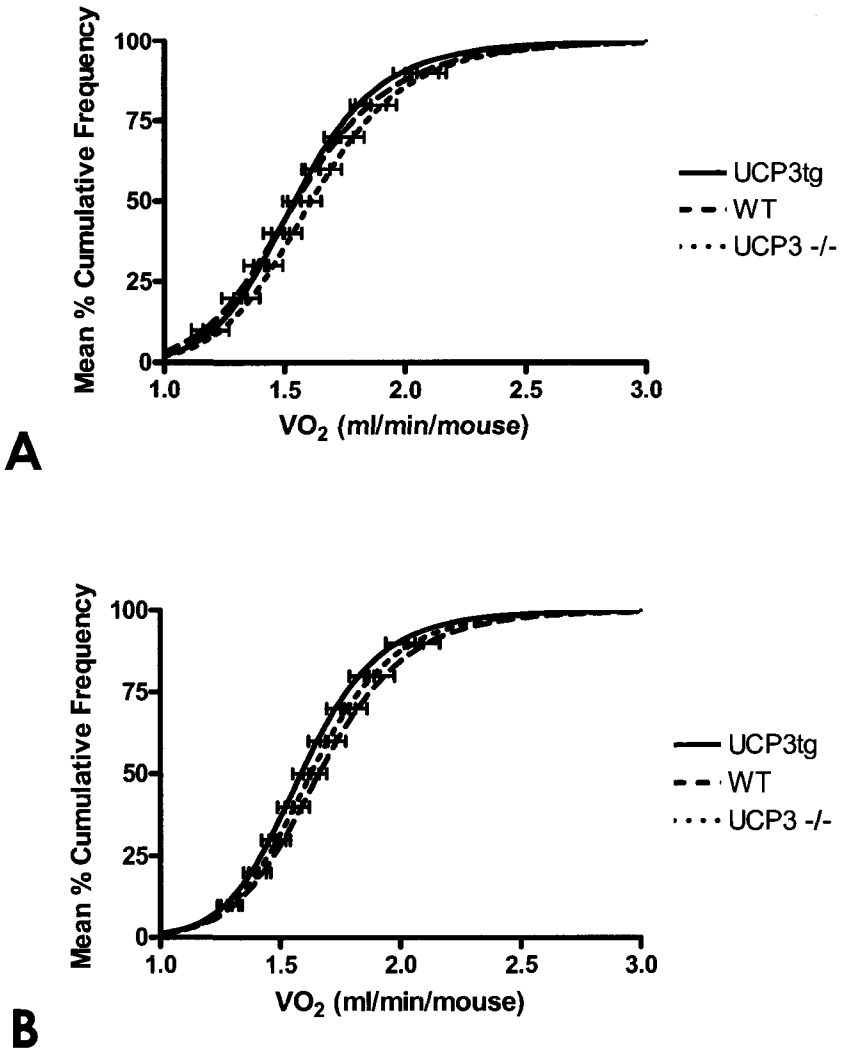

Figure 17: Percent relative cumulative frequency of oxygen consumption (VO_2) at 4 months (A) and 8 months (B). Means ± SEM, n=6-10 (a), n=5-10 (b). One-way ANOVA with Tukey post-test was used to test for any differences in means at 10, 20, 30, 40, 50, 60, 70, 80 and 90th percentile values. No significant differences between groups.

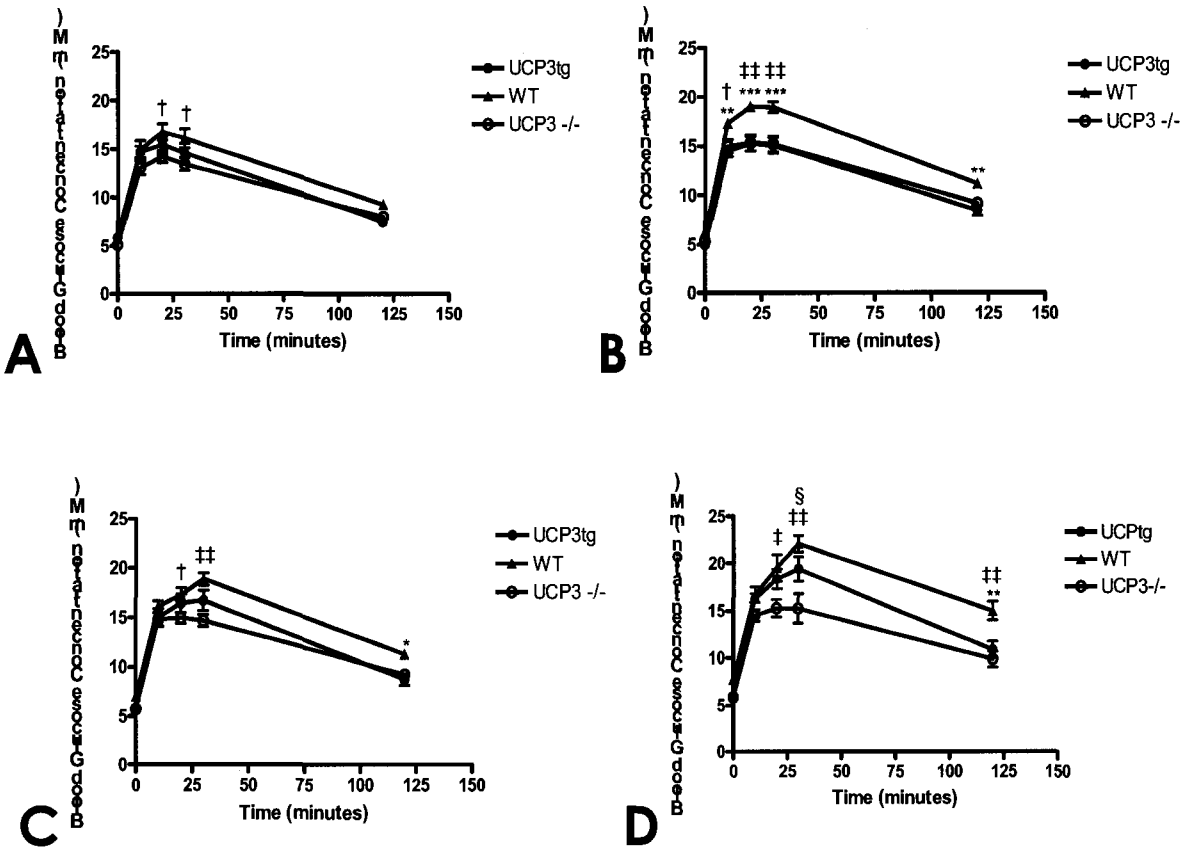

Figure 18: Glucose tolerance tests. Measurements taken at 1 month (A), 3 months (B), 4 months (C) and 8 months (D). Means ± SEM, n=20 (A-C), n=10 (D). Two-way ANOVA with Bonferroni correction. *p<0.05, **p<0.01, ***p<0.001 *UCP3tg* vs. WT. †p<0.05, ‡p<0.01, ‡‡p<0.001 WT vs. *Ucp3* -/-. §p<0.01 *UCP3tg* vs. *Ucp3* -/-. Both *UCP3tg* and *Ucp3* -/- mice are protected from the development of impaired glucose tolerance.

Insulin Tolerance

Both *UCP3tg* and *Ucp3* -/- mice showed some protection from the development of insulin resistance, as measured by insulin tolerance test (Figure 19). After 1 month on the diet, *UCP3tg* mice were more sensitive to insulin in the early part of the curve, in the first ~20 minutes post injection (Figure 19A). At 3 months, this difference disappeared (Figure 19B), but reappeared after 4 months on the diet: both *UCP3tg* and *Ucp3* -/- mice were more sensitive to insulin compared to wildtype mice in the first ~20 minutes post injection (Figure 19C). After 8 months on the diet, there was a trend for both *UCP3tg* and *Ucp3* -/- mice to be more insulin sensitive than wildtype mice, but this did not reach statistical significance (Figure 19D). These results were also surprising and again suggest that the *Ucp3* -/- mice might have developed mechanisms to compensate for the lack of UCP3.

2-Deoxy-[1-^{3}H]-Glucose Uptake

After 4 months on the diet, *Ucp3* -/- mice took up and phosphorylated more 2-deoxy-[1-^{3}H]-glucose in BAT (Figure 20A). Histological studies indicated that BAT from *UCP3tg* mice was more metabolically active and had smaller lipid droplets compared to wildtype and *Ucp3* -/- mice (Figure 21). *Ucp3* -/- also incorporated more 2-deoxy-[1-^{3}H]-glucose into liver glycogen compared to *UCP3tg* mice (Figure 20B).

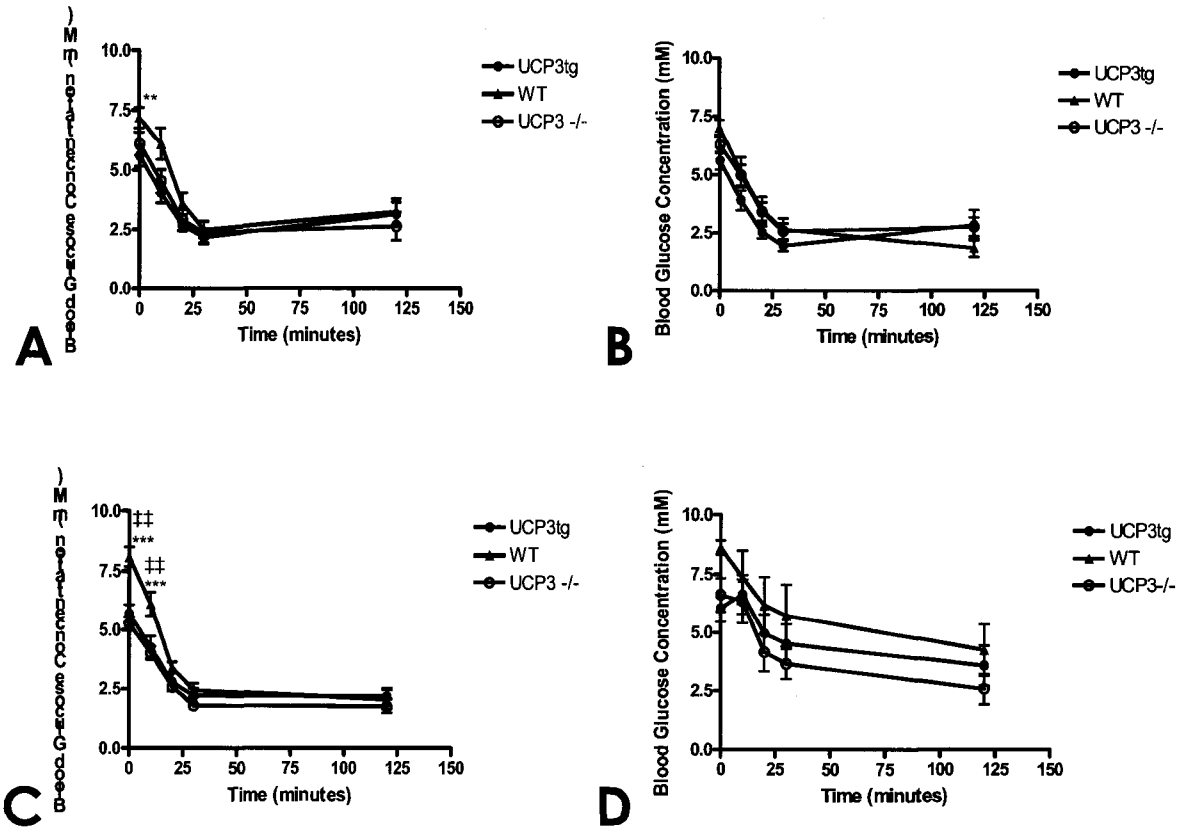

Figure 19: Insulin tolerance tests. Measurements taken at 1 month (A), 3 months (B), 4 months (C) and 8 months (D). Means ± SEM, n=19-20 (A), n=20 (B,C), n=10 (D). Two-way ANOVA with Bonferroni correction. **p<0.01, ***p<0.001 *UCP3tg* vs. WT. ‡‡p<0.001 WT vs. *Ucp3* -/-. Both *UCP3tg* and *Ucp3* -/- mice show some protection from the development of insulin resistance.

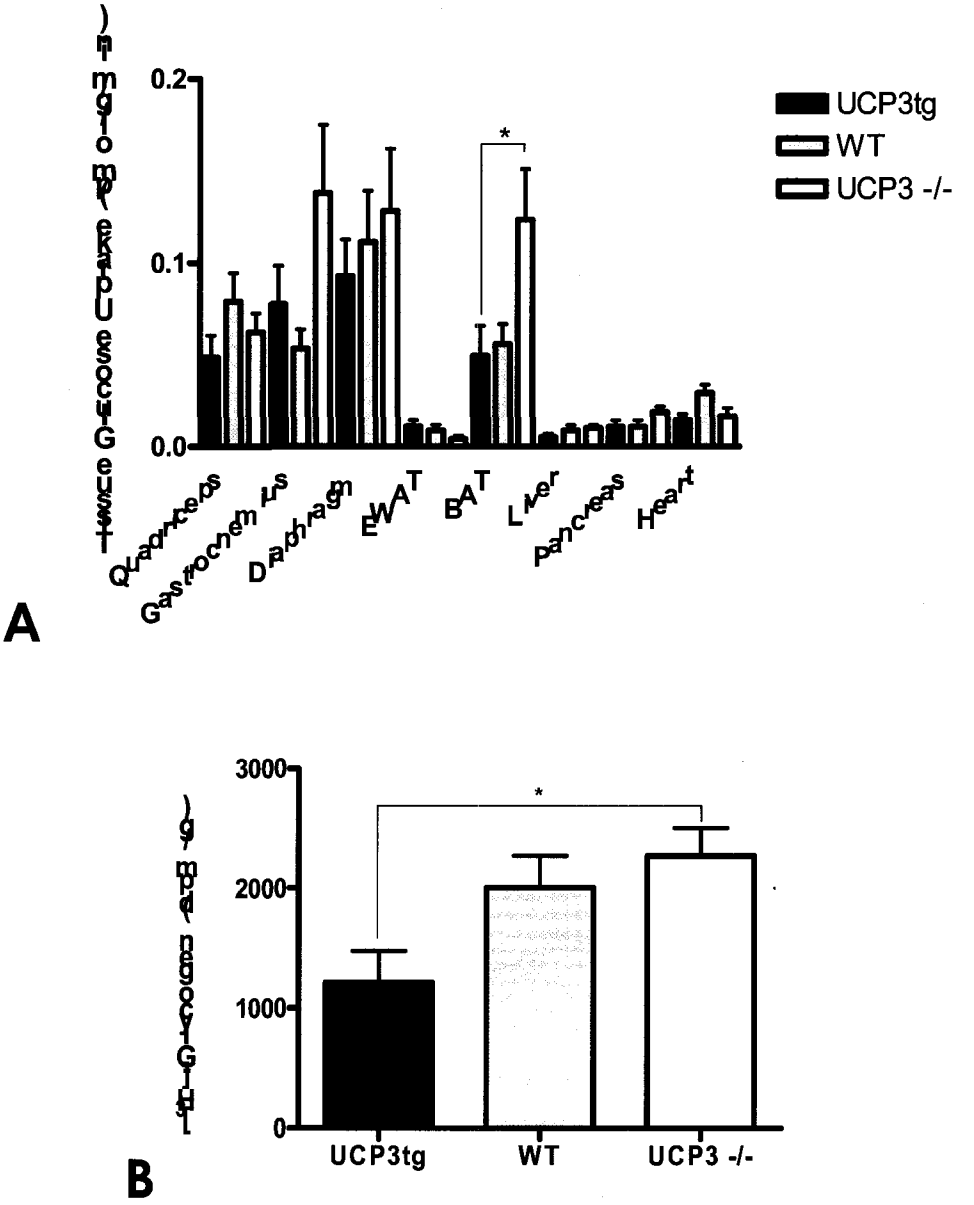

Figure 20: 2-deoxy-[^{3}H]-glucose uptake into tissues (A) and incorporation into liver glycogen (B) at 4 months. n=10, *p<0.05 *UCP3tg* vs. *Ucp3 -/-*. One-way ANOVA with Tukey post-test. *Ucp3 -/-* take up and phosphorylate more 2-deoxy-[^{3}H]-glucose into BAT compared to *UCP3tg*. Less glucose is incorporated into glycogen in *UCP3tg* compared to *Ucp3 -/-* mice.

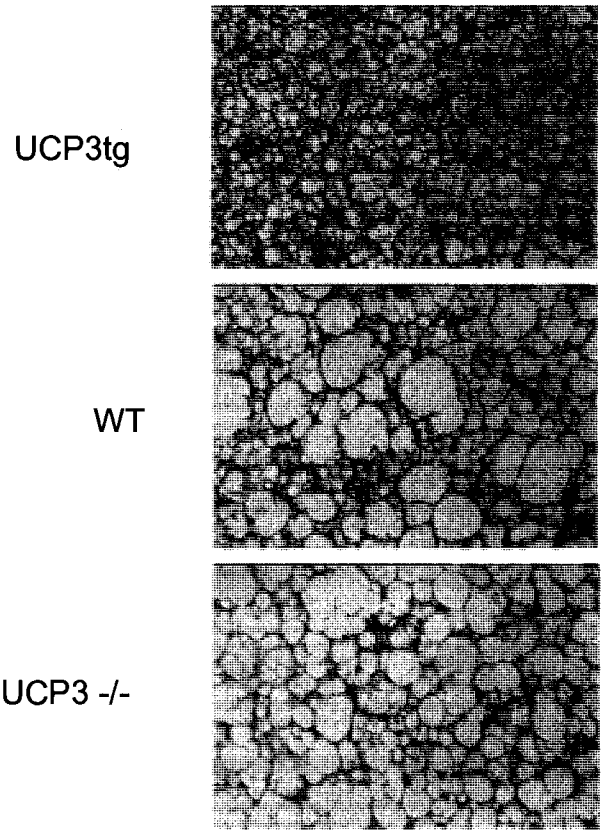

Figure 21: Brown adipose tissue (BAT) stained with haematoxylin and eosin (H&E).

Intramuscular Triglyceride (IMTG)

After 8 months on the diet, quadriceps from *UCP3tg* mice had less intramuscular triglyceride (IMTG) compared to quadriceps from both wildtype and *Ucp3* -/- mice (Figure 22A,C). In humans UCP3 protein is expressed most abundantly in type 2b fibers, less abundantly in type 2a fibers, and at even lower levels in type 1 fibers (18). In mice UCP3 protein is highest in gastrocnemius (1/3 type 1; 1/3 type 2a; and 1/3 type 2b), lowest in soleus (90% type 1) and intermediate in tibialis anterior (2/3 type 2a, and 1/3 type 2b) (12). Quadriceps muscle was assessed in our current study, as we hypothesized that the effects of UCP3 would be more apparent in muscles with a higher ratio of glycolytic to oxidative fibers. There was a trend for *Ucp3* -/- to store more triglyceride in their quadriceps compared to wildtype mice, however this did not reach statistical significance. In order to further challenge the genotypes with respect to IMTG accumulation, mice were fed a 45% fat diet for 8 months. Under these dietary conditions, *UCP3tg* mice were still protected from the accumulation of IMTG, however *Ucp3* -/- mice had higher levels of IMTG compared to both *UCP3tg* and wildtype mice (Figure 22B,D). Physiological overexpression of *UCP3* protected against the accumulation of triglyceride in muscle, whereas the lack of *Ucp3* promoted accumulation of IMTG.

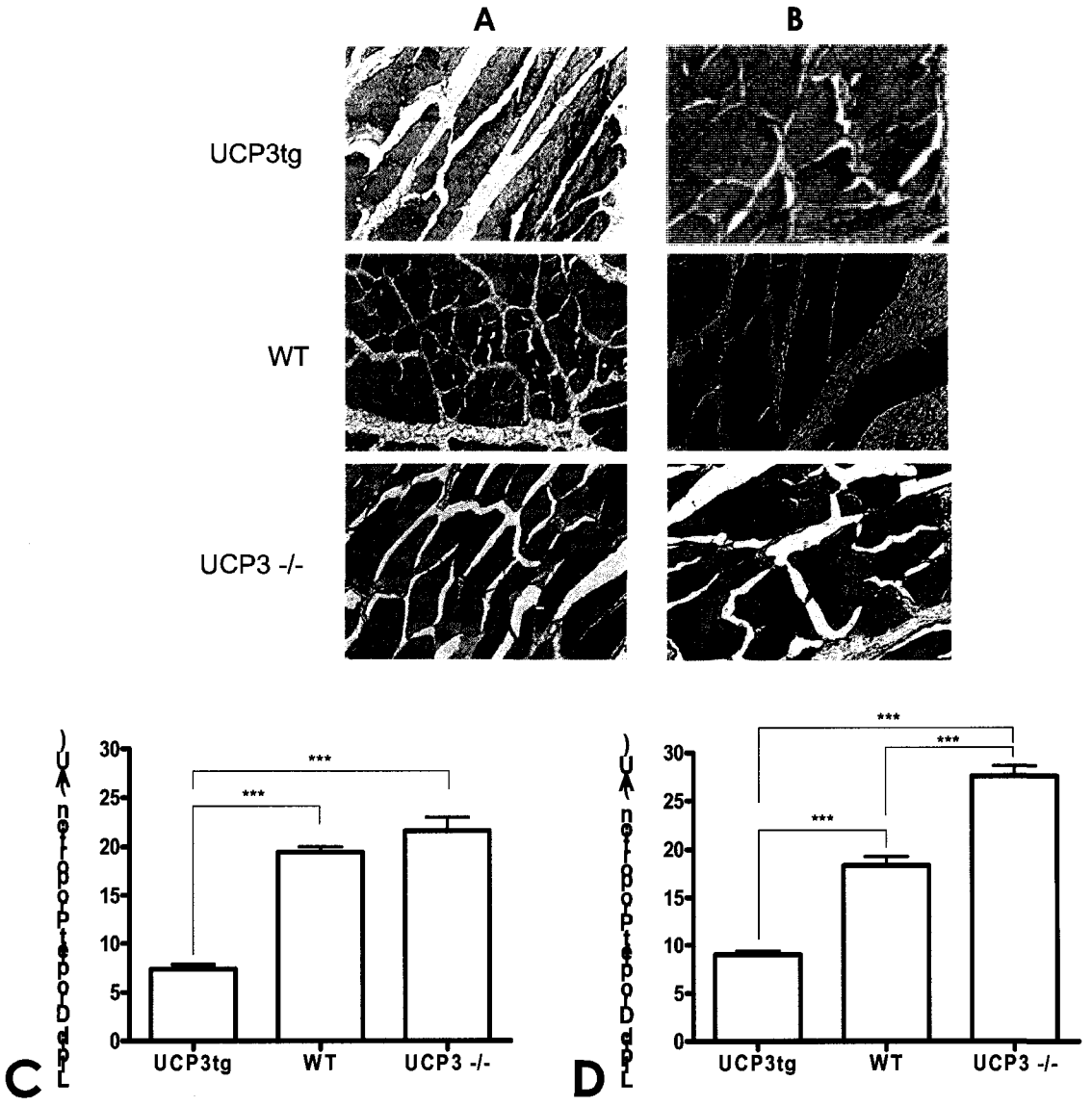

Figure 22: Quadriceps intramuscular triglyceride (IMTG) stained with osmium tetroxide (OsO_4) in mice fed a 10% fat diet (A) or a 45% fat diet (B) for 8 months. IMTG was measured as a proportion of surface area using imaging software for 10% fat fed mice (C) and 45% fat fed mice (D). Means ± SEM, n=3-5 (C) n-4-6 (D). One-way ANOVA with Tukey post-test, ***p<0.001. *UCP3tg* have less IMTG than WT and *Ucp3* -/- on both diets, *Ucp3* -/- have more IMTG than WT on the 45% fat diet.

Discussion

Contrary to our initial hypothesis, both *UCP3tg* and *Ucp3* -/- mice demonstrated protection from the development of glucose intolerance and insulin resistance. However, *UCP3tg* mice showed decreased overall adiposity, whereas *Ucp3* -/- mice showed increased lipid storage specifically in skeletal muscle.

Strengths of this study include the use of congenic transgenic and knockout mice backcrossed 10 generations into the C57BL/6 background. When identifying phenotypic differences between mice, comparing mice that have identical (or nearly-identical) genetic backgrounds increases confidence that identified differences are due to the gene being studied, not to random genetic variance (17). The use of a defined diet is also extremely important in metabolic studies such as these, as nutrient composition and macromolecule sources are consistent in such diets. Notably, the level of UCP3 overexpression in these transgenic mice was 2-2.5-fold compared to wildtype levels (4), and represents a physiological increase. Very high expression levels of uncoupling proteins can lead to artifactual uncoupling of oxidative phosphorylation (16, 32), which would mask the true metabolic effects of physiological increases of the protein *in vivo*.

Compared to wildtype mice, *UCP3tg* mice had lower body weights, lower fat pad and liver weights, less intramuscular triglyceride, and lower metabolic efficiencies. However, they showed no difference in food intake and no difference in metabolic rate or fatty acid oxidation (as measured by indirect calorimetry). Since there were no differences in food intake and no differences in energy expenditure, it appears as though neither one can account for the clear differences in metabolic efficiency observed. The explanation may lie in part in the ~5% error associated with indirect calorimetry (22). In addition, while food intake and metabolic efficiency determinations were conducted over long periods of time (4 or 8 months), indirect calorimetry was assessed only over a 24h period. Thus, small, but meaningful, differences in energy expenditure may not have been detected during this shorter time frame. Conversely, *Ucp3* -/- mice did not show any reduction in body weight, fat pad weight, liver weight or intramuscular triglyceride compared to wildtype mice, however they showed increased 2-deoxy-glucose uptake in BAT. *Ucp3* -/- mice showed no differences in food intake, metabolic rate, or fatty acid oxidation.

Interestingly, glucose and insulin tolerance tests demonstrated that both *UCP3tg* and *Ucp3* -/- mice were protected from the development of glucose intolerance and insulin resistance. These findings run counter to our original hypothesis that while transgenic mice would be protected from glucose and

insulin intolerance, knockout mice would be predisposed to the latter, compared to wildtype mice. In hindsight, given that these are germline genetic modifications and given the complexities of inter-tissue mechanisms involved in the development of glucose intolerance and insulin resistance, it could be considered somewhat naïve to expect that overexpressors and knockouts would have phenotypes mirror-imaging one another (17). Compensatory mechanisms are likely present. One possible explanation for the increased glucose and insulin tolerance in the *UCP3tg* mice may be that these mice are more lean compared to the wildtype and *Ucp3* -/- mice. In contrast this cannot explain why the *Ucp3* -/- mice also show increased glucose and insulin tolerance, as they have a similar degree of adiposity to wildtype mice. Further studies are underway in our laboratory to elucidate these mechanisms. Determining which genes are upregulated to compensate for UCP3 in its absence will hopefully be instructive with regard to the function of this protein.

In the examination of results from the various experimental approaches used herein, and in light of additional findings from our laboratory and others, a number of consistencies emerge. In these two experimental groups of mice it appears that improved glucose tolerance and insulin tolerance occurs through different mechanisms. In the transgenic mice there are decreases in muscle and BAT triglyceride contents, and decreases in the weights of fat

depots that coincide with the improved glucose and insulin tolerance. These findings are consistent with the ideas that the protection afforded to the mice occurs as a result of lipotoxicity prevention. Importantly there were no differences identified in total (whole body) energy expenditure and no differences in food intake, compared to wildtype controls.

UCP3tg mice had lower liver weights as well as a decreased incorporation of 2-deoxy-glucose into liver glycogen, thus identifying some important secondary effects of the muscle-specific changes in UCP3 content on liver fuel metabolism. In *Ucp3* -/- mice there were no changes in fat depot weights, or skeletal muscle, and yet these mice still had better glucose control overall than wildtype mice. The latter, in conjunction with the results from overexpressors, is consistent with the conclusion that UCP3 has little or no role in regulation of adiposity, but does play some role in the control of fuel substrate oxidation (glucose versus fatty acids) in some tissues where it is expressed (*e.g.*, BAT). Again, consistent with the results from overexpressors, there were no differences in total energy expenditure, or in food intake, compared to wildtype mice. The absence of *Ucp3* appears to have a significant effect on fuel metabolism in BAT. In *Ucp3* -/- mice, BAT took up and phosphorylated more glucose than did BAT of the other two groups of mice. This could explain the improved glucose tolerance and insulin tolerance in these mice compared to the other two groups. The latter

hypothetically occurs as a result of some impaired capacity to take up and/or oxidized fatty acids in BAT, leading to an increased reliance on glucose for fuel. Indeed in another series of studies conducted, we found that UCP3 played and important role in facilitating FA oxidation in muscle (4). However, the paradox remains as to why the absence of UCP3 in muscle does not lead to lipotoxicity in muscle, or even an increased reliance on glucose there as observed in BAT. Further research into this paradox is actively underway in our laboratory. Findings from this series of studies identify the need also for studies in conditional knockout and overexpressor mouse models, to avoid the issues of compensation that are associated with germline models.

Acknowledgments

We are very grateful to Linda Jui, Nicole Sabet, Mitra Abaeian, Kim Yates and Eileen Franklin for their assistance with histology, and care of the mice. This research was supported by funding from the Canadian Institutes of Health Research: Institute of Nutrition, Metabolism and Diabetes (M-E Harper).

References

1. **Anderson, S. C., and S. S. Schochet, Jr.** 1982. Osmium tetroxide-p-phenylenediamine stain for lipid in skeletal muscle. Arch Neurol **39:**383.

2. **Bevilacqua, L., J. J. Ramsey, K. Hagopian, R. Weindruch, and M. E. Harper.** 2005. Long-term caloric restriction increases UCP3 content but decreases proton leak and reactive oxygen species production in rat skeletal muscle mitochondria. Am J Physiol Endocrinol Metab.

3. **Bezaire, V., W. Hofmann, J. K. Kramer, L. P. Kozak, and M. E. Harper.** 2001. Effects of fasting on muscle mitochondrial energetics and fatty acid metabolism in Ucp3(-/-) and wild-type mice. Am J Physiol Endocrinol Metab **281:**E975-82.

4. **Bezaire, V., L. L. Spriet, S. Campbell, N. Sabet, M. Gerrits, A. Bonen, and M. E. Harper.** 2005. Constitutive UCP3 overexpression at physiological levels increases mouse skeletal muscle capacity for fatty acid transport and oxidation. Faseb J **19:**977-9.

5. **Boss, O., S. Samec, F. Kuhne, P. Bijlenga, F. Assimacopoulos-Jeannet, J. Seydoux, J. P. Giacobino, and P. Muzzin.** 1998. Uncoupling protein-3 expression in rodent skeletal muscle is modulated by food intake but not by changes in environmental temperature. J Biol Chem **273:**5-8.

6. **Boss, O., S. Samec, A. Paoloni-Giacobino, C. Rossier, A. Dulloo, J. Seydoux, P. Muzzin, and J. P. Giacobino.** 1997. Uncoupling protein-3: a new member of the mitochondrial carrier family with tissue-specific expression. FEBS Lett **408:**39-42.

7. **Brand, M. D., and T. C. Esteves.** 2005. Physiological functions of the mitochondrial uncoupling proteins UCP2 and UCP3. Cell Metab **2:**85-93.

8. **Cadenas, S., J. A. Buckingham, S. Samec, J. Seydoux, N. Din, A. G. Dulloo, and M. D. Brand.** 1999. UCP2 and UCP3 rise in starved rat skeletal muscle but mitochondrial proton conductance is unchanged. FEBS Lett **462:**257-60.

9. **Cadenas, S., K. S. Echtay, J. A. Harper, M. B. Jekabsons, J. A. Buckingham, E. Grau, A. Abuin, H. Chapman, J. C. Clapham, and M. D. Brand.** 2002. The basal proton conductance of skeletal muscle mitochondria from transgenic mice overexpressing or lacking uncoupling protein-3. J Biol Chem **277:**2773-8.

10. **Clapham, J. C., J. R. Arch, H. Chapman, A. Haynes, C. Lister, G. B. Moore, V. Piercy, S. A. Carter, I. Lehner, S. A. Smith, L. J. Beeley, R. J. Godden, N. Herrity, M. Skehel, K. K. Changani, P. D. Hockings, D. G. Reid, S. M. Squires, J. Hatcher, B. Trail, J. Latcham, S. Rastan, A. J. Harper, S. Cadenas, J. A. Buckingham, M. D. Brand, and A. Abuin.** 2000. Mice overexpressing human uncoupling protein-3 in skeletal muscle are hyperphagic and lean. Nature **406:**415-8.

11. **Cortright, R. N., D. Zheng, J. P. Jones, J. D. Fluckey, S. E. DiCarlo, D. Grujic, B. B. Lowell, and G. L. Dohm.** 1999. Regulation of skeletal muscle UCP-2 and UCP-3 gene expression by exercise and denervation. Am J Physiol **276:**E217-21.

12. **Giacobino, J. P.** 2001. Uncoupling protein 3 biological activity. Biochem Soc Trans **29:**774-7.

13. **Gong, D. W., Y. He, M. Karas, and M. Reitman.** 1997. Uncoupling protein-3 is a mediator of thermogenesis regulated by thyroid hormone, beta3-adrenergic agonists, and leptin. J Biol Chem **272:**24129-32.

14. **Gong, D. W., Y. He, and M. L. Reitman.** 1999. Genomic organization and regulation by dietary fat of the uncoupling protein 3 and 2 genes. Biochem Biophys Res Commun **256:**27-32.

15. **Gong, D. W., S. Monemdjou, O. Gavrilova, L. R. Leon, B. Marcus-Samuels, C. J. Chou, C. Everett, L. P. Kozak, C. Li, C. Deng, M. E. Harper, and M. L. Reitman.** 2000. Lack of obesity and normal response to fasting and thyroid hormone in mice lacking uncoupling protein-3. J Biol Chem **275:**16251-7.

16. **Harper, J. A., J. A. Stuart, M. B. Jekabsons, D. Roussel, K. M. Brindle, K. Dickinson, R. B. Jones, and M. D. Brand.** 2002. Artifactual uncoupling by uncoupling protein 3 in yeast mitochondria at the concentrations found in mouse and rat skeletal-muscle mitochondria. Biochem J **361:**49-56.

17. **Harper, M. E., and J. Himms-Hagen.** 2001. Mitochondrial efficiency: lessons learned from transgenic mice. Biochim Biophys Acta **1504:**159-72.

18. **Hesselink, M. K., H. A. Keizer, L. B. Borghouts, G. Schaart, C. F. Kornips, L. J. Slieker, K. W. Sloop, W. H. Saris, and P. Schrauwen.** 2001. Protein expression of UCP3 differs between human type 1, type 2a, and type 2b fibers. Faseb J **15:**1071-3.

19. **Himms-Hagen, J., and M. E. Harper.** 2001. Physiological role of UCP3 may be export of fatty acids from mitochondria when fatty acid oxidation predominates: an hypothesis. Exp Biol Med (Maywood) **226:**78-84.

20. **Hinz, W., S. Gruninger, A. De Pover, and M. Chiesi.** 1999. Properties of the human long and short isoforms of the uncoupling protein-3 expressed in yeast cells. FEBS Lett **462:**411-5.

21. **Krssak, M., K. Falk Petersen, A. Dresner, L. DiPietro, S. M. Vogel, D. L. Rothman, M. Roden, and G. I. Shulman.** 1999. Intramyocellular lipid concentrations are correlated with insulin sensitivity in humans: a 1H NMR spectroscopy study. Diabetologia **42:**113-6.

22. **Livesey, G., and M. Elia.** 1988. Estimation of energy expenditure, net carbohydrate utilization, and net fat oxidation and synthesis by indirect calorimetry: evaluation of errors with special reference to the detailed composition of fuels. Am J Clin Nutr **47:**608-28.

23. **Maclellan, J. D., M. F. Gerrits, A. Gowing, P. J. Smith, M. B. Wheeler, and M. E. Harper.** 2005. Physiological increases in uncoupling protein 3 augment Fatty Acid oxidation and decrease reactive oxygen species production without uncoupling respiration in muscle cells. Diabetes **54:**2343-50.

24. **Millet, L., H. Vidal, F. Andreelli, D. Larrouy, J. P. Riou, D. Ricquier, M. Laville, and D. Langin.** 1997. Increased uncoupling protein-2 and -3 mRNA expression during fasting in obese and lean humans. J Clin Invest **100:**2665-70.

25. **Moore, G. B., J. Himms-Hagen, M. E. Harper, and J. C. Clapham.** 2001. Overexpression of UCP-3 in skeletal muscle of mice results in increased expression of mitochondrial thioesterase mRNA. Biochem Biophys Res Commun **283:**785-90.

26. **Nedergaard, J., V. Golozoubova, A. Matthias, A. Asadi, A. Jacobsson, and B. Cannon.** 2001. UCP1: the only protein able to mediate adaptive non-shivering thermogenesis and metabolic inefficiency. Biochim Biophys Acta **1504:**82-106.

27. **Pan, D. A., S. Lillioja, A. D. Kriketos, M. R. Milner, L. A. Baur, C. Bogardus, A. B. Jenkins, and L. H. Storlien.** 1997. Skeletal muscle triglyceride levels are inversely related to insulin action. Diabetes **46:**983-8.

28. **Phillips, D. I., S. Caddy, V. Ilic, B. A. Fielding, K. N. Frayn, A. C. Borthwick, and R. Taylor.** 1996. Intramuscular triglyceride and muscle insulin sensitivity: evidence for a relationship in nondiabetic subjects. Metabolism **45:**947-50.

29. **Riachi, M., J. Himms-Hagen, and M. E. Harper.** 2004. Percent relative cumulative frequency analysis in indirect calorimetry: application to studies of transgenic mice. Can J Physiol Pharmacol **82:**1075-83.

30. **Schrauwen, P., M. K. Hesselink, E. E. Blaak, L. B. Borghouts, G. Schaart, W. H. Saris, and H. A. Keizer.** 2001. Uncoupling protein 3 content is decreased in skeletal muscle of patients with type 2 diabetes. Diabetes **50:**2870-3.

31. **Schrauwen, P., J. Xia, C. Bogardus, R. E. Pratley, and E. Ravussin.** 1999. Skeletal muscle uncoupling protein 3 expression is a determinant of energy expenditure in Pima Indians. Diabetes **48:**146-9.

32. **Stuart, J. A., J. A. Harper, K. M. Brindle, M. B. Jekabsons, and M. D. Brand.** 2001. Physiological levels of mammalian uncoupling protein 2 do not uncouple yeast mitochondria. J Biol Chem **276:**18633-9.

33. **Tsuboyama-Kasaoka, N., N. Tsunoda, K. Maruyama, M. Takahashi, H. Kim, S. Ikemoto, and O. Ezaki.** 1998. Up-regulation of uncoupling protein 3 (UCP3) mRNA by exercise training and down-regulation of UCP3 by denervation in skeletal muscle. Biochem Biophys Res Commun **247:**498-503.

34. **Vidal-Puig, A., G. Solanes, D. Grujic, J. S. Flier, and B. B. Lowell.** 1997. UCP3: an uncoupling protein homologue expressed preferentially and abundantly in skeletal muscle and brown adipose tissue. Biochem Biophys Res Commun **235:**79-82.

35. **Vincent, A. M., J. A. Olzmann, M. Brownlee, W. I. Sivitz, and J. W. Russell.** 2004. Uncoupling proteins prevent glucose-induced neuronal oxidative stress and programmed cell death. Diabetes **53:**726-34.

36. **Wang, S., A. Subramaniam, M. A. Cawthorne, and J. C. Clapham.** 2003. Increased fatty acid oxidation in transgenic mice overexpressing UCP3 in skeletal muscle. Diabetes Obes Metab **5:**295-301.

37. **Weigle, D. S., L. E. Selfridge, M. W. Schwartz, R. J. Seeley, D. E. Cummings, P. J. Havel, J. L. Kuijper, and H. BeltrandelRio.** 1998. Elevated free fatty acids induce uncoupling protein 3 expression in muscle: a potential explanation for the effect of fasting. Diabetes **47:**298-302.

38. **Zhang, C. Y., T. Hagen, V. K. Mootha, L. J. Slieker, and B. B. Lowell.** 1999. Assessment of uncoupling activity of uncoupling protein 3 using a yeast heterologous expression system. FEBS Lett **449:**129-34.

Chapter 3

Long-Term High Fat Feeding Induces Greater Fat Storage in Mice Lacking UCP3

Sheila R. Costford, Shehla N. Chaudhry, Mahmoud Salkhordeh, and Mary-Ellen Harper

Am J Physiol Endocrinol Metab (submitted)

Department of Biochemistry, Microbiology and Immunology
Faculty of Medicine, University of Ottawa
451 Smyth Rd., Ottawa, Ontario
Canada, K1H 8M5

Running Head: Lack of UCP3 Increases Fat Storage Following HF Feeding

Brief Description of Contents

This manuscript was submitted to the American Journal of Physiology: Endocrinology and Metabolism in December of 2007 and is currently in the revision stage. It describes the whole body energetics and development of insulin resistance in mice overexpressing or lacking uncoupling protein-3 (UCP3) compared to wildtype control animals when challenged long-term with a high fat diet. Overexpressor and knockout mice were both protected from the development of insulin resistance (as assessed by glucose and insulin tolerance tests) after short-term high fat feeding, however, this protection did not continue with long-term high fat feeding. Overexpressor mice had lower levels of adiposity whereas knockout mice had higher levels of adiposity compared to wildtype mice with long-term high fat feeding, indicating a protective effect of UCP3 against fat gain. Results are consistent with a role for UCP3 in the protection from fat gain induced by long-term high fat feeding, but indicate that UCP3 may not be involved in the protection from fat-induced insulin resistance.

Contribution of Collaborators

Sheila R. Costford

Mouse colony maintenance: changed cages, fed mice, weighed mice and rodent diet. Performed all experiments, analyzed all data, contributed all tables and figures, wrote the first draft of the manuscript, participated in the editing and submission of the manuscript.

Shehla N. Chaudhry

Assisted with mouse colony maintenance and the performance of all experiments.

Mahmoud Salkhordeh

Assisted with mouse colony maintenance and the performance of glucose and insulin tolerance tests, as well as 2-deoxy-[1-^{3}H]-glucose-6-phosphate uptake into tissues and incorporation into liver glycogen experiments.

Mary-Ellen Harper

Conceived and designed the study, contributed to data analysis, edited and submitted manuscript.

Abstract

Uncoupling protein-3 (UCP3) is a mitochondrial inner-membrane protein highly expressed in skeletal muscle. While UCP3's function is still unknown, it has been hypothesized to act as a fatty acid (FA) anion exporter, protecting mitochondria against lipid peroxidation, and/or facilitating FA oxidation. The aim of this study was to determine the effects of long-term feeding of a 45% fat diet on whole body indicators of muscle metabolism in congenic C57BL/6 mice that were either lacking *Ucp3* (*Ucp3* -/-) or had constitutive physiological (2-3 fold protein) overexpression of human *UCP3* (*UCP3tg*). Mice were fed the high fat (HF) diet for a period of either 4 or 8 months immediately following weaning. After long-term HF feeding, *UCP3tg* mice weighed less than wildtype mice and had lower metabolic efficiencies than both wildtype and *Ucp3* -/- mice. Additionally, *UCP3tg* mice had lower, while *Ucp3* -/- mice had higher levels of adiposity compared to wildtype mice, indicating a protective effect of UCP3 against fat gain. After 4 months on the diet, *UCP3tg* mice had lower whole body oxygen consumption compared to *Ucp3* -/- mice, however this difference disappeared after 8 months of HF feeding. Glucose and insulin tolerance tests revealed that both the *UCP3tg* and *Ucp3* -/- mice were more glucose tolerant and insulin sensitive compared to wildtype mice after short-term HF feeding, but this difference also disappeared after 8 months of HF feeding. Findings indicate that UCP3 is

involved in protection from fat gain induced by long-term HF feeding, but not in protection from insulin resistance.

Key Words: uncoupling protein-3, obesity, insulin resistance, type 2 diabetes mellitus, skeletal muscle

Introduction

Obesity is the excessive accumulation of body fat beyond what is normally considered healthy for a given height. Traditionally measured using the Body Mass Index (BMI), body mass divided by height squared (kg/m^2), obesity is defined as a BMI of 30 or above (World Health Organization, WHO). The prevalence of obesity has increased at an alarming rate over the past few decades. In the US, prevalence of obesity among adults increased from 15% in the mid-1970s to 32.2% in 2004 (12, 21, 27). Associated with several major health risks such as cardiovascular disease, type 2 diabetes mellitus (T2DM) and certain cancers (reviewed in (20)), obesity is caused by a positive energy balance (*i.e.*, energy consumption greater than energy expenditure). A number of factors influence energy balance (reviewed in (36)); both environmental (*e.g.*, high fat diet, physical inactivity) and genetic (28). There is a great need for more information regarding the genetic predisposition to obesity and its clinical sequalae, as well as the need for more effective treatment strategies.

Obesity treatment strategies must accomplish a decrease dietary energy intake, an increase in energy expenditure, or both. Increased energy expenditure can be achieved with increased physical activity/exercise or by decreasing metabolic efficiency. Metabolic efficiency, at the level of the

whole body, refers to the degree to which the energy in food substrates is captured as ATP. The majority of cellular ATP production occurs in the mitochondria through oxidative phosphorylation. When cellular fuel oxidation is tightly coupled to ATP production, metabolic efficiency is high. Energy conversion through oxidative phosphorylation is not perfect, however, and varies with several factors related to resting metabolic rate (RMR) (*e.g.*, thyroid status, reviewed in (16, 35)). The mitochondrial electron transport chain (ETC) pumps protons out of the mitochondrial matrix into the intermembrane space, creating an electrochemical gradient across the inner membrane. During 'coupled' oxidative phosphorylation, protons return to the matrix through ATP synthase (complex V) and ADP is phosphorylated to ATP. If protons return to the matrix by any means other than through ATP synthase, the potential energy across the membrane is lost as heat and ATP is not produced. This process is referred to as the 'uncoupling' of oxidative phosphorylation. Uncoupling occurs in all tissues, but at particularly high rates in brown adipose tissue (BAT) through uncoupling protein-1 (UCP1) for heat production during non-shivering thermogenesis (reviewed in (8, 26)). Uncoupling in skeletal muscle may account for up to 50% of resting energy expenditure (30, 31), and therefore can play a significant role in maintaining energy balance. For example, increased weight loss in a clinical weight loss program was associated with increased skeletal muscle mitochondrial uncoupling and uncoupling protein-3 (*UCP3*) mRNA expression (17).

The novel uncoupling proteins (UCPs 2-5) have been studied over the last decade; however their physiological functions are still unclear. UCP3 is expressed highly selectively in skeletal muscle, BAT and at low levels in the heart (3, 40). Early studies of *UCP3* overexpression in experimental systems ranging from yeast to mice were confounded by supra-physiological levels of expression (10, 15, 19, 37, 42). These high levels of protein expressed on the mitochondrial inner membrane induced artifactual proton leak (15, 37), making it difficult to draw conclusions about the true function of UCP3.

In this study our aim was to assess the effect of long-term (4 or 8 month-) high fat feeding on *Ucp3* -/- mice, wild type control mice, and in mice with increased levels of UCP3 that are physiological (*UCP3tg*). Here we report the effects of UCP3 on development of T2DM, whole body energetics and fuel storage.

Materials and Methods

Animal Models

Male *Ucp3 -/-*, wildtype and *UCP3tg* C57BL/6 mice (n=20 per genotype) back-crossed 10 generations were housed individually in clear polycarbonate cages from weaning and fed a high fat rodent diet (Research Diets, D12451, New Brunswick, NJ) *ad libitum*. The D12451 diet consisted of 20% protein (casein and L-cysteine), 35% carbohydrate (corn starch, maltodextrin and sucrose) and 45% fat (soybean oil and lard) by kilocalorie. Mice were housed at 23°C for 4 or 8 months with light from 0600-1800. The F1 generation of the *UCP3tg* mice has been previously described (10); these mice were provided originally by Dr. John Clapham at Glaxo-Smith-Kline (UK). The overexpressor mice used in this study express 2-3 fold the UCP3 protein levels of wildtype mice in skeletal muscle. The *Ucp3 -/-* mice have also been previously described, but on a mixed genetic background (13). Animals were cared for in accordance with the principles and guidelines of the Canadian Council on Animal Care and the Institute of Laboratory Animal Resources (National Research Council). The study was approved by the Animal Care Committee of the University of Ottawa.

Whole Body Analyses

Body weight and food intake were determined twice per week for the duration of the study. Food intake is expressed as the total amount of energy ingested over the study period divided by the same number of days (mean kcal ingested per day). Metabolic efficiency was calculated as total body weight gained divided by total amount of energy consumed during the study period (mg body weight gained per kcal ingested). Rectal body temperature was measured at 0730 immediately prior to sacrifice (Physitemp Thermalert, Model TH-8, Clifton, New Jersey) while naso-anal length was measured post-sacrifice.

Glucose and Insulin Tolerance Tests

Mice were assessed for glucose and insulin tolerance after 1, 2, 3, 4 and 8 months on the diet. Tests were carried out at one week intervals to allow recovery time. Saphenous blood was used to measure blood glucose using a glucometer (One Touch Basic, LifeScan, Burnaby, British Columbia). Prior to the tests, fasting blood glucose was measured and then mice were intraperitoneally injected with 1 mg glucose (10% dextrose in sterile saline) or 1×10^{-4} units human insulin (Humalog Rapid Acting, Eli Lilly, in sterile saline) per g body weight. Blood glucose was assessed again at 10, 20, 30 and 120 min post-injection.

Indirect Calorimetry

A customized four-chamber Oxymax system (Columbus Instruments, Columbus, OH) was used to measure oxygen consumption (VO_2) and carbon dioxide production (VCO_2) in the mice. The system was programmed to maintain chamber temperature at 24°C with lights on from 0600-1800. Flow rate was set at 0.5 L/min and the sample line-purge at 2 min. Mice were housed individually in the 2.5 L calorimetry chambers and given *ad libitum* access to water and the diet. Measurements were taken every twelve minutes for 60 s over a period of 24-hours. Energy expenditure was expressed as percent relative cumulative frequencies of all points collected, as described previously (29). Respiratory exchange ratios (RER) were calculated as the ratio of VCO_2 divided by VO_2.

Analysis of 2-Deoxy-[1-^{3}H]-Glucose-6-Phosphate in Tissue

This procedure was adapted from Wang *et al.* (41) with minor modifications and has been previously described (11). At 4 months, mice fasted overnight were injected intraperitoneally with 0.5 µCi 2-deoxy-[1-^{3}H]-glucose mixed with 10% dextrose to provide a fixed specific activity of 1 g glucose per kg body weight. 70 min post-injection, quadriceps, gastrocnemius, diaphragm, interscapular brown adipose tissue (IBAT), epididymal white adipose tissue (EWAT), liver, pancreas and heart were flash frozen in liquid nitrogen. Thawed tissues homogenized in 2% $HClO_4$ were incubated at 4°C overnight then

centrifuged for 10 min at 2000 x g. Total [^{3}H]-radioactivity was determined in 50% of the neutralized supernatant, and the other 50% was applied to a anion exchange resin-filled column (Ag1-X8) (BioRad, Mississauga, Ontario, Canada). [^{3}H]-radioactivity was measured in free 2-deoxyglucose and 2-deoxyglucose-6-phosphate eluantes. Tissue glucose uptake was determined by dividing tissue [^{3}H]-2-deoxyglucose-6-phosphate activity by the glucose specific activity.

Analysis of 2-Deoxy-[1-^{3}H]-Glucose-6-Phosphate in Liver Glycogen

This procedure was adapted from Wang *et al.* (41) with minor modifications and has been previously described (11). Preparation of liver samples was carried out as described above in the analysis of tissue 2-deoxy-[1-^{3}H]-glucose-6-phosphate. 2.5% oyster glycogen and 0.2% Na_2SO_4 were added to the neutralized supernatant prior to glycogen precipitation with ethanol. The resulting pellet was washed once and resuspended in distilled water before [^{3}H]-radioactivity counting.

Statistical Methods

One-way ANOVA with Tukey post-test was used to assess statistical significance for body weight, food intake, naso-anal length, body temperature, metabolic efficiency, tissue weights, oxygen consumption, respiratory exchange ratios, 2-deoxy-[1-3H]-glucose tissue uptake and

incorporation of 2-deoxy-[1-3H]-glucose into liver glycogen (Figures 23-27, 30; Table 6). Two-way ANOVA with Bonferroni correction was used to assess statistical significance for glucose tolerance tests and insulin tolerance tests (Figures 28 and 29).

Results

Whole Body Analysis

There were no differences in body weight after 4 months of HF feeding (Figure 23A), however, after 8 months on the diet, *UCP3tg* mice weighed less than wildtype mice (Figure 23B). There was a trend for *UCP3tg* mice to have lower body weights compared to *Ucp3* -/- mice at 8 months, although this did not reach statistical significance. *UCP3tg* mice did, however, have lower metabolic efficiencies compared to both wildtype and *Ucp3* -/- mice after 8 months of HF feeding, but not after 4 months (Figures 24A, 24B). There were no differences in food intake at either 4 months (*UCP3tg*: 10.18 ± 0.18 kcal/d; WT: 10.08 ± 0.25 kcal/d; *Ucp3* -/-: 10.31 ± 0.24 kcal/d; n=10-13, means ± SEM, One-way ANOVA, Tukey post-test, NS) or 8 months (*UCP3tg*: 12.67 ± 0.26 kcal/d; WT: 12.51 ± 0.38 kcal/d; *Ucp3* -/-: 12.89 ± 0.47 kcal/d; n=10, means ± SEM, One-way ANOVA, Tukey post-test, NS). There were no differences in naso-anal length at 8 months (*UCP3tg*: 8.5 ± 0.2 cm; WT: 9.0 ± 0.2 cm; *Ucp3* -/- : 9.0 ± 0.2 cm; n=10, means ± SEM, One-way ANOVA, Tukey post-test, NS), although there was an unexpected increase in body temperature of both *UCP3tg* and *Ucp3* -/- mice compared to wildtype mice (*UCP3tg*: 34.2 ± 0.4°C; WT: 30.3 ± 1.6°C; *Ucp3* -/-: 34.1 ± 0.4°C; n=10, means ± SEM, One-way ANOVA, Tukey post-test, *p<0.05 *UCP3tg* vs. WT, *p<0.05 *Ucp3* -/- vs. WT).

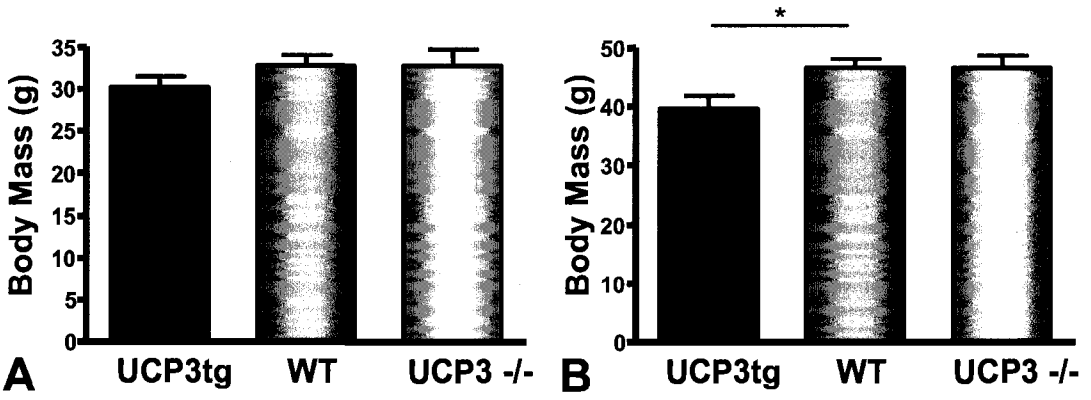

Figure 23: Body weight (g). Means ± SEM; one-way ANOVA, Tukey post-test. A) After 4 months of HF feeding; n=10-13; NS. B) After 8 months of HF feeding; n=10; *$p<0.05$.

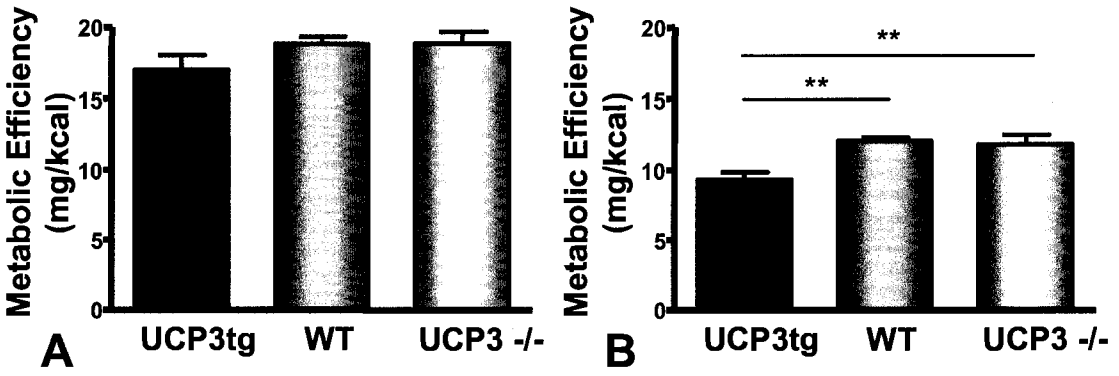

Figure 24: Metabolic efficiency (mg/kcal). Means ± SEM; one-way ANOVA, Tukey post-test. A) After 4 months of HF feeding; n=10-13; NS. B) After 8 months of HF feeding; n=10; **p<0.01.

Wet weight tissue analysis revealed no differences in muscle mass (gastrocnemius, soleus, quadriceps, diaphragm), interscapular brown adipose tissue (IBAT), or organ (pancreas, liver, heart, spleen) weights (Table 6). There were no differences in adiposity as measured by epididymal white adipose tissue (EWAT) mass at 4 months. However at 8 months of HF feeding, *UCP3tg* mice had smaller EWAT depots compared to *Ucp3* -/- mice, and *Ucp3* -/- mice had higher EWAT depots compared to wildtype mice (Figures 25A, 25B).

Indirect Calorimetry

After 4 months of HF feeding, *UCP3tg* mice had lower whole body oxygen consumption compared to *Ucp3* -/- mice, however, this difference disappeared after 8 months on the diet (Figures 26A, 26B). There were no differences in respiratory exchange ratio (RER) after either 4 or 8 months of HF feeding (Figures 27A, 27B).

Glucose Tolerance

After one month on the HF diet, *Ucp3* -/- mice had better glucose tolerance compared to wildtype mice, whereas after 2 and 3 months of HF feeding the *UCP3tg* and *Ucp3* -/- mice had better glucose tolerance compared to wildtype mice (Figures 28A, 28B, 28C). Differences in glucose tolerance were not evident after 4 months of HF feeding (Figures 28D, 28E).

4 months Tissue (g)	***UCP3tg***	**WT**	*Ucp3 -/-*
Soleus	0.03 ± 0.00	0.03 ± 0.01	0.02 ± 0.00
Gastrocnemius	0.37 ± 0.01	0.34 ± 0.01	0.33 ± 0.04
Quadriceps	0.37 ± 0.02	0.37 ± 0.02	0.32 ± 0.02
Diaphragm	0.09 ± 0.01	0.11 ± 0.01	0.10 ± 0.01
IBAT	0.10 ± 0.01	0.14 ± 0.01	0.13 ± 0.04
Pancreas	0.19 ± 0.02	0.21 ± 0.03	0.23 ± 0.02
Liver	0.92 ± 0.03	1.02 ± 0.04	0.99 ± 0.10
Heart	0.15 ± 0.01	0.18 ± 0.01	0.15 ± 0.01
Spleen	0.08 ± 0.01	0.10 ± 0.01	0.10 ± 0.02
8 months Tissue (g)	***UCP3tg***	**WT**	*Ucp3 -/-*
Soleus	0.02 ± 0.00	0.03 ± 0.01	0.03 ± 0.01
Gastrocnemius	0.32 ± 0.01	0.34 ± 0.01	0.35 ± 0.02
Quadriceps	0.32 ± 0.01	0.30 ± 0.01	0.29 ± 0.03
Diaphragm	0.10 ± 0.01	0.11 ± 0.01	0.14 ± 0.02
IBAT	0.29 ± 0.04	0.33 ± 0.04	0.32 ± 0.04
Pancreas	0.31 ± 0.04	0.28 ± 0.01	0.34 ± 0.03
Liver	1.57 ± 0.20	2.31 ± 0.18	1.87 ± 0.37
Heart	0.17 ± 0.01	0.16 ± 0.01	0.18 ± 0.02
Spleen	0.09 ± 0.01	0.10 ± 0.01	0.10 ± 0.02

Table 6: Wet tissue weight analysis. Means ± SEM, n=10-13 (4 months), n=10 (8 months), One-way ANOVA, Tukey post-test, NS.

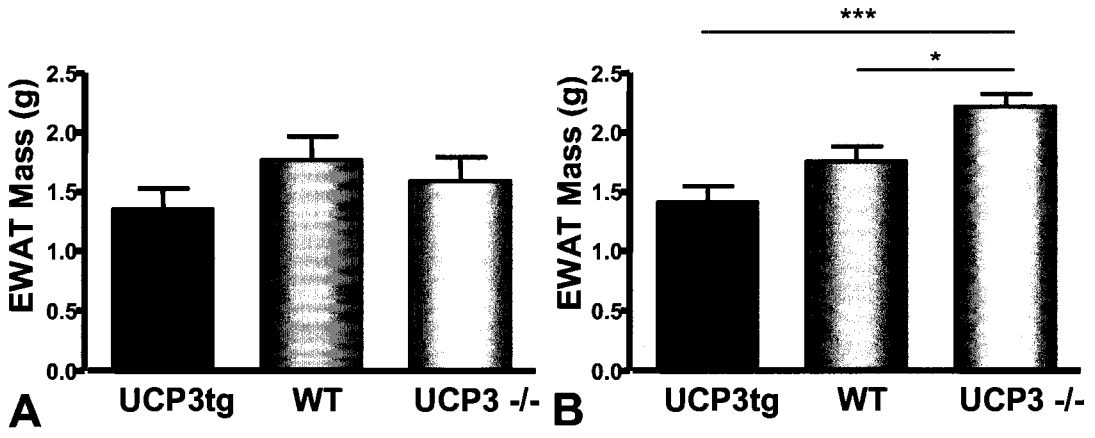

Figure 25: Epididymal white adipose tissue (EWAT) mass (g). Means ± SEM; one-way ANOVA, Tukey post-test. A) After 4 months of HF feeding; n=10-13; NS. B) After 8 months of HF feeding; n=10; *p<0.05, ***p<0.001.

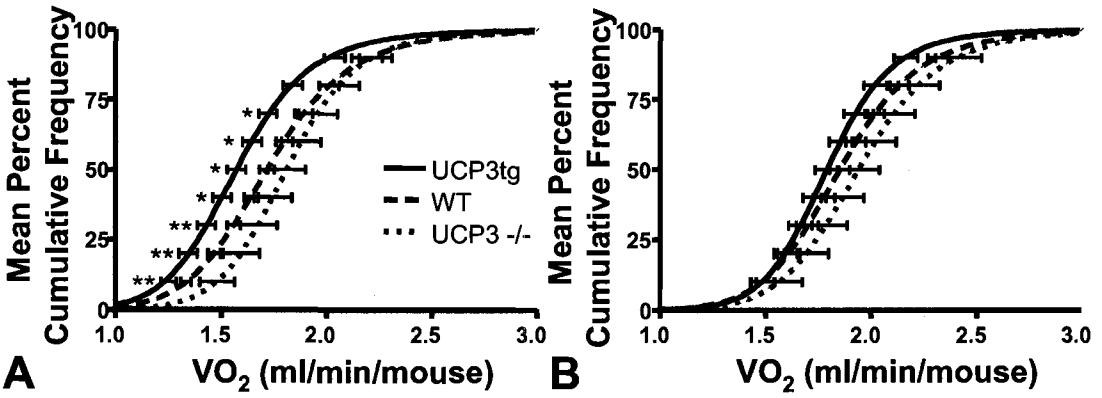

Figure 26: Mean percentage of cumulative frequency (PRCF) of oxygen consumption (VO2). One-way ANOVA, Tukey post-test at 10th, 20th, 30th, 40th, 50th, 60th, 70th, 80th, and 90th percentiles. A) After 4 months of HF feeding; n=7-11; *p<0.05, **p<0.01 *UCP3tg* vs. *Ucp3* -/-. B) After 8 months of HF feeding; n=7-10; NS.

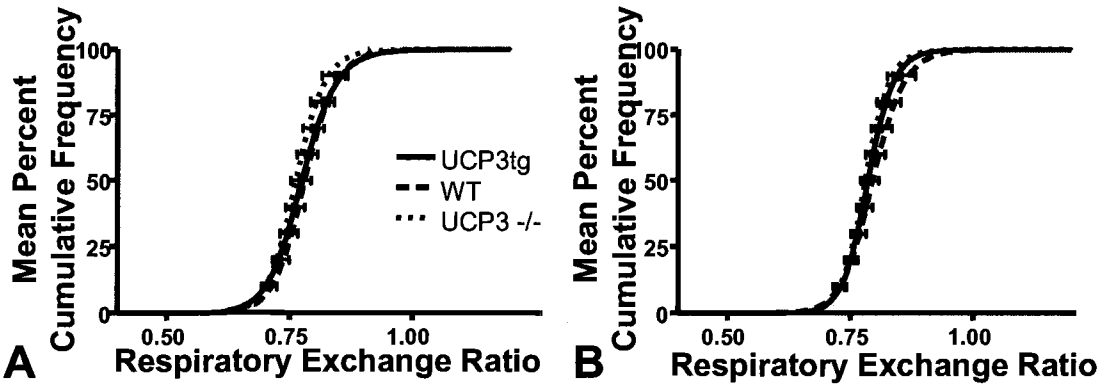

Figure 27: Mean percentage of cumulative frequency (PRCF) of respiratory exchange ratio (RER). One-way ANOVA, Tukey post-test at 10th, 20th, 30th, 40th, 50th, 60th, 70th, 80th, and 90th percentiles. A) After 4 months of HF feeding; n=7-11; NS. B) After 8 months of HF feeding; n=5-9; NS.

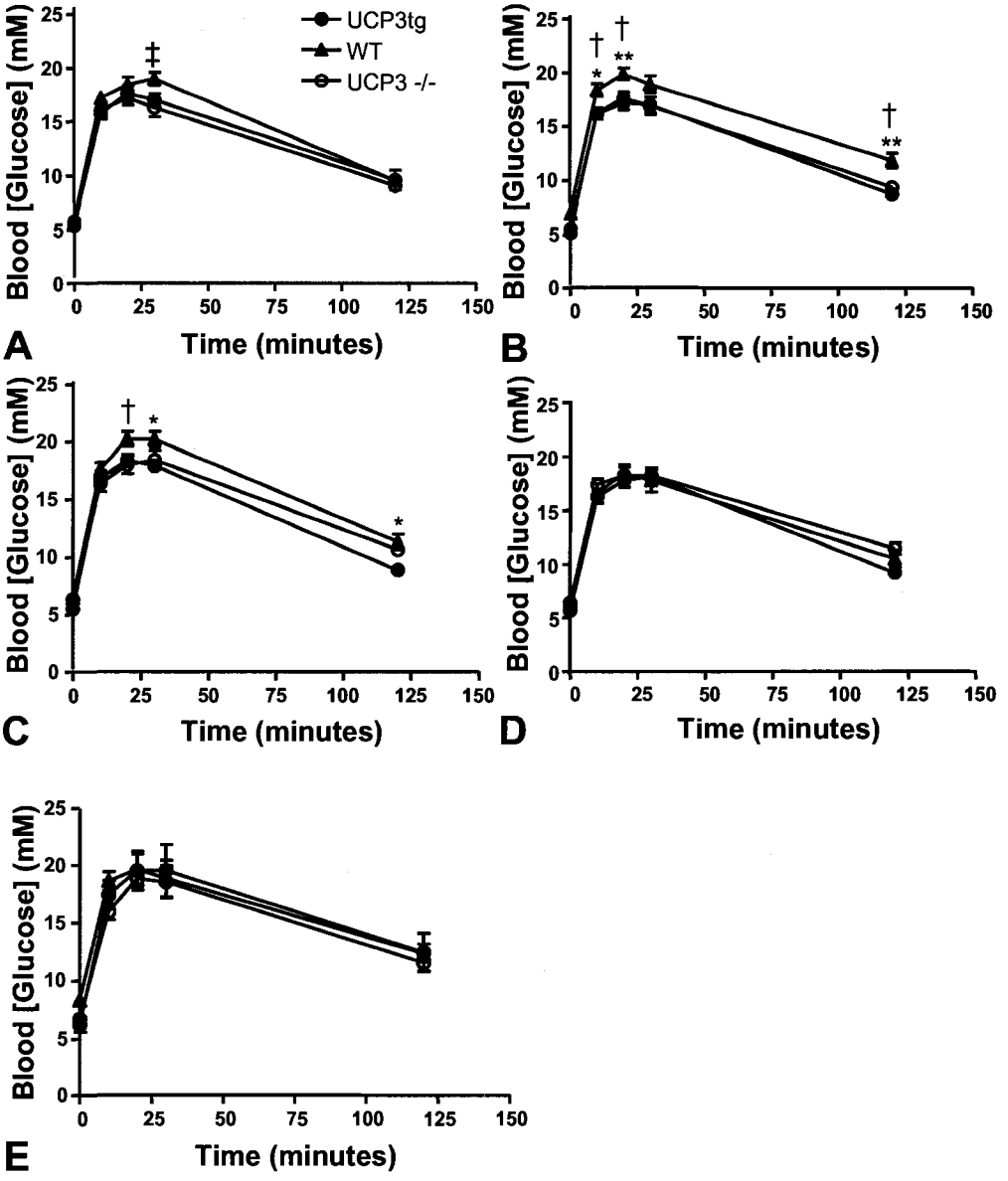

Figure 28: Glucose tolerance tests. Means ± SEM; two-way ANOVA, Bonferroni correction. A) After 1 month of HF feeding; n=20; ‡p<0.01 WT vs. *Ucp3* -/-. B) After 2 months of HF feeding; n=20; *p<0.05, **p<0.01 *UCP3tg* vs. WT; †p<0.05 WT vs. *Ucp3* -/-. C) After 3 months of HF feeding; n=20; *p<0.05 *UCP3tg* vs. WT; †p<0.05 WT vs. *Ucp3* -/-. D) After 4 months of HF feeding; n=20; NS. E) After 8 months of HF feeding; n=10; NS.

Insulin Tolerance

There were no differences in insulin tolerance during the first 2 months of HF feeding (Figures 29A, 29B), however, both *UCP3tg* and *Ucp3 -/-* mice were more insulin sensitive compared to wildtype mice after 3 and 4 months of HF feeding (Figures 29C, 29D). As seen with glucose tolerance, long-term HF feeding caused this difference to disappear: there were no differences in insulin sensitivity between the genotypes after 8 months on the HF diet (Figure 29E).

2-Deoxy-[1-^{3}H]-Glucose Uptake

In accordance with glucose tolerance data, there were no differences in 2-deoxy-[1-^{3}H]-glucose uptake into any tissue (Figure 30A) or in incorporation of 2-deoxy-[1-^{3}H]-glucose into liver glycogen (Figure 30B) after 4 months of HF feeding.

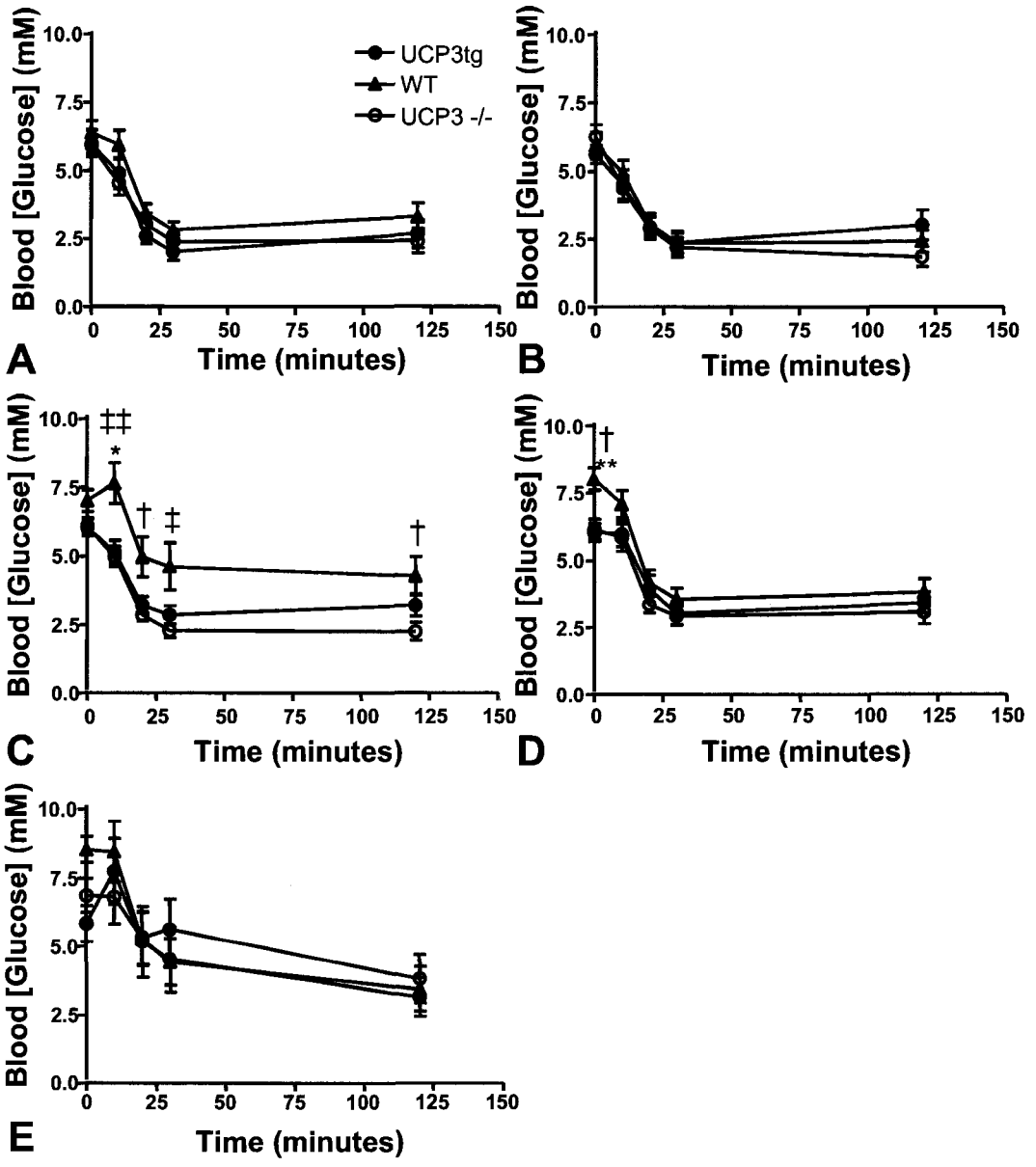

Figure 29: Insulin tolerance tests. Means ± SEM; two-way ANOVA, Bonferroni correction. A) After 1 month of HF feeding; n=19-20; NS. B) After 2 months of HF feeding; n=2-; NS. C) After 3 months of HF feeding; n=20; *p<0.05 *UCP3tg* vs. WT; †p<0.05 ‡p<0.01, ‡‡p<0.001 WT vs. *Ucp3* -/-. D) After 4 months of HF feeding; n=20; **p<0.01 *UCP3tg* vs. WT; †p<0.05 WT vs. *Ucp3* -/-. E) After 8 months of HF feeding; n=10; NS.

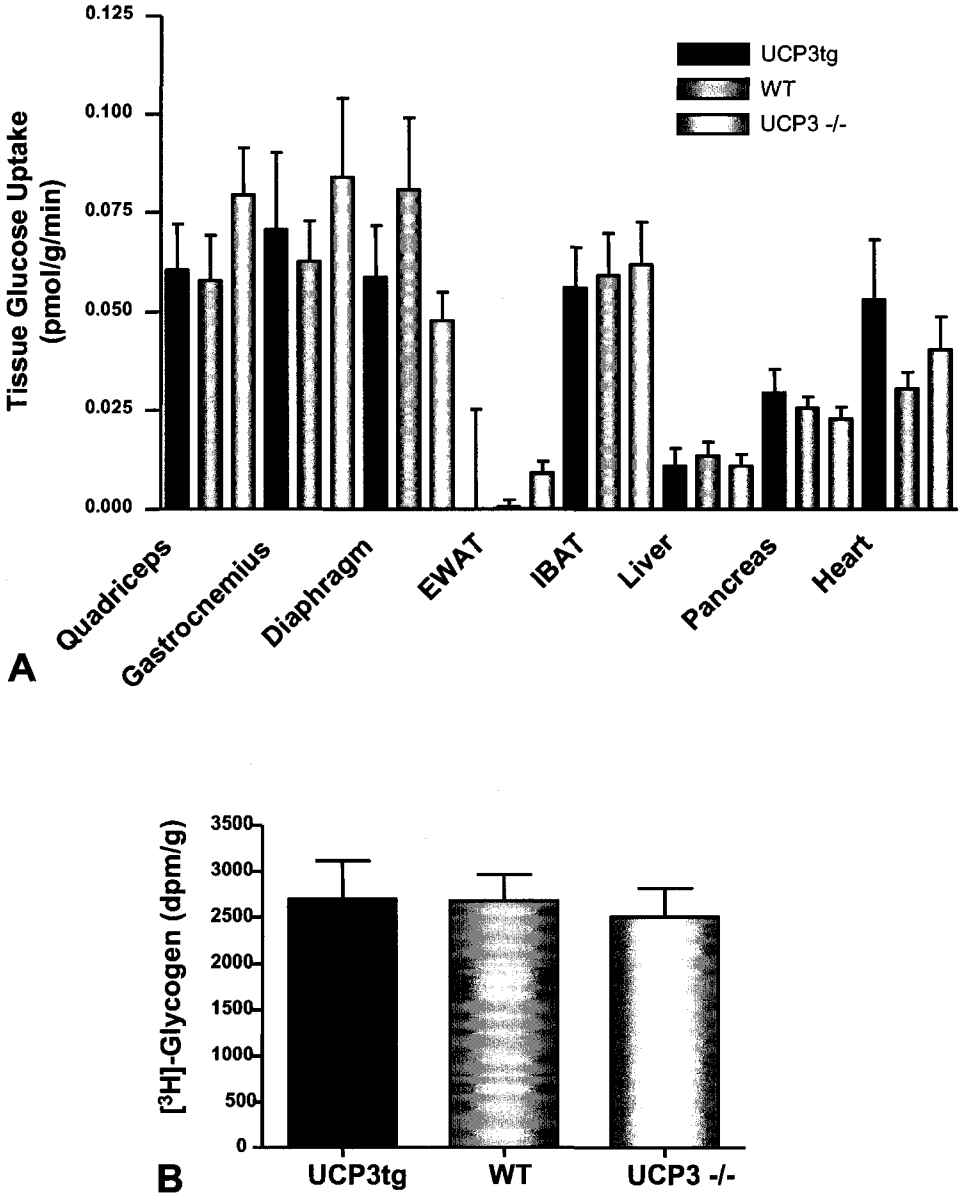

Figure 30: A) Mean 2-deoxy-[^{3}H]-glucose uptake into tissues ± SEM after 4 months of HF feeding. One-way ANOVA, Tukey post-test, NS. B) Mean incorporation of 2-deoxy-[^{3}H]-glucose into liver glycogen ± SEM after 4 months of HF feeding. One-way ANOVA, Tukey post-test, NS.

Discussion

Given the hypothesized roles for UCP3 in skeletal muscle energy expenditure and lipid handling, our aim overall was to assess the impact of the long-term feeding of a high fat diet. To achieve this, we studied congenic mice either lacking, or having physiological overexpression of *UCP3*, compared to wildtype control mice. After 8 months of HF feeding, *UCP3tg* mice showed reduced adiposity compared to *Ucp3* -/- mice, and *Ucp3* -/- mice showed increased adiposity compared to wildtype mice (Figure 25B). Differences in body weight were also observed after 8 months on the HF diet: *UCP3tg* mice had decreased body weight compared to wildtype controls (Figure 23B). There were no differences in muscle (soleus, gastrocnemius, quadriceps, diaphragm), IBAT or organ (pancreas, liver, heart, spleen) weights following 4 or 8 months of HF feeding (Table 6). Therefore, the only tissue to be significantly affected by the absence and physiological overexpression of *UCP3* was adipose tissue. Thus we can conclude that UCP3 plays an important role in mitigating HF diet-induced obesity.

Our results demonstrate that there were no differences in dietary energy intake between the three genotypes, resulting in lower metabolic efficiency in *UCP3tg* mice compared to both wildtype and *Ucp3* -/- mice over 8 months of HF feeding (Figure 24B). Since there were no differences in food

intake, the increased adiposity in *Ucp3* -/- must be explained by differences in energy expenditure. Energy expenditure was measured as oxygen consumption using whole body indirect calorimetry, but we were unable to detect differences in oxygen consumption after 8 months of HF feeding (Figure 26B). It can be difficult to detect small differences in whole body energy expenditure via indirect calorimetry due to the ~5% error associated with this technique (22). Interestingly, compared to *Ucp3* -/- mice, *UCP3tg* mice displayed lower oxygen consumption after 4 months of HF feeding (Figure 26A), despite no differences in body weight (Figure 23A), EWAT weight (Figure 25A), food intake or metabolic efficiency (Figure 24A). However, there were no statistical differences in oxygen consumption between *UCP3tg* mice and wildtype controls. Spontaneous physical activity was not assessed, although differences in this parameter could account for the oxygen consumption results at this early time point.

We previously published a study in which we assessed the absence and the overexpression of *UCP3* in congenic C57Bl6 mice fed a 10% fat defined diet (11). Although *UCP3tg* mice were protected from obesity and the development of insulin resistance, *Ucp3* -/- mice were also protected from insulin resistance. However, when challenged with a high fat (45%) diet, *Ucp3* -/- showed increased accumulation of intramuscular triglyceride (IMTG) compared to wildtypes, whereas *UCP3tg* mice showed decreased IMTG

content. Accumulation of IMTG is known to be closely linked with development of insulin resistance (reviewed in (14)). Additionally, Choi and colleagues demonstrated that *UCP3tg* mice were protected from the development of insulin resistance after short term (10 day-) high fat feeding (9). The latter finding was recently corroborated by Tiraby et al (38). However, neither of these reports included analyses of *Ucp3* -/- mice.

Paradoxically, *Ucp3* -/- mice as well as *UCP3tg* mice were protected from the development of glucose intolerance and insulin resistance when fed a 10% fat diet (11). Similar glucose tolerance results were obtained when mice were fed the 45% fat diet for the first 3 months, although these differences disappeared as of 4 months on the diet (Figures 28A-E). *UCP3tg* and *Ucp3* -/- mice also showed protection from insulin resistance after 3 and 4 months of high fat feeding, but these differences disappeared after 8 months of consumption of the HF diet (Figures 29A-E). Unlike *Ucp3* -/- mice fed the 10% fat diet which showed increased 2-deoxy-[1-^{3}H]-glucose in BAT at 4 months, there were no genotype differences in 2-deoxy-[1-^{3}H]-glucose uptake in any of the muscles, fat depots or organs examined (Figure 30A). In addition, there were no differences in 2-deoxy-[1-^{3}H]-glucose incorporation into liver glycogen in mice fed the HF fat diet (Figure 30B). Altogether, 2-deoxy-[1-^{3}H]-glucose uptake results are consistent with the glucose tolerance data at 4 months (Figure 28D).

Due to its high sequence homology to the original uncoupling protein expressed in BAT, UCP1, UCP3 was first hypothesized to dissipate the proton gradient across the mitochondrial inner membrane in skeletal muscle, thereby uncoupling oxidative phosphorylation and releasing energy as heat. Since its discovery in 1997, several studies have shown that UCP3 is likely not responsible for basal proton leak in muscle (1, 7). In fact, the adenine nucleotide translocator (ANT) is probably responsible for the majority of proton leak in this tissue (6). However, it may be possible that UCP3, upon activation by a fatty acid, a reactive oxygen species (ROS), or a lipid by-product of ROS (*e.g.*, 4-hydroxynonenal) can cause increases in proton leak (5). UCP3 expression is increased in situations of increased reliance on fatty acid oxidation, such as fasting (4, 25), high fat feeding (24, 33) and acute exercise (32, 39). These expression patterns led to two hypotheses implicating UCP3 as a fatty acid anion transporter; either to increase fatty acid oxidation capacity (18) or for the protection from lipid peroxidation (34). Indeed the content and/or activity of key proteins involved in FA uptake and oxidation are increased in *UCP3tg* muscle, supporting a role for UCP3 in FA metabolism (2). MacLellan *et al* also demonstrated that the physiological overexpression of *UCP3* in L6 muscle cells resulted in increased FA oxidation, and decreased reactive oxygen species production (23). However, the molecular mechanisms through which UCP3 functions in FA metabolism are yet to be elucidated.

In conclusion, our results support a role for UCP3 in the protection from fat gain when exposed to a HF diet over a prolonged period of time, but not a role for long-term protection against HF-induced insulin resistance. The physiological function of UCP3 and its molecular mechanism require further investigation, although it appears likely that this protein is involved in fuel management.

Acknowledgements

We would like to thank Linda Jui for assistance with histology, as well as Kim Yates, Eileen Franklin, Nicole Sabet and Mitra Abaeian for their help in animal care. This research was supported by funding from the Canadian Institutes of Health Research: Institute of Nutrition, Metabolism and Diabetes (M-E Harper).

References

1. **Bezaire, V., W. Hofmann, J. K. Kramer, L. P. Kozak, and M. E. Harper.** 2001. Effects of fasting on muscle mitochondrial energetics and fatty acid metabolism in Ucp3(-/-) and wild-type mice. Am J Physiol Endocrinol Metab **281**:E975-82.

2. **Bezaire, V., L. L. Spriet, S. Campbell, N. Sabet, M. Gerrits, A. Bonen, and M. E. Harper.** 2005. Constitutive UCP3 overexpression at physiological levels increases mouse skeletal muscle capacity for fatty acid transport and oxidation. Faseb J **19**:977-9.

3. **Boss, O., S. Samec, A. Dulloo, J. Seydoux, P. Muzzin, and J. P. Giacobino.** 1997. Tissue-dependent upregulation of rat uncoupling protein-2 expression in response to fasting or cold. FEBS Lett **412**:111-4.

4. **Boss, O., S. Samec, F. Kuhne, P. Bijlenga, F. Assimacopoulos-Jeannet, J. Seydoux, J. P. Giacobino, and P. Muzzin.** 1998. Uncoupling protein-3 expression in rodent skeletal muscle is modulated by food intake but not by changes in environmental temperature. J Biol Chem **273**:5-8.

5. **Brand, M. D., and T. C. Esteves.** 2005. Physiological functions of the mitochondrial uncoupling proteins UCP2 and UCP3. Cell Metab **2**:85-93.

6. **Brand, M. D., J. L. Pakay, A. Ocloo, J. Kokoszka, D. C. Wallace, P. S. Brookes, and E. J. Cornwall.** 2005. The basal proton conductance of mitochondria depends on adenine nucleotide translocase content. Biochem J **392**:353-62.

7. **Cadenas, S., J. A. Buckingham, S. Samec, J. Seydoux, N. Din, A. G. Dulloo, and M. D. Brand.** 1999. UCP2 and UCP3 rise in starved rat skeletal muscle but mitochondrial proton conductance is unchanged. FEBS Lett **462**:257-60.

8. **Cannon, B., and J. Nedergaard.** 2004. Brown adipose tissue: function and physiological significance. Physiol Rev **84**:277-359.

9. **Choi, C. S., J. J. Fillmore, J. K. Kim, Z. X. Liu, S. Kim, E. F. Collier, A. Kulkarni, A. Distefano, Y. J. Hwang, M. Kahn, Y. Chen, C. Yu, I. K. Moore, R. M. Reznick, T. Higashimori, and G. I. Shulman.** 2007. Overexpression of uncoupling protein 3 in skeletal muscle protects against fat-induced insulin resistance. J Clin Invest **117**:1995-2003.

10. **Clapham, J. C., J. R. Arch, H. Chapman, A. Haynes, C. Lister, G. B. Moore, V. Piercy, S. A. Carter, I. Lehner, S. A. Smith, L. J. Beeley, R. J. Godden, N. Herrity, M. Skehel, K. K. Changani, P. D. Hockings, D. G. Reid, S. M. Squires, J. Hatcher, B. Trail, J. Latcham, S. Rastan, A. J. Harper, S. Cadenas, J. A. Buckingham, M. D. Brand, and A. Abuin.** 2000. Mice overexpressing human uncoupling protein-3 in skeletal muscle are hyperphagic and lean. Nature **406**:415-8.

11. **Costford, S. R., S. N. Chaudhry, M. Salkhordeh, and M. E. Harper.** 2006. Effects of the Presence, Absence and Overexpression of Uncoupling Protein-3 on Adiposity and Fuel Metabolism in Congenic Mice. Am J Physiol Endocrinol Metab. **290**: E1304-12.

12. **Flegal, K. M., M. D. Carroll, R. J. Kuczmarski, and C. L. Johnson.** 1998. Overweight and obesity in the United States: prevalence and trends, 1960-1994. Int J Obes Relat Metab Disord **22**:39-47.

13. **Gong, D. W., S. Monemdjou, O. Gavrilova, L. R. Leon, B. Marcus-Samuels, C. J. Chou, C. Everett, L. P. Kozak, C. Li, C. Deng, M. E. Harper, and M. L. Reitman.** 2000. Lack of obesity and normal response to fasting and thyroid hormone in mice lacking uncoupling protein-3. J Biol Chem **275**:16251-7.

14. **Goodpaster, B. H., and D. E. Kelley.** 2002. Skeletal muscle triglyceride: marker or mediator of obesity-induced insulin resistance in type 2 diabetes mellitus? Curr Diab Rep **2**:216-22.

15. **Harper, J. A., J. A. Stuart, M. B. Jekabsons, D. Roussel, K. M. Brindle, K. Dickinson, R. B. Jones, and M. D. Brand.** 2002. Artifactual uncoupling by uncoupling protein 3 in yeast mitochondria at the concentrations found in mouse and rat skeletal-muscle mitochondria. Biochem J **361**:49-56.

16. **Harper, M. E., J. S. Ballantyne, M. Leach, and M. D. Brand.** 1993. Effects of thyroid hormones on oxidative phosphorylation. Biochem Soc Trans 21 **(Pt 3)**:785-92.

17. **Harper, M. E., R. Dent, S. Monemdjou, V. Bezaire, L. Van Wyck, G. Wells, G. N. Kavaslar, A. Gauthier, F. Tesson, and R. McPherson.** 2002. Decreased mitochondrial proton leak and reduced expression of uncoupling protein 3 in skeletal muscle of obese diet-resistant women. Diabetes **51**:2459-66.

18. **Himms-Hagen, J., and M. E. Harper.** 2001. Physiological role of UCP3 may be export of fatty acids from mitochondria when fatty acid oxidation predominates: an hypothesis. Exp Biol Med (Maywood) **226**:78-84.

19. **Hinz, W., S. Gruninger, A. De Pover, and M. Chiesi.** 1999. Properties of the human long and short isoforms of the uncoupling protein-3 expressed in yeast cells. FEBS Lett **462**:411-5.

20. **Kopelman, P. G.** 2000. Obesity as a medical problem. Nature **404**:635-43.

21. **Kuczmarski, R. J., K. M. Flegal, S. M. Campbell, and C. L. Johnson.** 1994. Increasing prevalence of overweight among US adults. The National Health and Nutrition Examination Surveys, 1960 to 1991. Jama **272**:205-11.

22. **Livesey, G., and M. Elia.** 1988. Estimation of energy expenditure, net carbohydrate utilization, and net fat oxidation and synthesis by indirect calorimetry: evaluation of errors with special reference to the detailed composition of fuels. Am J Clin Nutr **47**:608-28.

23. **Maclellan, J. D., M. F. Gerrits, A. Gowing, P. J. Smith, M. B. Wheeler, and M. E. Harper.** 2005. Physiological increases in uncoupling protein 3 augment Fatty Acid oxidation and decrease reactive oxygen species production without uncoupling respiration in muscle cells. Diabetes **54**:2343-50.

24. **Matsuda, J., K. Hosoda, H. Itoh, C. Son, K. Doi, T. Tanaka, Y. Fukunaga, G. Inoue, H. Nishimura, Y. Yoshimasa, Y. Yamori, and K. Nakao.** 1997. Cloning of rat uncoupling protein-3 and uncoupling protein-2 cDNAs: their gene expression in rats fed high-fat diet. FEBS Lett **418**:200-4.

25. **Millet, L., H. Vidal, F. Andreelli, D. Larrouy, J. P. Riou, D. Ricquier, M. Laville, and D. Langin.** 1997. Increased uncoupling protein-2 and -3 mRNA expression during fasting in obese and lean humans. J Clin Invest **100**:2665-70.

26. **Nicholls, D. G., and R. M. Locke.** 1984. Thermogenic mechanisms in brown fat. Physiol Rev **64**:1-64.

27. **Ogden, C. L., M. D. Carroll, L. R. Curtin, M. A. McDowell, C. J. Tabak, and K. M. Flegal.** 2006. Prevalence of overweight and obesity in the United States, 1999-2004. Jama **295**:1549-55.

28. **Rankinen, T., A. Zuberi, Y. C. Chagnon, S. J. Weisnagel, G. Argyropoulos, B. Walts, L. Perusse, and C. Bouchard.** 2006. The human obesity gene map: the 2005 update. Obesity (Silver Spring) **14**:529-644.

29. **Riachi, M., J. Himms-Hagen, and M. E. Harper.** 2004. Percent relative cumulative frequency analysis in indirect calorimetry: application to studies of transgenic mice. Can J Physiol Pharmacol **82**:1075-83.

30. **Rolfe, D. F., and M. D. Brand.** 1996. Contribution of mitochondrial proton leak to skeletal muscle respiration and to standard metabolic rate. Am J Physiol **271**:C1380-9.

31. **Rolfe, D. F., J. M. Newman, J. A. Buckingham, M. G. Clark, and M. D. Brand.** 1999. Contribution of mitochondrial proton leak to respiration rate in working skeletal muscle and liver and to SMR. Am J Physiol **276**:C692-9.

32. **Schrauwen, P., M. K. Hesselink, I. Vaartjes, E. Kornips, W. H. Saris, J. P. Giacobino, and A. Russell.** 2002. Effect of acute exercise on uncoupling protein 3 is a fat metabolism-mediated effect. Am J Physiol Endocrinol Metab **282**:E11-7.

33. **Schrauwen, P., H. Hoppeler, R. Billeter, A. H. Bakker, and D. R. Pendergast.** 2001. Fiber type dependent upregulation of human skeletal muscle UCP2 and UCP3 mRNA expression by high-fat diet. Int J Obes Relat Metab Disord **25**:449-56.

34. **Schrauwen, P., W. H. Saris, and M. K. Hesselink.** 2001. An alternative function for human uncoupling protein 3: protection of mitochondria against accumulation of nonesterified fatty acids inside the mitochondrial matrix. Faseb J **15**:2497-502.

35. **Seifert, E. L., and M. Harper.** 2007. Thyroid effects on mitochondrial function. Thyroid In press.

36. **Speakman, J. R.** 2004. Obesity: the integrated roles of environment and genetics. J Nutr **134**:2090S-2105S.

37. **Stuart, J. A., J. A. Harper, K. M. Brindle, M. B. Jekabsons, and M. D. Brand.** 2001. Physiological levels of mammalian uncoupling protein 2 do not uncouple yeast mitochondria. J Biol Chem **276**:18633-9.

38. **Tiraby, C., G. Tavernier, F. Capel, A. Mairal, F. Crampes, J. Rami, C. Pujol, J. A. Boutin, and D. Langin.** 2007. Resistance to high-fat-diet-induced obesity and sexual dimorphism in the metabolic responses of transgenic mice with moderate uncoupling protein 3 overexpression in glycolytic skeletal muscles. Diabetologia **50**:2190-9.

39. **Tsuboyama-Kasaoka, N., N. Tsunoda, K. Maruyama, M. Takahashi, H. Kim, S. Ikemoto, and O. Ezaki.** 1998. Up-regulation of uncoupling protein 3 (UCP3) mRNA by exercise training and down-regulation of UCP3 by denervation in skeletal muscle. Biochem Biophys Res Commun **247**:498-503.

40. **Vidal-Puig, A., G. Solanes, D. Grujic, J. S. Flier, and B. B. Lowell.** 1997. UCP3: an uncoupling protein homologue expressed preferentially and abundantly in skeletal muscle and brown adipose tissue. Biochem Biophys Res Commun **235**:79-82.

41. **Wang, S., A. Subramaniam, M. A. Cawthorne, and J. C. Clapham.** 2003. Increased fatty acid oxidation in transgenic mice overexpressing UCP3 in skeletal muscle. Diabetes Obes Metab **5**:295-301.

42. **Zhang, C. Y., T. Hagen, V. K. Mootha, L. J. Slieker, and B. B. Lowell.** 1999. Assessment of uncoupling activity of uncoupling protein 3 using a yeast heterologous expression system. FEBS Lett **449**:129-34.

General Discussion

The Necessity of Novel Therapies for Energy Regulation Disorders

In a country where ~6 in 10 adults and ~3 in 10 children are overweight or obese (64), there can be no disputing the necessity of action in this area. The medical implications of maintaining a state of over-nutrition are clear (reviewed in (40)) and include Canada's leading causes of death, cardiovascular disease and cancer (65). Another risk factor associated with overweight/obesity is the energy management disorder T2DM (reviewed in (40)). Over 2 million Canadians are currently living with DM, and this number is expected to grow by 50% by the time we reach the year 2010 (CDA). The association between overweight/obesity and T2DM is well documented (10, 13, 20, 58) and adds to the complexity of dissecting this energy management disorder. With the majority of our population living in a state of positive energy balance and an increasing number of Canadians succumbing to insulin resistance and T2DM, the need for the development of effective treatment strategies has become essential.

Weight loss and/or halting/reversing the progression of T2DM through lifestyle management is possible, but difficult for many people in today's obesigenic society. A negative energy balance can be achieved through a decrease in energy intake (via caloric restriction) and/or an increase in energy

expenditure (via physical activity). Weight loss has been shown to be effective in improving glucose tolerance and insulin sensitivity in type 2 diabetics (27, 44), and even muscle contraction alone is extremely beneficial as it elicits glucose uptake through the insulin-independent pathway (42, 46, 51, 52, 70, 75, 78). However, adherence to this traditional 'diet and exercise' regimen has proven to be easier said than done for many individuals.

Targeting energy intake is an active area of research, as discussed in the *Whole Body Energy Regulation* section of the General Introduction of this thesis. Exploiting neuro-endocrine pathways to control feelings of hunger and satiety may be an effective way to regulate food intake in humans (28). Targeting energy expenditure at the molecular level may also be possible through the activation of uncoupling of oxidative phosphorylation in skeletal muscle or converted WAT (reviewed in (15)), also discussed in the General Introduction in the *Treatment of Energy Regulation Disorders* section. Regardless of the targeting strategy, it is clear that research into the basic mechanisms underlying whole body energy management and tissue-specific cellular energy homeostasis will be crucial for the development of novel therapies to stem the energy disregulation epidemic in our society.

AMPKγ_3 Activation as a Treatment for T2DM and Obesity

AMPK is touted as the master regulator of energy in the cell (30, 32) and fascinatingly contributes to the regulation of energy balance at the level of the whole body as well (reviewed in (39)). When activated (through a fall in cellular ATP levels and subsequent rise in AMP levels) by muscle contraction, low glucose, hypoxia or ischemia (33, 76), AMPK 'turns on' ATP producing pathways and associated processes such as glucose uptake, glycolysis, fatty acid oxidation and mitochondrial biogenesis. Activated AMPK 'turns off' ATP consuming pathways such as those responsible for the synthesis of glycogen, fatty acids, sterols and proteins. It thus restores energy charge in the cell (reviewed in (29)).

Since the activation of AMPK elicits glucose uptake into the cell in an insulin-independent manner (48) and suppresses gluconeogenesis in the liver (45), it is a logical target for T2DM therapy. In fact, AMPK activation in skeletal muscle has been shown to reduce the level of insulin resistance and T2DM in experimental animals (4, 8, 9, 74). Metformin, an anti-diabetic drug of widespread use, indirectly activates AMPK (24, 77) through the tumor suppressor LKB1(62) to improve glucose clearance in type 2 diabetics. Rosiglitazone and pioglitazone, both TZDs and also commonly prescribed in cases of T2DM, have been shown to carry out their effects partly through PPARγ/adiponectin-mediated activation of AMPK (24, 41, 43, 49, 55). The

positive effects of these drugs in skeletal muscle and liver are clear, however, metformin and TZDs are non-specific activators of AMPK, therefore activating AMPK in all tissues. Activation of AMPK in the hypothalamus results in increased food intake (reviewed in (39)), which is obviously undesirable in obesity and T2DM. Also, certain missense mutations in the AMPKγ_2 isoform have been shown to be constitutively active when expressed in the AMPK yeast homologue (SNF1/SNF4) (2) (although some controversy exists here (18)) and result in increased glycogen storage in the heart, WPW syndrome, conduction system disease and cardiac hypertrophy (2, 25, 26). In fact, it was recently revealed that some subjects treated with rosiglitazone have a slightly elevated risk of death from a cardiovascular event (50), and it has been suggested that this risk may arise from the activation of AMPK in the heart (31).

It therefore seems rational that more specific activators of AMPK would be of great benefit for the treatment of T2DM. Since AMPK has three subunits, each with various isoforms, one way to target tissue-specific AMPK activation would be to develop a pharmaceutical that activates only one isoform of a particular subunit. The gamma-3 isoform is expressed exclusively in skeletal muscle, and it is thought that only three AMPK complexes are expressed in human *vastus lateralis*: $\alpha_1/\beta_2/\gamma_1$, $\alpha_2/\beta_2/\gamma_1$ and $\alpha_2/\beta_2/\gamma_3$ (5). Further, only the gamma-3 containing complex is phosphorylated and activated during high

intensity exercise (5). Based on studies in purebred Hampshire Rendement Napole pigs, AMPKγ_3 containing the R225Q mutation has been shown to result in increased AMPK activity, increased glycogen storage in skeletal muscle (but not in heart or liver) and decreased muscle fat (1, 35, 71). Increased muscle glycogen content may seem contradictory in a situation of AMPK activation since AMPK is known to inhibit glycogen synthase; however, it is thought that increased glucose uptake rates overcompensate for this inhibition, resulting in the accumulation of glycogen in muscle tissue. In fact, it has been shown that R225Q pigs re-synthesize glycogen at faster rates than control pigs due to increased muscle glucose uptake rates following an exercise challenge (1, 35). Development of a pharmaceutical that would act specifically on the gamma-3 subunit of AMPK could be an effective way to increase glucose uptake in skeletal muscle of individuals with T2DM without eliciting negative effects in the brain or heart. Unfortunately, hepatic glucose production would not be decreased (as is it with metformin treatment (3, 37)) as AMPKγ_3 is not expressed in the liver.

Prior to development of such a drug, we now have a model of how it might affect humans: the recently identified naturally occurring AMPKγ_3 R225W mutation results in both increased basal and AMP-stimulated AMPK activity in skeletal muscle, increased muscle glycogen and decreased IMTG in the absence of a change in fiber type ratio (17). Additionally, it may cause

increased glucose uptake in skeletal muscle following exercise (preliminary results in Appendix A), as seen in the R225Q pigs (1, 35). Further characterization of the AMPKγ_3 R225W carriers is required. In an ongoing study, we are continuing to assess glucose uptake into skeletal muscle *in vivo* in the resting and exercised states through positron emission tomography (PET) (described in Appendix A). We will also investigate glucose uptake following a VO_2max treadmill test and look at whole body oxygen consumption and respiratory exchange ratios via indirect calorimetry in the resting and exercised states. Another muscle biopsy of these carriers and their matched controls is planned so that we can look at metabolic characteristics of isolated muscle cells grown up and differentiated in culture. Experiments planned include biochemical determination of glycogen and IMTG, oxygen consumption and metabolic flexibility using fluorescence technologies (Seahorse Bioscience Extracellular Flux Analyzer), mitochondrial membrane potential and ROS production through the use of fluorescence probes, and glucose uptake using radiotracer approaches. Activities of key enzymes known to be affected by AMPK will also be measured. It is our hope that a full characterization of the effects of the AMPKγ_3 R225W mutation *in vivo* and *in vitro* will lead to the development of novel pharmacotherapies for individuals with T2DM, as we now know that individuals with T2DM or obesity have deceased AMPK activation during exercise (63).

There is less evidence to support AMPK as an effective target for obesity treatment, although long-term AICAR treatment in rats has been shown to decrease intra-abdominal fat content (73). The stimulation of pathways such as glycolysis and fatty acid oxidation through activation of AMPK may initially appear to be instigating a shift towards an increase in energy expenditure; however, the end result of these pathways is the production of ATP. Phosphogen levels are tightly regulated in the cell: the ATP:ADP ratio is maintained at 10:1 (reviewed in (34)). ATP is a direct inhibitor of AMPK, therefore high cellular levels of ATP inactivate AMPK (14, 19). This negative feedback loop would make achieving a negative energy balance impossible strictly through the activation of AMPK. In order to maintain activation of AMPK (and its downstream effectors), ATP levels in the cell would need to be depleted through the utilization of ATP, or ATP production would have to be prevented through uncoupling of oxidative phosphorylation, where the energy associated with reducing equivalents entering the ETC would be dissipated as heat. It is worth noting, however, that whole body energy balance has many major players besides AMPK (*e.g.*, NPY, endocannabinoids and GRP; reviewed in (28)). Activation of AMPK in peripheral tissues may be (over-)compensated for by other neuro-endocrine players in order to affect whole body energy balance. The ability of ATP to inhibit skeletal muscle AMPK activity in AMPKγ_3 R225W carriers has yet to be assessed.

The Physiological Function of UCP3

The physiological role of UCP3 is still elusive, despite 10 years of active research since its discovery. Probably the most striking phenotype of the UCP3 overexpressor mouse is its leanness, even when challenged with a high fat diet (12, 16, 66); however, UCP3 protein levels do not correlate with BMI in humans (59). One possibility that could explain this phenotype in the overexpressor mice (and lack of the opposite phenotype in the knockout mice) is that even a 2 to 3-fold increase in UCP3 protein causes artifactual uncoupling. This possibility has yet to be tested.

It has been shown that individuals with T2DM have lower levels of UCP3 protein in *vastus lateralis* (59), and several studies have shown improved glucose and insulin tolerance in UCP3 overexpressor mice (11, 12, 16); however, UCP3 knockout mice display the same protection from the development of insulin resistance (16), and neither UCP3 overexpressors or knockouts are protected from the development of insulin resistance when challenged with long-term high fat feeding (Costford *et al., submitted*).

Uncoupling of oxidative phosphorylation in skeletal muscle accounts for up to 50% of the tissue's resting metabolic rate (53, 54). Uncoupling in this tissue is therefore a reasonable target for increasing energy expenditure in the treatment of obesity. The discovery that UCP3 is expressed predominantly in

skeletal muscle and has high sequence homology to UCP1 (7, 69) sparked the logical hypothesis that it was indeed responsible for the high rates of uncoupling in resting muscle. UCP3 was subsequently found to be upregulated in response to situations of dependence on fatty acid oxidation and/or energy deficit such as fasting (6, 47, 72), acute exercise (60, 68) or high fat feeding (56, 57). No consistent correlations have been observed between UCP3 expression and altered *in vivo* energy expenditure. The uncoupling hypothesis therefore became inconsistent with UCP3's expression patterns. Two hypotheses for the function of UCP3 in fat metabolism were put forward in 2001: as a facilitator of beta oxidation (36) or as a protector from lipotoxicity (61). Another hypothesis was subsequently proposed implicating UCP3 in the protection from ROS and oxidative damage via mediation of an inducible proton leak (21-23). Very recently, it has also been proposed that the UCPs play important roles in mitochondrial calcium import (67).

The studies described in this thesis do not advance our understanding of the molecular mechanism of UCP3 action; however, they do support a role for UCP3 in fat metabolism. Under both low and high fat feeding circumstances, UCP3 appears to prevent the accumulation of lipid storage in muscle (16), although this does not necessarily translate into protection from the development of fat-induced insulin resistance in the long-term (Costford *et al., submitted*). UCP3 protected against increased storage of lipid in BAT

under low fat feeding conditions (16) and protected against the accumulation of adipose tissue during long-term high fat feeding conditions (Costford *et al., submitted*). Based on these studies, it is possible that UCP3 may be an effective target for the prevention of fat gain; however, inducible transgenic mouse models are required for the determination of whether inducing increased expression of UCP3 is effective in initiating weight loss and reversing obesity. Regardless, further studies into the mechanistic action of this elusive protein are required for a better understanding of its physiological role.

Conclusions

Energy regulation disorders are complex. The heterogeneity of these disorders, especially obesity (reviewed in (38)), necessitates interdisciplinary routes of therapy. Investigated in this thesis were the roles of two potential obesity/T2DM therapeutic targets, AMPK and UCP3, in skeletal muscle fuel metabolism.

Although further characterization is required, the identification of the naturally occurring AMPKγ_3 R225W mutation in humans, the subsequent discovery of its gain-of-function nature and the associated skeletal muscle fuel storage characteristics has set the stage for the development of a gamma-3 specific pharmaceutical activator of AMPK. Such an activator

would increase AMPK activity in skeletal muscle and promote increased glucose uptake in this tissue without altering AMPK activity or eliciting unwanted effects in other tissues.

The physiological function of UCP3 has yet to be elucidated, however it is clear that overexpression of this mitochondrial inner membrane protein leads to the prevention of fat gain, even following long-term high fat feeding. UCP3 may play a role in the protection from the development of insulin resistance, but only in situations of low fat feeding or short-term high fat feeding. There is ample evidence that UCP3 plays a role in the management or regulation of fat metabolism, however, mechanistic studies are now required to determine its molecular role in the cell.

AMPK and UCP3 are undoubtedly important players in the bioenergetics of skeletal muscle. There is potential for each as a target for novel pharmacotherapies, although further investigation in these areas is still required.

References

1. **Andersson, L.** 2003. Identification and characterization of AMPK gamma 3 mutations in the pig. Biochem Soc Trans **31**:232-5.

2. **Arad, M., D. W. Benson, A. R. Perez-Atayde, W. J. McKenna, E. A. Sparks, R. J. Kanter, K. McGarry, J. G. Seidman, and C. E. Seidman.** 2002. Constitutively active AMP kinase mutations cause glycogen storage disease mimicking hypertrophic cardiomyopathy. J Clin Invest **109**:357-62.

3. **Bailey, C. J., and R. C. Turner.** 1996. Metformin. N Engl J Med **334**:574-9.

4. **Bergeron, R., J. M. Ren, K. S. Cadman, I. K. Moore, P. Perret, M. Pypaert, L. H. Young, C. F. Semenkovich, and G. I. Shulman.** 2001. Chronic activation of AMP kinase results in NRF-1 activation and mitochondrial biogenesis. Am J Physiol Endocrinol Metab **281**:E1340-6.

5. **Birk, J. B., and J. F. Wojtaszewski.** 2006. Predominant alpha2/beta2/gamma3 AMPK activation during exercise in human skeletal muscle. J Physiol **577**:1021-32.

6. **Boss, O., S. Samec, F. Kuhne, P. Bijlenga, F. Assimacopoulos-Jeannet, J. Seydoux, J. P. Giacobino, and P. Muzzin.** 1998. Uncoupling protein-3 expression in rodent skeletal muscle is modulated by food intake but not by changes in environmental temperature. J Biol Chem **273**:5-8.

7. **Boss, O., S. Samec, A. Paoloni-Giacobino, C. Rossier, A. Dulloo, J. Seydoux, P. Muzzin, and J. P. Giacobino.** 1997. Uncoupling protein-3: a new member of the mitochondrial carrier family with tissue-specific expression. FEBS Lett **408**:39-42.

8. **Buhl, E. S., N. Jessen, R. Pold, T. Ledet, A. Flyvbjerg, S. B. Pedersen, O. Pedersen, O. Schmitz, and S. Lund.** 2002. Long-term AICAR administration reduces metabolic disturbances and lowers blood pressure in rats displaying features of the insulin resistance syndrome. Diabetes **51**:2199-206.

9. **Buhl, E. S., N. Jessen, O. Schmitz, S. B. Pedersen, O. Pedersen, G. D. Holman, and S. Lund.** 2001. Chronic treatment with 5-aminoimidazole-4-carboxamide-1-beta-D-ribofuranoside increases insulin-stimulated glucose uptake and GLUT4 translocation in rat skeletal muscles in a fiber type-specific manner. Diabetes **50**:12-7.

10. **Chan, J. M., E. B. Rimm, G. A. Colditz, M. J. Stampfer, and W. C. Willett.**

1994. Obesity, fat distribution, and weight gain as risk factors for clinical diabetes in men. Diabetes Care **17:**961-9.

11. **Choi, C. S., J. J. Fillmore, J. K. Kim, Z. X. Liu, S. Kim, E. F. Collier, A. Kulkarni, A. Distefano, Y. J. Hwang, M. Kahn, Y. Chen, C. Yu, I. K. Moore, R. M. Reznick, T. Higashimori, and G. I. Shulman.** 2007. Overexpression of uncoupling protein 3 in skeletal muscle protects against fat-induced insulin resistance. J Clin Invest **117:**1995-2003.

12. **Clapham, J. C., J. R. Arch, H. Chapman, A. Haynes, C. Lister, G. B. Moore, V. Piercy, S. A. Carter, I. Lehner, S. A. Smith, L. J. Beeley, R. J. Godden, N. Herrity, M. Skehel, K. K. Changani, P. D. Hockings, D. G. Reid, S. M. Squires, J. Hatcher, B. Trail, J. Latcham, S. Rastan, A. J. Harper, S. Cadenas, J. A. Buckingham, M. D. Brand, and A. Abuin.** 2000. Mice overexpressing human uncoupling protein-3 in skeletal muscle are hyperphagic and lean. Nature **406:**415-8.

13. **Colditz, G. A., W. C. Willett, A. Rotnitzky, and J. E. Manson.** 1995. Weight gain as a risk factor for clinical diabetes mellitus in women. Ann Intern Med **122:**481-6.

14. **Corton, J. M., J. G. Gillespie, S. A. Hawley, and D. G. Hardie.** 1995. 5-aminoimidazole-4-carboxamide ribonucleoside. A specific method for activating AMP-activated protein kinase in intact cells? Eur J Biochem **229:**558-65.

15. **Costford, S., A. Gowing, and M. E. Harper.** 2007. Mitochondrial uncoupling as a target in the treatment of obesity. Curr Opin Clin Nutr Metab Care **10:**671-8.

16. **Costford, S. R., S. N. Chaudhry, M. Salkhordeh, and M. E. Harper.** 2006. Effects of the presence, absence, and overexpression of uncoupling protein-3 on adiposity and fuel metabolism in congenic mice. Am J Physiol Endocrinol Metab **290:**E1304-12.

17. **Costford, S. R., N. Kavaslar, N. Ahituv, S. N. Chaudhry, W. S. Schackwitz, R. Dent, L. A. Pennacchio, R. McPherson, and M. E. Harper.** 2007. Gain-of-function R225W mutation in human AMPKgamma3 causing increased glycogen and decreased triglyceride in skeletal muscle. PLoS ONE **2:**e903.

18. **Daniel, T., and D. Carling.** 2002. Functional analysis of mutations in the gamma 2 subunit of AMP-activated protein kinase associated with

cardiac hypertrophy and Wolff-Parkinson-White syndrome. J Biol Chem **277:**51017-24.

19. **Davies, S. P., N. R. Helps, P. T. Cohen, and D. G. Hardie.** 1995. 5'-AMP inhibits dephosphorylation, as well as promoting phosphorylation, of the AMP-activated protein kinase. Studies using bacterially expressed human protein phosphatase-2C alpha and native bovine protein phosphatase-2AC. FEBS Lett **377:**421-5.

20. **Dunstan, D. W., P. Z. Zimmet, T. A. Welborn, M. P. De Courten, A. J. Cameron, R. A. Sicree, T. Dwyer, S. Colagiuri, D. Jolley, M. Knuiman, R. Atkins, and J. E. Shaw.** 2002. The rising prevalence of diabetes and impaired glucose tolerance: the Australian Diabetes, Obesity and Lifestyle Study. Diabetes Care **25:**829-34.

21. **Echtay, K. S., T. C. Esteves, J. L. Pakay, M. B. Jekabsons, A. J. Lambert, M. Portero-Otin, R. Pamplona, A. J. Vidal-Puig, S. Wang, S. J. Roebuck, and M. D. Brand.** 2003. A signalling role for 4-hydroxy-2-nonenal in regulation of mitochondrial uncoupling. Embo J **22:**4103-10.

22. **Echtay, K. S., M. P. Murphy, R. A. Smith, D. A. Talbot, and M. D. Brand.** 2002. Superoxide activates mitochondrial uncoupling protein 2 from the matrix side. Studies using targeted antioxidants. J Biol Chem **277:**47129-35.

23. **Echtay, K. S., D. Roussel, J. St-Pierre, M. B. Jekabsons, S. Cadenas, J. A. Stuart, J. A. Harper, S. J. Roebuck, A. Morrison, S. Pickering, J. C. Clapham, and M. D. Brand.** 2002. Superoxide activates mitochondrial uncoupling proteins. Nature **415:**96-9.

24. **Fryer, L. G., A. Parbu-Patel, and D. Carling.** 2002. The Anti-diabetic drugs rosiglitazone and metformin stimulate AMP-activated protein kinase through distinct signaling pathways. J Biol Chem **277:**25226-32.

25. **Gollob, M. H., M. S. Green, A. S. Tang, T. Gollob, A. Karibe, A. S. Ali Hassan, F. Ahmad, R. Lozado, G. Shah, L. Fananapazir, L. L. Bachinski, and R. Roberts.** 2001. Identification of a gene responsible for familial Wolff-Parkinson-White syndrome. N Engl J Med **344:**1823-31.

26. **Gollob, M. H., J. J. Seger, T. N. Gollob, T. Tapscott, O. Gonzales, L. Bachinski, and R. Roberts.** 2001. Novel PRKAG2 mutation responsible for the genetic syndrome of ventricular preexcitation and conduction system disease with childhood onset and absence of cardiac hypertrophy. Circulation **104:**3030-3.

27. **Goodpaster, B. H., D. E. Kelley, R. R. Wing, A. Meier, and F. L. Thaete.** 1999. Effects of weight loss on regional fat distribution and insulin sensitivity in obesity. Diabetes **48**:839-47.

28. **Halford, J. C., G. D. Cooper, and T. M. Dovey.** 2004. The pharmacology of human appetite expression. Curr Drug Targets **5**:221-40.

29. **Hardie, D. G.** 2007. AMP-activated/SNF1 protein kinases: conserved guardians of cellular energy. Nat Rev Mol Cell Biol **8**:774-85.

30. **Hardie, D. G.** 1994. An emerging role for protein kinases: the response to nutritional and environmental stress. Cell Signal **6**:813-21.

31. **Hardie, D. G.** 2008. Role of AMP-activated protein kinase in the metabolic syndrome and in heart disease. FEBS Lett **582**:81-9.

32. **Hardie, D. G., D. Carling, and N. Halford.** 1994. Roles of the Snf1/Rkin1/AMP-activated protein kinase family in the response to environmental and nutritional stress. Semin Cell Biol **5**:409-16.

33. **Hardie, D. G., S. A. Hawley, and J. W. Scott.** 2006. AMP-activated protein kinase--development of the energy sensor concept. J Physiol **574**:7-15.

34. **Hardie, D. G., J. W. Scott, D. A. Pan, and E. R. Hudson.** 2003. Management of cellular energy by the AMP-activated protein kinase system. FEBS Lett **546**:113-20.

35. **Hedegaard, J., P. Horn, R. Lametsch, H. Sondergaard Moller, P. Roepstorff, C. Bendixen, and E. Bendixen.** 2004. UDP-glucose pyrophosphorylase is upregulated in carriers of the porcine RN-mutation in the AMP-activated protein kinase. Proteomics **4**:2448-54.

36. **Himms-Hagen, J., and M. E. Harper.** 2001. Physiological role of UCP3 may be export of fatty acids from mitochondria when fatty acid oxidation predominates: an hypothesis. Exp Biol Med (Maywood) **226**:78-84.

37. **Hundal, R. S., M. Krssak, S. Dufour, D. Laurent, V. Lebon, V. Chandramouli, S. E. Inzucchi, W. C. Schumann, K. F. Petersen, B. R. Landau, and G. I. Shulman.** 2000. Mechanism by which metformin reduces glucose production in type 2 diabetes. Diabetes **49**:2063-9.

38. **Ichihara, S., and Y. Yamada.** 2007. Genetic factors for human obesity. Cell Mol Life Sci.

39. **Kahn, B. B., T. Alquier, D. Carling, and D. G. Hardie.** 2005. AMP-activated protein kinase: ancient energy gauge provides clues to modern understanding of metabolism. Cell Metab **1:**15-25.

40. **Kopelman, P. G.** 2000. Obesity as a medical problem. Nature **404:**635-43.

41. **Kubota, N., Y. Terauchi, T. Kubota, H. Kumagai, S. Itoh, H. Satoh, W. Yano, H. Ogata, K. Tokuyama, I. Takamoto, T. Mineyama, M. Ishikawa, M. Moroi, K. Sugi, T. Yamauchi, K. Ueki, K. Tobe, T. Noda, R. Nagai, and T. Kadowaki.** 2006. Pioglitazone ameliorates insulin resistance and diabetes by both adiponectin-dependent and -independent pathways. J Biol Chem **281:**8748-55.

42. **Lee, A. D., P. A. Hansen, and J. O. Holloszy.** 1995. Wortmannin inhibits insulin-stimulated but not contraction-stimulated glucose transport activity in skeletal muscle. FEBS Lett **361:**51-4.

43. **Lehmann, J. M., L. B. Moore, T. A. Smith-Oliver, W. O. Wilkison, T. M. Willson, and S. A. Kliewer.** 1995. An antidiabetic thiazolidinedione is a high affinity ligand for peroxisome proliferator-activated receptor gamma (PPAR gamma). J Biol Chem **270:**12953-6.

44. **Lemieux, S., D. Prud'homme, A. Nadeau, A. Tremblay, C. Bouchard, and J. P. Despres.** 1996. Seven-year changes in body fat and visceral adipose tissue in women. Association with indexes of plasma glucose-insulin homeostasis. Diabetes Care **19:**983-91.

45. **Lochhead, P. A., I. P. Salt, K. S. Walker, D. G. Hardie, and C. Sutherland.** 2000. 5-aminoimidazole-4-carboxamide riboside mimics the effects of insulin on the expression of the 2 key gluconeogenic genes PEPCK and glucose-6-phosphatase. Diabetes **49:**896-903.

46. **Lund, S., G. D. Holman, O. Schmitz, and O. Pedersen.** 1995. Contraction stimulates translocation of glucose transporter GLUT4 in skeletal muscle through a mechanism distinct from that of insulin. Proc Natl Acad Sci U S A **92:**5817-21.

47. **Millet, L., H. Vidal, F. Andreelli, D. Larrouy, J. P. Riou, D. Ricquier, M. Laville, and D. Langin.** 1997. Increased uncoupling protein-2 and -3 mRNA expression during fasting in obese and lean humans. J Clin Invest **100:**2665-70.

48. **Mu, J., J. T. Brozinick, Jr., O. Valladares, M. Bucan, and M. J. Birnbaum.** 2001. A role for AMP-activated protein kinase in contraction- and

hypoxia-regulated glucose transport in skeletal muscle. Mol Cell **7:**1085-94.

49. **Nawrocki, A. R., M. W. Rajala, E. Tomas, U. B. Pajvani, A. K. Saha, M. E. Trumbauer, Z. Pang, A. S. Chen, N. B. Ruderman, H. Chen, L. Rossetti, and P. E. Scherer.** 2006. Mice lacking adiponectin show decreased hepatic insulin sensitivity and reduced responsiveness to peroxisome proliferator-activated receptor gamma agonists. J Biol Chem **281:**2654-60.

50. **Nissen, S. E., and K. Wolski.** 2007. Effect of rosiglitazone on the risk of myocardial infarction and death from cardiovascular causes. N Engl J Med **356:**2457-71.

51. **Richter, E. A., L. P. Garetto, M. N. Goodman, and N. B. Ruderman.** 1984. Enhanced muscle glucose metabolism after exercise: modulation by local factors. Am J Physiol **246:**E476-82.

52. **Richter, E. A., L. P. Garetto, M. N. Goodman, and N. B. Ruderman.** 1982. Muscle glucose metabolism following exercise in the rat: increased sensitivity to insulin. J Clin Invest **69:**785-93.

53. **Rolfe, D. F., and M. D. Brand.** 1996. Contribution of mitochondrial proton leak to skeletal muscle respiration and to standard metabolic rate. Am J Physiol **271:**C1380-9.

54. **Rolfe, D. F., J. M. Newman, J. A. Buckingham, M. G. Clark, and M. D. Brand.** 1999. Contribution of mitochondrial proton leak to respiration rate in working skeletal muscle and liver and to SMR. Am J Physiol **276:**C692-9.

55. **Saha, A. K., P. R. Avilucea, J. M. Ye, M. M. Assifi, E. W. Kraegen, and N. B. Ruderman.** 2004. Pioglitazone treatment activates AMP-activated protein kinase in rat liver and adipose tissue in vivo. Biochem Biophys Res Commun **314:**580-5.

56. **Samec, S., J. Seydoux, and A. G. Dulloo.** 1998. Interorgan signaling between adipose tissue metabolism and skeletal muscle uncoupling protein homologs: is there a role for circulating free fatty acids? Diabetes **47:**1693-8.

57. **Samec, S., J. Seydoux, and A. G. Dulloo.** 1998. Role of UCP homologues in skeletal muscles and brown adipose tissue: mediators of thermogenesis or regulators of lipids as fuel substrate? Faseb J **12:**715-

24.

58. **Satman, I., T. Yilmaz, A. Sengul, S. Salman, F. Salman, S. Uygur, I. Bastar, Y. Tutuncu, M. Sargin, N. Dinccag, K. Karsidag, S. Kalaca, C. Ozcan, and H. King.** 2002. Population-based study of diabetes and risk characteristics in Turkey: results of the turkish diabetes epidemiology study (TURDEP). Diabetes Care **25:**1551-6.

59. **Schrauwen, P., M. K. Hesselink, E. E. Blaak, L. B. Borghouts, G. Schaart, W. H. Saris, and H. A. Keizer.** 2001. Uncoupling protein 3 content is decreased in skeletal muscle of patients with type 2 diabetes. Diabetes **50:**2870-3.

60. **Schrauwen, P., M. K. Hesselink, I. Vaartjes, E. Kornips, W. H. Saris, J. P. Giacobino, and A. Russell.** 2002. Effect of acute exercise on uncoupling protein 3 is a fat metabolism-mediated effect. Am J Physiol Endocrinol Metab **282:**E11-7.

61. **Schrauwen, P., W. H. Saris, and M. K. Hesselink.** 2001. An alternative function for human uncoupling protein 3: protection of mitochondria against accumulation of nonesterified fatty acids inside the mitochondrial matrix. Faseb J **15:**2497-502.

62. **Shaw, R. J., K. A. Lamia, D. Vasquez, S. H. Koo, N. Bardeesy, R. A. Depinho, M. Montminy, and L. C. Cantley.** 2005. The kinase LKB1 mediates glucose homeostasis in liver and therapeutic effects of metformin. Science **310:**1642-6.

63. **Sriwijitkamol, A., D. K. Coletta, E. Wajcberg, G. B. Balbontin, S. M. Reyna, J. Barrientes, P. A. Eagan, C. P. Jenkinson, E. Cersosimo, R. A. DeFronzo, K. Sakamoto, and N. Musi.** 2007. Effect of acute exercise on AMPK signaling in skeletal muscle of subjects with type 2 diabetes: a time-course and dose-response study. Diabetes **56:**836-48.

64. **StatisticsCanada.** 2004. Canadian Community Health Survey.

65. **StatisticsCanada.** 2005. Selected leading causes of death, by sex. Health Statistics Division.

66. **Tiraby, C., G. Tavernier, F. Capel, A. Mairal, F. Crampes, J. Rami, C. Pujol, J. A. Boutin, and D. Langin.** 2007. Resistance to high-fat-diet-induced obesity and sexual dimorphism in the metabolic responses of transgenic mice with moderate uncoupling protein 3 overexpression in glycolytic skeletal muscles. Diabetologia **50:**2190-9.

67. **Trenker, M., R. Malli, I. Fertschai, S. Levak-Frank, and W. F. Graier.** 2007. Uncoupling proteins 2 and 3 are fundamental for mitochondrial Ca2+ uniport. Nat Cell Biol **9**:445-52.

68. **Tsuboyama-Kasaoka, N., N. Tsunoda, K. Maruyama, M. Takahashi, H. Kim, S. Ikemoto, and O. Ezaki.** 1998. Up-regulation of uncoupling protein 3 (UCP3) mRNA by exercise training and down-regulation of UCP3 by denervation in skeletal muscle. Biochem Biophys Res Commun **247**:498-503.

69. **Vidal-Puig, A., G. Solanes, D. Grujic, J. S. Flier, and B. B. Lowell.** 1997. UCP3: an uncoupling protein homologue expressed preferentially and abundantly in skeletal muscle and brown adipose tissue. Biochem Biophys Res Commun **235**:79-82.

70. **Wallberg-Henriksson, H., and J. O. Holloszy.** 1985. Activation of glucose transport in diabetic muscle: responses to contraction and insulin. Am J Physiol **249**:C233-7.

71. **Walling, G. A., P. M. Visscher, L. Andersson, M. F. Rothschild, L. Wang, G. Moser, M. A. Groenen, J. P. Bidanel, S. Cepica, A. L. Archibald, H. Geldermann, D. J. de Koning, D. Milan, and C. S. Haley.** 2000. Combined analyses of data from quantitative trait loci mapping studies. Chromosome 4 effects on porcine growth and fatness. Genetics **155**:1369-78.

72. **Weigle, D. S., L. E. Selfridge, M. W. Schwartz, R. J. Seeley, D. E. Cummings, P. J. Havel, J. L. Kuijper, and H. BeltrandelRio.** 1998. Elevated free fatty acids induce uncoupling protein 3 expression in muscle: a potential explanation for the effect of fasting. Diabetes **47**:298-302.

73. **Winder, W. W., B. F. Holmes, D. S. Rubink, E. B. Jensen, M. Chen, and J. O. Holloszy.** 2000. Activation of AMP-activated protein kinase increases mitochondrial enzymes in skeletal muscle. J Appl Physiol **88**:2219-26.

74. **Wojtaszewski, J. F., J. B. Birk, C. Frosig, M. Holten, H. Pilegaard, and F. Dela.** 2005. 5'AMP activated protein kinase expression in human skeletal muscle: effects of strength training and type 2 diabetes. J Physiol **564**:563-73.

75. **Yeh, J. I., E. A. Gulve, L. Rameh, and M. J. Birnbaum.** 1995. The effects of wortmannin on rat skeletal muscle. Dissociation of signaling

pathways for insulin- and contraction-activated hexose transport. J Biol Chem **270:**2107-11.

76. **Yeh, L. A., K. H. Lee, and K. H. Kim.** 1980. Regulation of rat liver acetyl-CoA carboxylase. Regulation of phosphorylation and inactivation of acetyl-CoA carboxylase by the adenylate energy charge. J Biol Chem **255:**2308-14.

77. **Zhou, G., R. Myers, Y. Li, Y. Chen, X. Shen, J. Fenyk-Melody, M. Wu, J. Ventre, T. Doebber, N. Fujii, N. Musi, M. F. Hirshman, L. J. Goodyear, and D. E. Moller.** 2001. Role of AMP-activated protein kinase in mechanism of metformin action. J Clin Invest **108:**1167-74.

78. **Zierath, J. R.** 1995. In vitro studies of human skeletal muscle: hormonal and metabolic regulation of glucose transport. Acta Physiol Scand Suppl **626:**1-96.

Appendix A

Real-time skeletal muscle glucose uptake in AMPKγ_3 R225W carriers using positron emission tomography

Contribution of Collaborators

Ottawa Hospital Weight Management Clinic
Robert Dent, MD – study design, subject recruitment

University of Ottawa Heart Institute Lipid Research Laboratory
Ruth McPherson, MD, PhD – study design, subject recruitment
Brenda Bradley – subject recruitment, pre-screening
Sybil Hebert – subject recruitment, pre-screening

University of Ottawa Heart Institute Molecular Function & Imaging Group
Robert Beanlands, MD – study design, data analysis
Jean da Silva, PhD – manufacturing of [^{18}F]-fluorodeoxyglucose
Robert deKemp, PhD – study design, data analysis
Michael Gollob, MD – study design
May Aung – positron emission tomography technician, data analysis
Ed Gannon – study design
Kimberly Gardner – positron emission tomography technician
Michaela Garkisch – blood sampling
Linda Garrard – study design, subject recruitment, pre-screening, serum analysis

University of Ottawa School of Human Kinetics
Dany Lafontaine, PhD – study design, KinCom, electromyography, data analysis
Mario Lamontagne, PhD – study design
Stéfanie Pagé – KinCom, electromyography

Mitochondrial Bioenergetics Laboratory
Mary-Ellen Harper, PhD – study design, data analysis, involved in all experiments
Sheila Costford – study design, data analysis, involved in all experiments
Sean Crawford – study design, data analysis, involved in all experiments

Rationale

Upon activation, AMPK has been shown to increase glucose uptake in skeletal muscle by causing GLUT4 vesicle translocation to the plasma membrane (6) through AS160 (5, 8). Since the AMPKγ_3 R225W mutation leads to increased basal and AMP-stimulated AMPK activity (3), we hypothesized that R225W carriers would display increased glucose uptake in both resting and exercising skeletal muscle.

To investigate the effects of the AMPKγ_3 R225W mutation on glucose uptake *in vivo*, we collaborated with the University of Ottawa School of Human Kinetics and the Molecular Functioning and Imaging (MFI) Group at the University of Ottawa Heart Institute to determine real-time skeletal muscle glucose uptake in R225W carriers using [^{18}F]-fluorodeoxyglucose (FDG) positron emission tomography (PET).

Condensed Protocol

Pre-Screening

Control subjects for R225W carriers were matched for age, gender, BMI and physical activity. Prior to inclusion in the study, all subjects completed a standard Physical Activity Readiness Questionnaire (PAR-Q) to evaluate exercise eligibility.

Visit #1

Subjects fasted overnight before undergoing testing at the University of Ottawa School of Human Kinetics to determine the maximal force output of the quadriceps muscle group in their dominant leg using a KinCom leg extension machine. This value was used to calculate the load for the exercise intervention prior to PET analysis. Electromyography (EMG) was also performed during a series of fatigue tests to evaluate resistance to muscular fatigue.

Visit #2

Subjects underwent an overnight fast prior to arriving at the PET Facility at the University of Ottawa Heart Institute. An intravenous (IV) line was inserted in one arm (for FDG injection) and an arterialized IV line was inserted in the other line (for blood sampling). A baseline blood sample was taken

immediately before the initiation of the exercise intervention for the determination of free fatty acid (FFA), cortisol, insulin, lactate and glucose concentrations.

Subjects performed 30 minutes of leg extensions on their dominant leg with 1 second duration for the concentric contraction and 2 seconds duration for the eccentric contraction (timed using a metronome). Subjects lifted an ankle weight bearing a load which required them to generate 11% of their maximal force output, as determined on Visit #1 (Figure 31). Ten minutes after the initiation of exercise, subjects were injected with the FDG (this time point is referred to as 'time 0'). After the completion of 30 minutes of exercise, subjects were transferred immediately to the CT/PET scanner, where they underwent a CT scan followed by a 15-minute PET scan (Figure 32). Subjects remained in the scanner until 70 minutes post-exercise initiation ('time 60'). After the initial sampling, blood was drawn for metabolite determinations immediately following injection of FDG, 20 minutes post-injection and 60 minutes post-injection. Blood samples for [^{18}F] activity determination were taken immediately following injection, every 20 seconds for the first 3 minutes, then every 10 minutes until 60 minutes post-injection (Figure 33).

Figure 31: Image of subject performing leg extensions with ankle weight during test run of procedure.

Figure 32: Image of subject undergoing PET scan during test run of the procedure.

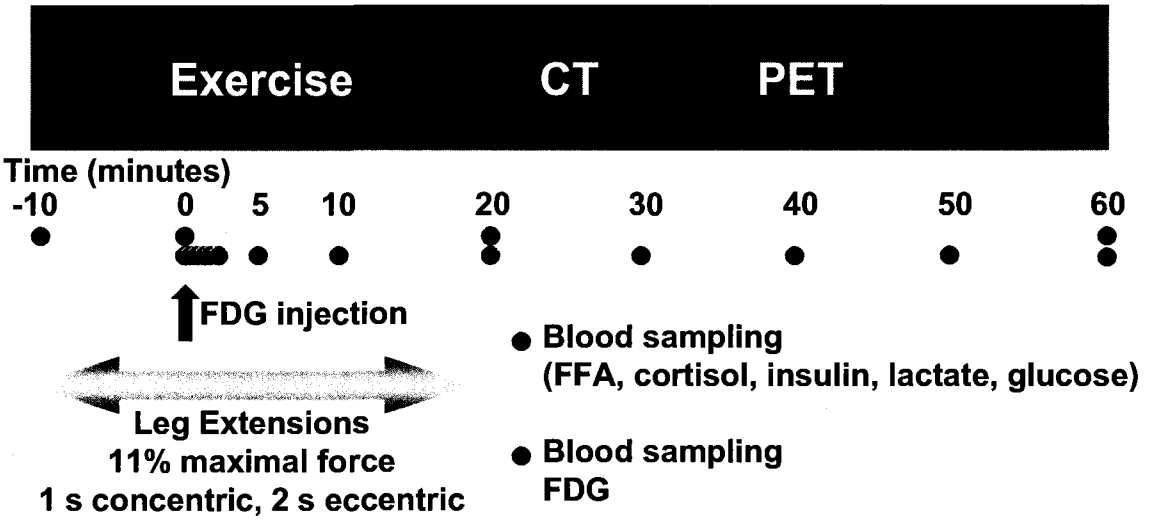

Figure 33: FDG PET exercise intervention protocol.

Results to Date

Maximal Muscular Force Output

To date (n=2), there are no differences in maximal force output of the quadriceps between R225W carriers and matched controls (Figure 34).

Muscular Fatigue

Subjects also underwent a series of muscular fatigue tests during which EMG was performed. We anticipate that R225W subjects will have higher resistance to muscular fatigue as they have increased muscle glycogen content (3), however the data as of yet is too preliminary to analyze.

Real-Time Glucose Uptake

There is a trend for R225W patients to have increased FDG uptake during exercise, but not at rest under fasting conditions (Figure 35 and 36).

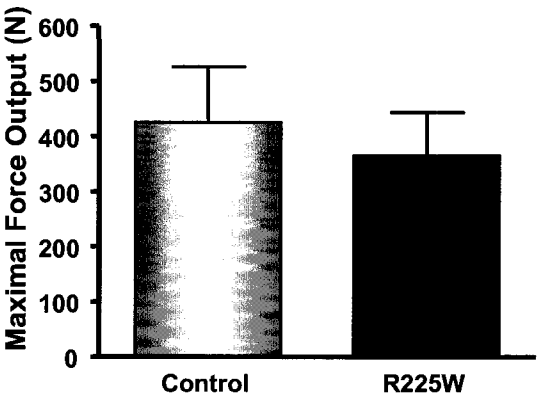

Figure 34: Maximal force output generated during extension of the leg. n=2, means ± SEM. Student's *t* test, NS.

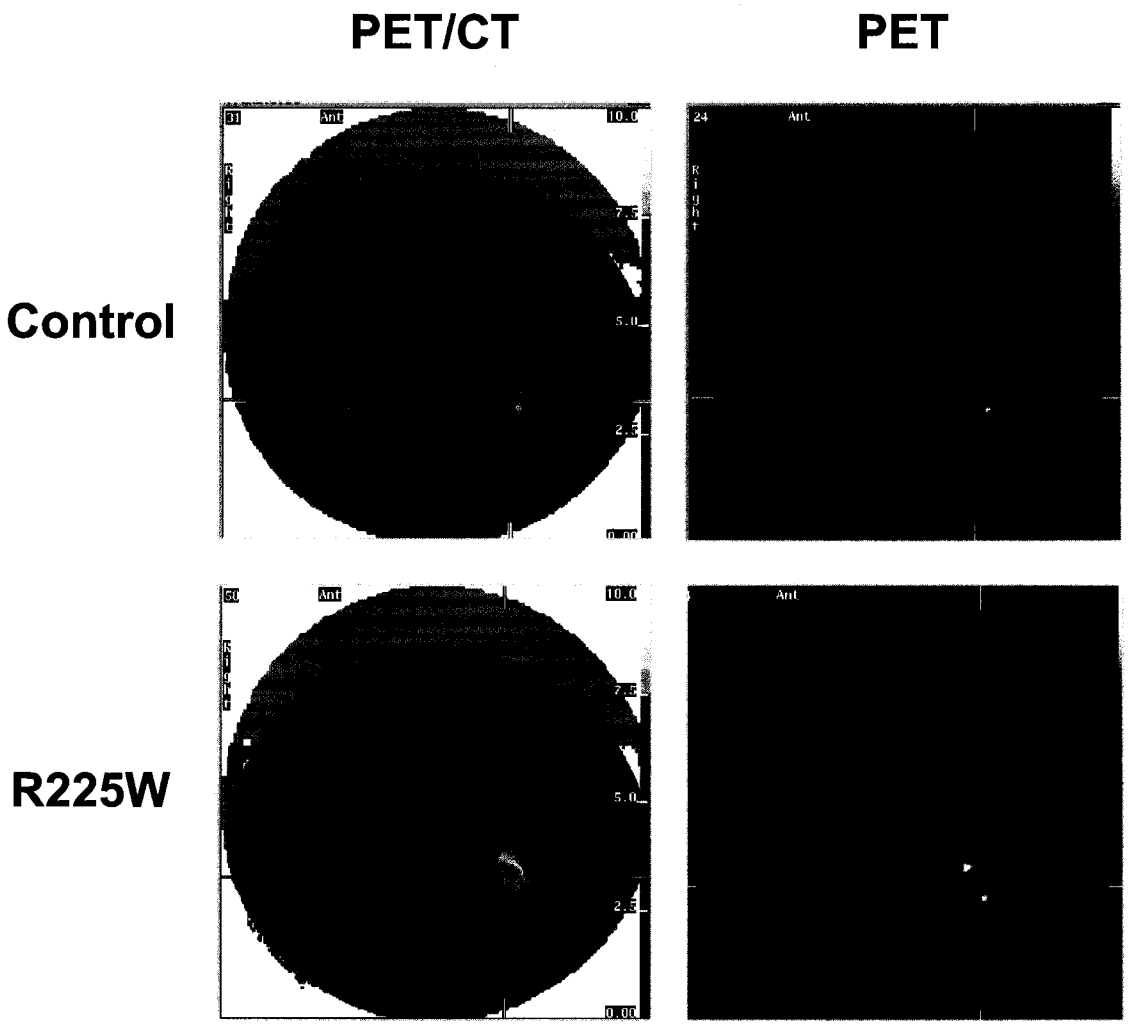

Figure 35: PET/CT and PET images of cross section of thighs in R225W carrier and matched control following exercise intervention. FDG indicated by colour intensity scale on right of each image (colour at top of scale indicates highest concentration of FDG). Anterior thigh: top; posterior thigh: bottom. Resting leg on left, exercised leg on right.

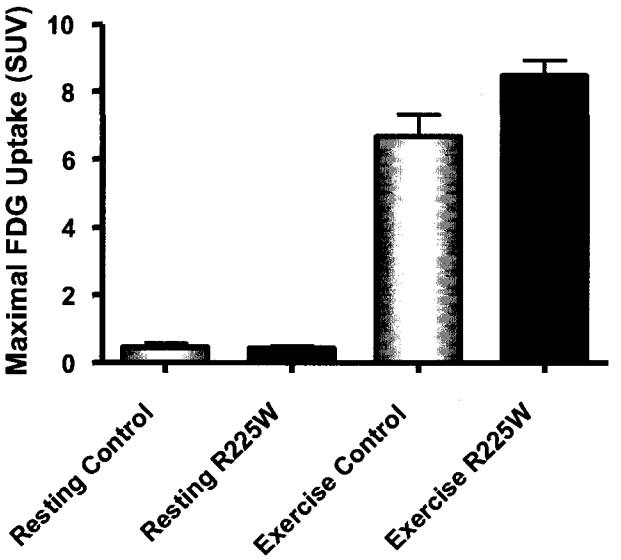

Figure 36: Quantification of PET images: maximal FDG uptake represented in standard uptake values (SUV). n=2, means ± SEM. One-way ANOVA, NS between R225W carriers and controls.

Summary

Muscle Function

There were no differences in maximal force output of the quadriceps between R225W carriers and matched controls (Figure 34), however this result was not unexpected. There is evidence that AMPK is involved in the molecular adaptation to endurance exercise (reviewed in (9)), therefore we hypothesized that R225W carriers would have increased resistance to muscular fatigue. The sample size is as yet too small to be able to draw conclusions from the EMG data, however we are currently recruiting more subjects for this study.

Skeletal Muscle Glucose Uptake

FDG PET has recently begun to be used to examine glucose uptake into skeletal muscles and tendons during exercise (4, 7). We compared FDG uptake in resting and exercised quadriceps muscles in R225W carriers and matched control subjects. We hypothesized that R225W carriers would have increased glucose uptake in both the resting and the exercised state compared to matched controls, due to their increased basal and AMP-stimulated AMPK activity in skeletal muscle (3). R225W carriers also exhibit increased muscle glycogen storage (3), which is paradoxical as AMPK is known to inhibit glycogen synthase (1, 2, 10). Increased glucose uptake,

however, may be able to explain the excess storage of glycogen in these subjects.

Our data indicate that there is no difference in FDG uptake in the resting state between R225W carriers and controls (Figure 36). However, PET may not be sensitive enough to detect differences in such low levels of glucose uptake in skeletal muscle as during the fasting state. There is a trend for R225W carriers to take up more FDG into the quadriceps muscles during the exercised state compared to control subjects. We anticipate that this result will reach statistical significance with an increased sample size.

References

1. **Carling, D., and D. G. Hardie.** 1989. The substrate and sequence specificity of the AMP-activated protein kinase. Phosphorylation of glycogen synthase and phosphorylase kinase. Biochim Biophys Acta **1012:**81-6.

2. **Chen, Z., J. Heierhorst, R. J. Mann, K. I. Mitchelhill, B. J. Michell, L. A. Witters, G. S. Lynch, B. E. Kemp, and D. Stapleton.** 1999. Expression of the AMP-activated protein kinase beta1 and beta2 subunits in skeletal muscle. FEBS Lett **460:**343-8.

3. **Costford, S. R., N. Kavaslar, N. Ahituv, S. N. Chaudhry, W. S. Schackwitz, R. Dent, L. A. Pennacchio, R. McPherson, and M. E. Harper.** 2007. Gain-of-function R225W mutation in human AMPKgamma3 causing increased glycogen and decreased triglyceride in skeletal muscle. PLoS ONE **2:**e903.

4. **Kalliokoski, K. K., J. Bojsen-Moller, M. Seppanen, J. Johansson, M. Kjaer, M. Teras, and S. P. Magnusson.** 2007. Contraction-induced [18F]-fluoro-deoxy-glucose uptake can be measured in human calf muscle using high-resolution PET. Clin Physiol Funct Imaging **27:**239-41.

5. **Kramer, H. F., C. A. Witczak, E. B. Taylor, N. Fujii, M. F. Hirshman, and L. J. Goodyear.** 2006. AS160 regulates insulin- and contraction-stimulated glucose uptake in mouse skeletal muscle. J Biol Chem **281:**31478-85.

6. **Kurth-Kraczek, E. J., M. F. Hirshman, L. J. Goodyear, and W. W. Winder.** 1999. 5' AMP-activated protein kinase activation causes GLUT4 translocation in skeletal muscle. Diabetes **48:**1667-71.

7. **Shimada, H., Y. Kimura, T. Suzuki, T. Hirata, M. Sugiura, Y. Endo, K. Yasuhara, K. Shimada, K. Kikuchi, M. Hashimoto, M. Ishikawa, K. Oda, K. Ishii, and K. Ishiwata.** 2007. The use of positron emission tomography and [18F]fluorodeoxyglucose for functional imaging of muscular activity during exercise with a stride assistance system. IEEE Trans Neural Syst Rehabil Eng **15:**442-8.

8. **Treebak, J. T., S. Glund, A. Deshmukh, D. K. Klein, Y. C. Long, T. E. Jensen, S. B. Jorgensen, B. Viollet, L. Andersson, D. Neumann, T. Wallimann, E. A. Richter, A. V. Chibalin, J. R. Zierath, and J. F. Wojtaszewski.** 2006. AMPK-mediated AS160 phosphorylation in skeletal muscle is dependent on AMPK catalytic and regulatory subunits. Diabetes **55:**2051-8.

9. **Winder, W. W., E. B. Taylor, and D. M. Thomson.** 2006. Role of AMP-activated protein kinase in the molecular adaptation to endurance exercise. Med Sci Sports Exerc **38:**1945-9.

10. **Wojtaszewski, J. F., S. B. Jorgensen, Y. Hellsten, D. G. Hardie, and E. A. Richter.** 2002. Glycogen-dependent effects of 5-aminoimidazole-4-carboxamide (AICA)-riboside on AMP-activated protein kinase and glycogen synthase activities in rat skeletal muscle. Diabetes **51:**284-92.

Curriculum Vitae

Sheila Costford
Mitochondrial Bioenergetics Laboratory
Department of Biochemistry, Microbiology & Immunology
Faculty of Medicine, University of Ottawa

FORMAL EDUCATION

Ph.D. Candidate	University of Ottawa, Faculty of Medicine, Jan 2003-08 *Department of **Biochemistry**, Microbiology & Immunology*
B.Sc. (Hon)	University of Ottawa, Faculty of Science, 2002 ***Biochemistry** Program*

ACADEMIC/RESEARCH/TEACHING AWARDS & SCHOLARSHIPS

December 2007	Award of Excellence in Graduate Studies ($500) For outstanding achievement in research, scholarship, education and other contributions to the life of the Faculty. *Faculty of Medicine, University of Ottawa*
October 2007	Young Investigator Travel Award ($500) *The Obesity Society Annual Scientific Meeting*
May 2007	2nd Place Poster: Biochemistry, Ph.D. Category *Department of Biochemistry, Microbiology and Immunology Graduate Student Poster Day*
May 2007	Award for Best Presentation Skills *Department of Biochemistry, Microbiology and Immunology Graduate Student Poster Day*

ACADEMIC/RESEARCH/TEACHING AWARDS & SCHOLARSHIPS CONTINUED

February 2007	Connexion Award: Inaugural Recipient In recognition of outstanding contribution to *YMCA-YWCA Education Centre* as an exceptional leader & volunteer
November 2006	University of Ottawa Doctoral Research Scholarship Awarded to 2 recipients at the University of Ottawa (Equivalent of tuition fees for remainder of doctoral degree)
November 2006	Winner of a AMP-Activated Protein Kinase in Obesity, Metabolic Node and Beyond Student Travel Award ($500) *Canadian Obesity Network*
July 2006	Selected as one of 24 trainees to attend Canadian Obesity Network/University of Laval Obesity Boot Camp Training Program *Canadian Obesity Network/University of Laval*
March 2006	Teaching Assistant of the Year, 2004-2005 *University of Ottawa, Faculty of Science, Biochemistry Program*
May 2005	Ontario Graduate Scholarship in Science & Technology ($15,000 per year for 2 years)
March 2005	3rd Place Poster: Biochemistry, Ph.D. Category *Department of Biochemistry, Microbiology and Immunology Graduate Student Poster Day*
June 2003	Winner of a Christine Gagnon Memorial Travel Award ($250) *Canadian Society for Nutritional Sciences (CSNS)*
June 2003	Nestlé Nutrition Graduate Student Competition – FINALIST *Canadian Federation for Biological Societies Annual Meeting*
April 2003	Visual Presentation Award – University of Ottawa *Department of Biochemistry, Microbiology and Immunology Graduate Student Poster Day*

RESEARCH PUBLICATIONS

Peer-Reviewed Articles

Sheila Costford, Shehla Chaudhry, Mahmoud Salkhordeh and Mary-Ellen Harper. Long-term high fat feeding induces greater fat storage in mice lacking UCP3. (*Am J Physiol Endocrinol Metab, submitted*)

Sheila Costford, Erin Seifert, Veronic Bezaire, Martin Gerrits, Lisa Bevilacqua, Adrienne Gowing and Mary-Ellen Harper. The Energetic Implications of Uncoupling Protein-3 in Skeletal Muscle. Review. Appl Physiol Nutr Metab, 2007 Oct;32(5):884-894.

Sheila Costford, Adrienne Gowing and Mary-Ellen Harper. Mitochondrial uncoupling as a target for the treatment of obesity. Review. Curr Opin Clin Nutr Metab Care, Nov;10(6):671–678.

Sheila Costford, Nihan Kavaslar, Nadav Ahituv, Shehla Chaudhry, Wendy Schackwitz, Robert Dent, Len Pennacchio, Ruth McPherson and Mary-Ellen Harper. Identification of a gain-of-function R225W mutation in human AMPKγ3 that causes increased skeletal muscle glycogen. PLoS ONE, 2007 Sep 19;2(9):e903.

Sheila Costford, Shehla Chaudhry, Mahmoud Salkhordeh and Mary-Ellen Harper. Effects of the Presence, Absence and Overexpression of Uncoupling Protein-3 on Adiposity and Fuel Metabolism in Congenic Mice. Am J Physiol Endocrinol Metab 290: E1304-E1312, 2006.

Book Chapter

Mary-Ellen Harper, Lisa Bevilacqua, **Sheila Costford**, Lorenne Doucet, Mahmoud Salkhordeh and Martin Gerrits. Uncoupling protein 3 (UCP3) and fatty acid metabolism in muscle. In: Progress in Obesity Research: 9. Eds. G. Mederios-Neta, A. Halpern and C. Bouchard. John Libbey Eurotext Ltd. Surrey, United Kingdom (2003).

RESEARCH PUBLICATIONS CONTINUED

Abstracts

Sheila Costford, Nihan Kavaslar, Nadav Ahituv, Shehla Chaudhry, Wendy Schackwitz, Robert Dent, Len Pennacchio, Ruth McPherson and Mary-Ellen Harper. Characterization of R225W Mutation in Human AMPKγ_3 Causing Increased Muscle Glycogen and Decreased Muscle Triglyceride. (2007). The Obesity Society Annual Scientific Meeting.

Sheila Costford, Shehla Chaudhry, Nihan Kavaslar, Nadav Ahituv, Len Pennacchio, Robert Dent, Ruth McPherson and Mary-Ellen Harper. Novel Mutations in the Gamma-3 Subunit of AMP-Activated Protein Kinase Affect Protein Function in Humans. (2006). Biochemistry of Exercise 13th International Conference.

Sheila Costford, Shehla Chaudhry, Mahmoud Salkhordeh and Mary-Ellen Harper. Uncoupling protein-3 protects against accumulation of intramuscular triglyceride and insulin resistance. (2005). 48th Annual Meeting of the Canadian Federation of Biological Societies.

Sheila Costford, Shehla Chaudhry and Mary-Ellen Harper. UCP3 overexpression improves insulin sensitivity and prevents lipid accumulation in muscle in the absence of altered energy expenditure or intake in mice. (2004). North American Association for the Study of Obesity 2004 Annual Scientific Meeting.

Sheila Costford, Mahmoud Salkhordeh and Mary-Ellen Harper. Effects of the overexpression or absence of uncoupling protein-3 on the development of insulin resistance in C57BL/6 mice. (2003). 46th Annual Meeting of the Canadian Federation of Biological Societies.

Sheila Costford, Lorenne Doucet and Mary-Ellen Harper. UCP3 overexpression in muscle of mice fed a high fat diet protects against obesity and impaired glucose tolerance. (2003). Experimental Biology.

RESEARCH PRESENTATIONS and POSTERS

October 2007	The Obesity Society Annual Scientific Meeting *Oral Presentation* (New Orleans, LA)
October 2006	Biochemistry of Exercise 13th International Conference *Poster Presentation* (Seoul, Korea)
May 2006	University of Ottawa Centre for Catalysis Research and Innovation Grand Opening, *Poster Presentation* (Ottawa, ON)
February 2006	University of Ottawa Biochemistry, Microbiology & Immunology Research Symposia, *Oral Presentation* (Ottawa, ON)
June 2005	48th Annual Meeting of the Canadian Federation for Biological Societies, *Poster Presentation* (Guelph, ON)
March 2005	University of Ottawa, BMI Graduate Student Poster Day *Poster Presentation* (Ottawa, ON)
November 2004	North American Association for the Study of Obesity 2004 Annual Scientific Meeting, *Poster Presentation* (Las Vegas, NV)
January 2004	Centre for Catalysis Research and Innovation Workshop-III *Poster Presentation* (Ottawa, ON)
June 2003	46th Annual Meeting of the Canadian Federation for Biological Societies, *Nestle Nutrition Graduate Student Competition Finalist* *Oral Presentation* (Ottawa, ON)
June 2003	46th Annual Meeting of the Canadian Federation for Biological Societies *Poster Presentation* (Ottawa, ON)
June 2003	Centre for Research of Biopharmaceuticals - Diabetes/Obesity Research Day, *Poster Presentation* (Ottawa, ON)
April 2003	University of Ottawa, BMI Graduate Student Poster Day *Poster Presentation* (Ottawa, ON)

RESEARCH PRESENTATIONS and POSTERS CONTINUED

April 2003 — Experimental Biology 2003 Conference
Poster Presentation (San Diego, CA)

INVITED LECTURES

February 2007 — Connexion Fitness Conference
Keynote Address (Ottawa, ON)

ACADEMIC SERVICE

Jan-Dec 2006 — University of Ottawa BMI Graduate Students' Association
Vice President Internal Affairs

Mar 05-Dec 2006 — University of Ottawa Faculty of Medicine Graduate Student Representative Committee, *Member*

Oct 04-Dec 2006 — University of Ottawa Biochemistry Graduate Studies Committee
Graduate Student Representative

May 04-Dec 2006 — University of Ottawa Biochemistry, Microbiology & Immunology Council, *Graduate Student Representative*

Jan 03-Dec 2005 — University of Ottawa BMI Graduate Students' Association, *Secretary*

TEACHING EXPERIENCE

Jan 07-Apr 2007	Teaching Assistant: Lecturer *University of Ottawa, Faculty of Science*
Jan 04-Apr 2006	Teaching Assistant: Marker/Corrector *University of Ottawa, Faculty of Science*
Sep 03-Sep 2006	Teaching Assistant: Laboratory Demonstrator *University of Ottawa, Faculty of Science*
May 02-Dec 07	Health & Fitness Trainer/Presenter *National Capital Region YMCA-YWCA Education Centre*

MEDIA & CONSULTING

November 2006	Program Development for Canada's First Women's Only YMCA Centre, *National Capital Region YMCA-YWCA*
Jan-Dec 2006	Health & Fitness Columnist *University of Ottawa Biochemistry, Microbiology & Immunology Bulletin*
February 2003	Invited Interview: CBC Radio One, Ottawa Morning (with Anthony Germain). Topic: Nutrition: Breakfast 101

PROFESSIONAL MEMBERSHIPS

Since 2003	American College of Sports Medicine
Since 2002	American Physiological Society
Since 2002	Canadian Society for Nutritional Sciences
Since 2002	Canadian Federation for Biological Societies
Since 2002	Centre for Science in the Public Interest
Since 2001	Canadian Fitness Professionals

REFERENCES

Mary-Ellen Harper, PhD
Associate Professor of Biochemistry
Department of Biochemistry, Microbiology and Immunology
Faculty of Medicine
University of Ottawa

Ruth McPherson MD, PhD, FRCPC
Director, Lipid Clinic,
Lipid Research Laboratory
University of Ottawa Heart Institute
Professor, Medicine & Biochemistry
University of Ottawa

Additional references available upon request.